

Supporting Information

Catalytic Role of the Enol Ether Intermediate in the Intramolecular Stetter Reaction: A Computational Perspective

Gou-Tao Huang[†] and Jen-Shiang K. Yu^{*,†,‡,¶}

[†]Department of Biological Science and Technology, [‡]Institute of Bioinformatics and Systems Biology, and [¶]Center for Intelligent Drug Systems and Smart Bio-devices (IDS²B), National Yang Ming Chiao Tung University, Hsinchu City 300, Taiwan

E-mail: jsyu@mail.nctu.edu.tw

Phone: +886 (3)5729287. Fax: +886 (3)5729288

*To whom correspondence should be addressed

[†]National Yang Ming Chiao Tung University

[‡]National Yang Ming Chiao Tung University

[¶]National Yang Ming Chiao Tung University

Contents

1	Conformational search by CREST	S8
2	Assessment of computational accuracy by DLPNO-CCSD(T)	S10
2.1	Energy profile	S10
3	Reaction mechanism	S13
3.1	Isomers of enones and enolates	S13
3.2	Intramolecular reactions starting from the PA	S14
3.2.1	Direct [1,2] proton transfer	S14
3.2.2	Direct [1,2] hydride transfer	S15
3.2.3	Oxa-Michael reaction	S17
3.2.4	Proton transfer with a chiral carbene	S27
3.3	Formation of the BI	S29
3.3.1	Intramolecular mechanism	S29
3.3.2	Intermolecular mechanism	S30
3.4	C–C Michael reaction	S39
4	Kinetics simulations	S44
4.1	Rate equation for each species	S44
4.2	Kinetic simulations at five reaction stages	S46
4.3	Determination of the reaction order by the VTNA	S49
4.4	Rate constant for enol ether formation	S51
4.5	Steady-state approximation	S54
4.6	Kinetic simulation with increasing k_{11} and k_{-11}	S58
4.7	NHC-assisted mechanism	S59
5	Cartesian coordinates of optimized structures	S60

List of Figures

- S1 Free energy profiles ($\Delta G_{\text{DFT, sol}}$ and $\Delta G_{\text{CC, sol}}$ in kcal mol⁻¹) based on the most stable conformer. The values shown in red and blue refer to the free energies computed at the levels of $\omega\text{B97X-D}$ and DLPNO-CCSD(T), respectively. S11
- S2 Relative electronic energies (ΔE_{ele} in kcal mol⁻¹) computed at the DLPNO-CCSD(T)/def2-TZVP and DLPNO-CCSD(T)/CBS levels. The energy of the reactant (**1** + **2**) is employed as the baseline energy. S12
- S3 Charge analyses (in e) of **ts4** and **ts4keto**. S16
- S4 Four stereoisomeric TSs involved in the oxa-conjugate addition (**ts8**). The reported activation energies are relative to the reference energy of separated reactants, **1** + **2**. S19
- S5 Optimized TS structures of **ts8** in terms of stereochemistry of *si*-(*scis-re*) and *si*-(*strans-re*). The most stable conformer is shown by the ball-and-stick representation, and eight low-energy conformers are aligned with respect to the five-membered NHC ring. Bond lengths are given in Å. S19
- S6 16 stereoisomeric TSs involved in the proton transfer (**ts9**). The proton transfer of the oxa-Michael reaction can proceed in (a) syn, and (b) anti modes. The reported activation energies are relative to the reference energy of separated reactants, **1** + **2**. S20
- S7 Optimized TS structures of **ts9** in terms of stereochemistry of *si*-(*scis-re-si*)-*E*, *si*-(*scis-re-si*)-*Z*, *si*-(*scis-re-re*)-*E*, and *si*-(*scis-re-re*)-*Z*. The most stable conformer is shown by the ball-and-stick representation, and eight low-energy conformers are aligned with respect to the five-membered NHC ring. Bond lengths are given in Å. S21

S8	Optimized TS structures of ts9 in terms of stereochemistry of <i>si</i> -(<i>trans-re-si</i>)- <i>E</i> , <i>si</i> -(<i>trans-re-si</i>)- <i>Z</i> , <i>si</i> -(<i>trans-re-re</i>)- <i>E</i> , and <i>si</i> -(<i>trans-re-re</i>)- <i>Z</i> . The most stable conformer is shown by the ball-and-stick representation, and eight low-energy conformers are aligned with respect to the five-membered NHC ring. Bond lengths are given in Å.	S22
S9	Four stereoisomers of enol ether 9 . The reported energies are relative to the reference energy of separated reactants, 1 + 2	S23
S10	Free energy profiles (in kcal mol ⁻¹) for the formation of enol ether 9 . The oxa-Michael reactions with respect to the <i>scis</i> - and <i>trans</i> -enones are shown in red and blue, respectively.	S24
S11	(a) Structural analysis of ts8-A . Relative free energies and distances are given in kcal mol ⁻¹ and Å, respectively. For the low energy conformers, the O⋯HC distances smaller than 2.60 Å are marked in orange. (b) NCI analysis of the lowest energy conformer. The NCI surface corresponds to <i>s</i> = 0.5 au and the NCI color scale ranges from 0.04 to 0.02 au.	S25
S12	(a) Structural analysis of ts9-A . Relative free energies and distances are given in kcal mol ⁻¹ and Å, respectively. For the low energy conformers, the O⋯HC distances smaller than 2.60 Å are marked in orange. (b) NCI analysis of the lowest energy conformer. The NCI surface corresponds to <i>s</i> = 0.5 au and the NCI color scale ranges from 0.04 to 0.02 au.	S26
S13	Stereoisomeric TSs with respect to the proton transfer using a chiral carbene. The reported activation energies (in kcal mol ⁻¹) are relative to the reference energy of separated reactants.	S27

S14	(a) Structural analysis of ts9-A with a chiral carbene. Relative free energies and distances are given in kcal mol ⁻¹ and Å, respectively. For the low energy conformers, the O⋯HC distances smaller than 2.60 Å are marked in orange. (b) NCI analysis of the lowest energy conformer. The NCI surface corresponds to $s = 0.5$ au and the NCI color scale ranges from 0.04 to 0.02 au.	S28
S15	Eight stereoisomeric TSs with respect to the C–O _β bond cleavage. The (<i>R</i>)-PA and the (<i>S</i>)-PA are used as the bases. The free energies shown in orange (in kcal mol ⁻¹) are relative to the reference energy of 9 + 3	S34
S16	Lowest-energy conformers of the stereoisomeric TSs with respect to C–O bond cleavage. The (<i>R</i>)/(<i>S</i>)-PA moiety is highlighted in orange. The <i>E/Z</i> -geometry of the Michael acceptor is shown in cyan. Distances are given in Å.	S35
S17	Computed energy profile (in kcal mol ⁻¹) for the BI formation assisted by the PA. The symbols shown in cyan indicate the olefin geometry of the Michael acceptor to be re-generated. For consistency, the (<i>Z</i>)/(<i>E</i>)-configurations of the enolates in ts10 , 10 , and 10i (shown in magenta) are represented by the corresponding <i>s-cis/s-trans</i> of the enones. The reported free energies are relative to the reference energy of 9 + 3	S36
S18	Optimized structures of ts5 in terms of four stereochemical configurations of <i>re-(scis-si)</i> , <i>re-(strans-si)</i> , <i>re-(scis-re)</i> and <i>re-(strans-si)</i> . The Newman projections along the C _β –C ₂ bond to form, highlighted in cyan, are also shown for the most stable conformer. Distances are in Å.	S41
S19	Kinetic simulations at different reaction stages.	S47
S20	Kinetic simulations including all five reaction stages. The gray regions indicate the BI formation with or without the hydrogen-bonded complex (4·3) considered.	S48

S21	Variable time normalization analysis: (a) variation of the initial concentration of catalyst 1 , where the initial concentration of substrate 2 is fixed; (b) variation of the initial concentration of substrate 2 , where the initial concentration of catalyst 1 is fixed.	S50
S22	Relationship between the rate-constant representation (eq. s18) and the energy representation (eq. s19).	S52
S23	Relationship between the rate-constant representation and the energy representation in eqs. s34 and s35.	S57
S24	(a) Kinetic simulation using the initial concentrations of $[\mathbf{1}]_0 = 0.005$ M and $[\mathbf{2}]_0 = 0.025$ M. The barrier heights with respect to k_{11} and k_{-11} are lowered by 0.5 kcal mol ⁻¹ while other parameters remain unchanged. (b) VTNA using the data obtained from kinetic simulations.	S58
S25	Kinetic simulation based on the reaction profile of the NHC-assisted mechanism.	S59

List of Tables

S1	Numbers of conformers and constrained parameters.	S9
S2	Free energy profiles based on the most stable conformer for each species (in the second column). The Boltzmann-weighted energies are also listed for comparison (in the third column).	S42
S3	Rate constants calculated at 0°C by the Eyring-Polanyi equation using DFT-computed activation energies ($\Delta G_{\text{act}}^\ddagger$ in kcal mol ⁻¹).	S45

1 Conformational search by CREST

Owing to conformational flexibility, the CREST program was employed to yield possible conformers. Table S1 shows the number of the conformers obtained from the CREST sampling. Additional constraints were applied in search of TS conformers: the constrained parameters were utilized according to DFT-computed structures (the technical detail statement is provided in the CREST’s manual). For example, the initial addition involves the bond formation between carbene **1** and aldehyde **2**, and the distance of the C...C bond to be created is set at 2.02 Å during the ensemble sampling. In several cases, structural constraints might be necessary to maintain the desired geometry. The purpose of the structural constraint is to obtain the reasonable conformers, which are employed as the initial structures for geometry optimization at the DFT level. Table S1 lists the constrained parameters during the conformational search.

The PA-assisted mechanism (**9** + **3** \rightleftharpoons **4** + **3**) is an intermolecular reaction, where the PA **3** moiety can be oriented in multiple directions towards the enol ether **9**. To explore conformational ensembles, we have attempted to place the PA and the enol ether in different orientation and position. The procedure was performed for the conformational search of the structures, **ts10**, **10**, **10i**, **ts11**, **11**, **ts4·3**, and **4·3**. Other stereochemical pathways are examined by the same procedure.

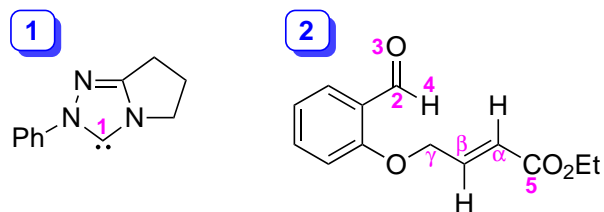


Table S1: Numbers of conformers and constrained parameters.

	number of conformers	constraints during conformational search
1	1	not required
2	101	not required
initial addition		
ts3	1001	C1...C2: 2.02 Å
3	603	C1-C2-O3: 105°, C5-C _α -C _β -C _γ : 180°, C5-C _α -C _β -H _β : 0°
oxa-Michael reaction		
ts8-A	313	O3...C _β : 1.95 Å
8-A	22	not required
ts9-A	34	C2...H4: 1.30 Å, C _α ...H4: 1.52 Å
9	440	not required
[1,2] proton transfer		
ts4	354	C2...H4: 1.19 Å, C3...H4: 1.29 Å
4	571	not required
[1,2] hydride transfer		
ts4keto	431	C2...H4: 1.44 Å, C1...H4: 1.45 Å
4keto	1263	not required
[1,3] hydrogen transfer (intramolecular)		
H _S transfer	32	O3...H4: 1.17 Å, O3...C _β : 1.72 Å, H4...C _α : 1.51 Å,
H _R transfer	45	O3...H _α : 1.17 Å, O3...C _β : 1.74 Å, H _α ...C _α : 1.51 Å
the BI with the <i>Z</i> -form Michael acceptor	982	not required
PA-assisted (intermolecular)		
ts10	6574	C _α ...H4: 1.51 Å, O3'...H4: 1.13 Å
10	9995	O3'H4...O _{enolate} : 1.55 Å
10i	7732	O3'H4...O3: 1.72 Å, O3...C _β : 1.54 Å
ts11	2360	O3...H4: 1.52 Å, O3'...H4: 1.00 Å, O3...C _β : 1.87 Å
11	1000	O3'H4...O3: 1.42 Å
ts4-3	8920	O3...H4: 1.25 Å, H4...O3': 1.15 Å
4-3	1739	H4...O3': 1.49 Å
C-C Michael reaction		
ts5-A	101	C2...C _β : 2.25 Å
ts5-B	73	C2...C _β : 2.13 Å
5-A	87	not required
ts6-A	82	H4...C _α : 1.40 Å H4...O3: 1.21 Å
ts6-B	100	H4...C _α : 1.44 Å H4...O3: 1.18 Å
6	199	not required
catalyst expulsion		
ts7	501	C1...C2: 2.03 Å
7	92	not required

2 Assessment of computational accuracy by DLPNO-CCSD(T)

2.1 Energy profile

To assess the accuracy of the DFT-computed energetics, the free energy profile was re-computed by the high-level DLPNO-CCSD(T) method.^{1,2} The DFT-computed lowest energy conformers were used to construct the energy profiles shown in Figure S1. Single-point DLPNO-CCSD(T)/def2-TZVP calculations ($\Delta G_{\text{CC, sol}}$) were performed to re-compute the free energies according to the equation

$$G_{\text{CC, sol}} = G_{\text{DFT, sol}} - E_{\text{DFT, gas}} + E_{\text{CC, gas}},$$

where $E_{\text{DFT, gas}}$ and $E_{\text{CC, gas}}$ represent the gas-phase electronic energies at $\omega\text{B97X-D/def2-TZVP}$ and DLPNO-CCSD(T)/def2-TZVP levels, respectively (that is, the DFT energy of $G_{\text{DFT, gas}}$ is replaced by $G_{\text{CC, gas}}$). Other terms including zero-point energies and solvation energies were taken from the previous DFT calculations. The coupled cluster computations were carried out by the ORCA software.³ Density fitting was employed to accelerate two-electron integrals.

Figure S1 shows the comparison of the energy profiles computed at the $\omega\text{B97X-D}$ and DLPNO-CCSD(T) levels. In the DFT calculations, the two key TSs, **ts8-A** and **ts9-A**, have similar energies, and the formation of the enol ether intermediate (**9**) is exergonic. Other intramolecular reactions including [1,2] proton shift (**ts4**) and hydride transfer (**ts4keto**) require high activation energies. Among the three intermediates of **9**, **4** and **4keto**, the enol ether species (**9**) is the most thermodynamically favored. The energetic trends mentioned above are reproduced by the DLPNO-CCSD(T) calculations. Therefore, the $\omega\text{B97X-D}$ level can offer a reliable description in energetics.

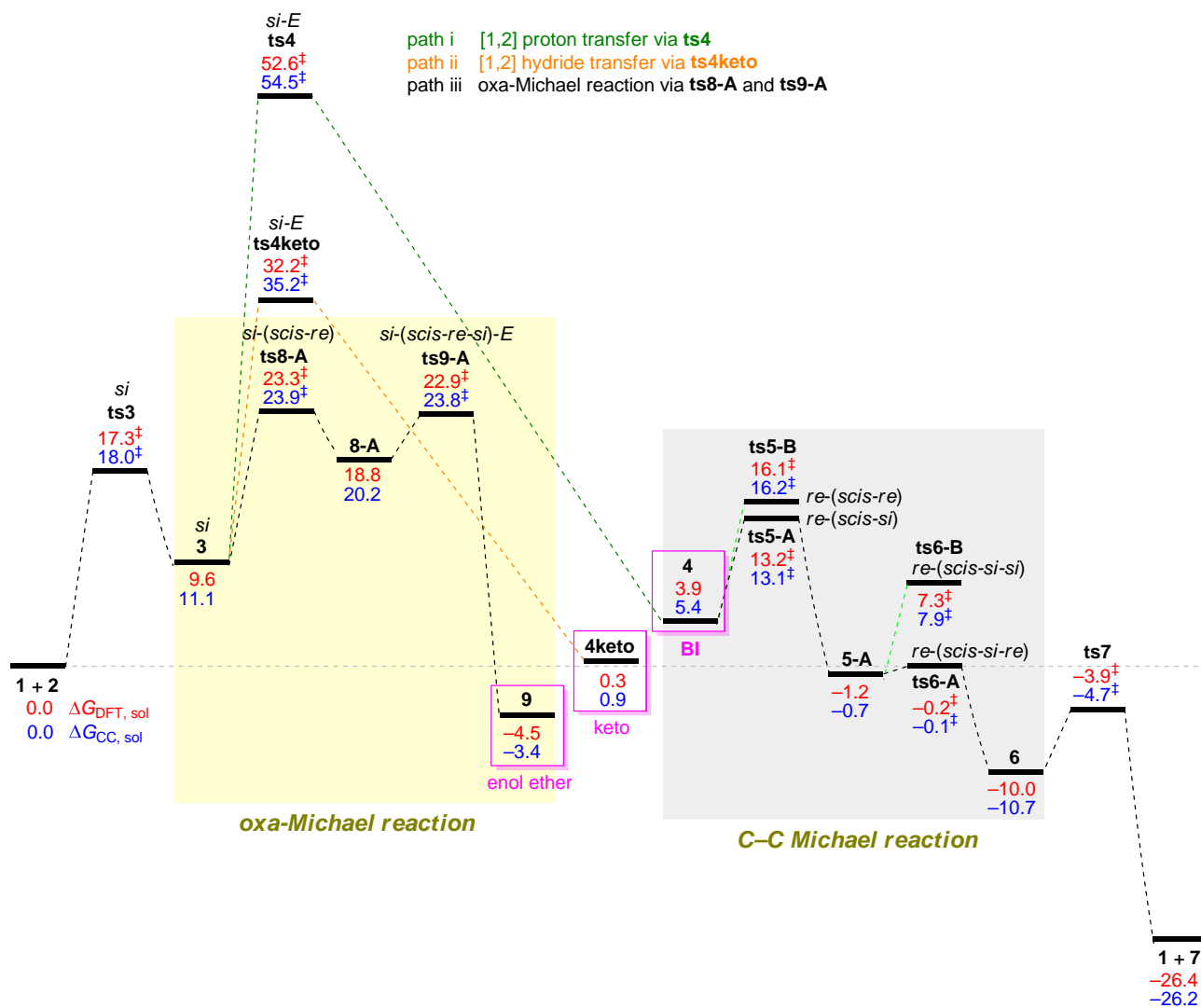


Figure S1: Free energy profiles ($\Delta G_{\text{DFT, sol}}$ and $\Delta G_{\text{CC, sol}}$ in kcal mol⁻¹) based on the most stable conformer. The values shown in red and blue refer to the free energies computed at the levels of $\omega\text{B97X-D}$ and DLPNO-CCSD(T), respectively.

In order to examine the effect of the basis set size on the energetics, we performed a TZ/QZ extrapolation toward the complete basis set (CBS) limit. The relative electronic energies along the pathway of the enol ether formation were computed at the DLPNO-CCSD(T)/def2-TZVP and DLPNO-CCSD(T)/CBS levels. The DLPNO-CCSD(T) single-point calculations were performed using the lowest-energy conformer optimized at the DFT level. The def2-TZVP basis set yielded a deviation within 1 kcal mol⁻¹ as compared to the CBS.

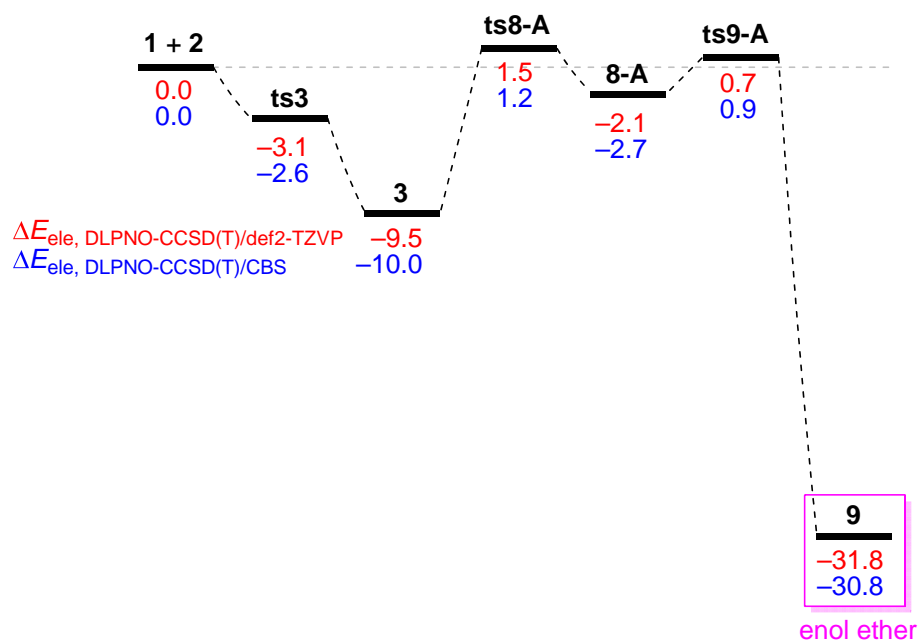


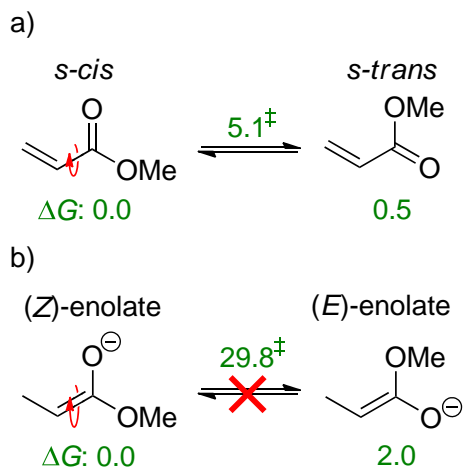
Figure S2: Relative electronic energies (ΔE_{ele} in kcal mol⁻¹) computed at the DLPNO-CCSD(T)/def2-TZVP and DLPNO-CCSD(T)/CBS levels. The energy of the reactant (**1 + 2**) is employed as the baseline energy.

3 Reaction mechanism

3.1 Isomers of enones and enolates

An enone exists in two configurations of *s-cis* and *s-trans*, while an enolate has (*Z*)- and (*E*)-isomers. The model calculations shown in Scheme S1a suggest that the *s-cis* and *s-trans* conformers undergo a rapid interconversion due to a small barrier of 5.1 kcal mol⁻¹, and thus coexist in an equilibrium.⁴ In contrast, the (*Z*)- and (*E*)-enolate isomers are unable to interconvert through the rotation around the carbon-carbon double bond, with a high rotational barrier of 29.8 kcal mol⁻¹ (Scheme S1b).

Scheme S1: (a) Structures of the *s-cis* and *s-trans* enoates. The reported free energies (in kcal mol⁻¹) are computed at the ω B97X-D level. (b) Structures of the (*Z*)- and (*E*)-enolates.

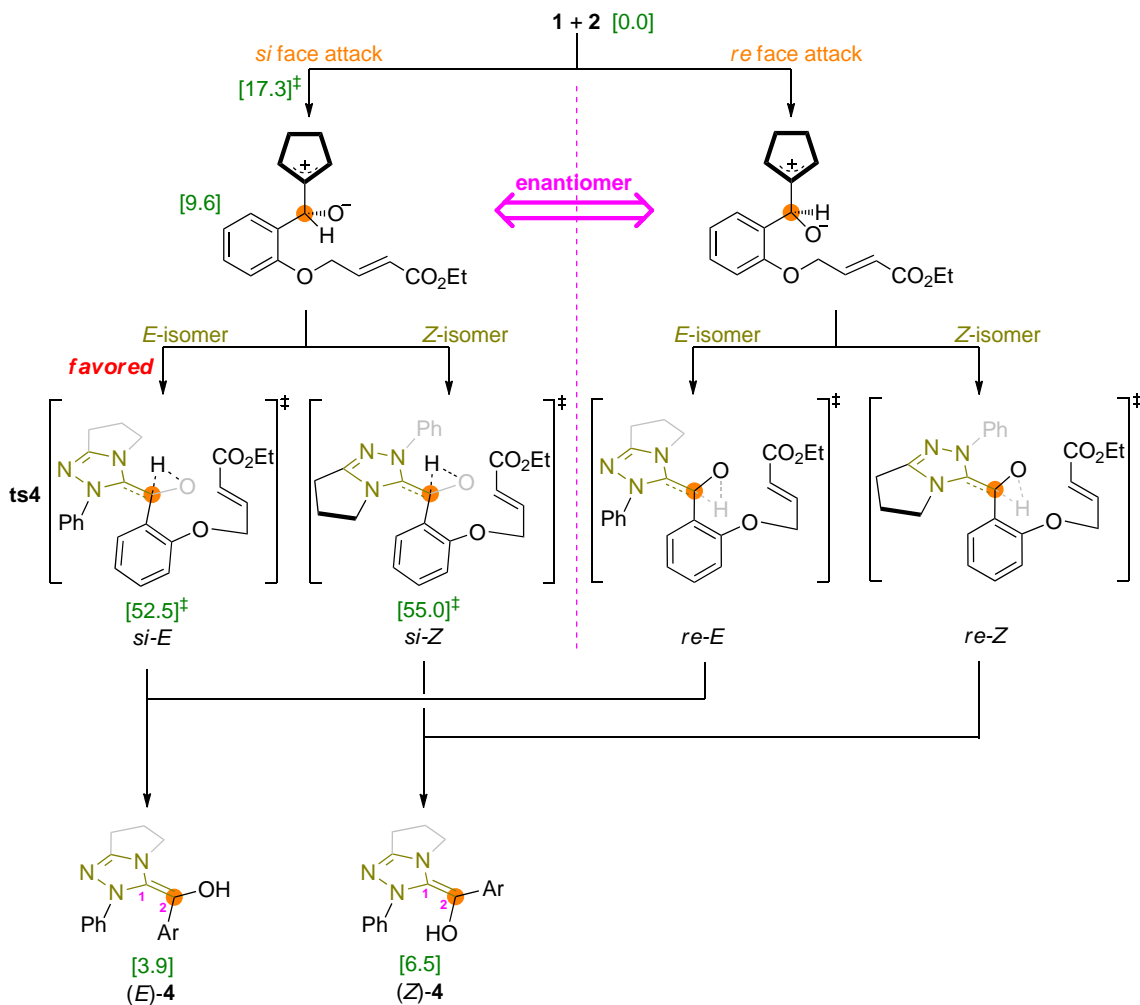


3.2 Intramolecular reactions starting from the PA

The PA undergoes three types of intramolecular reactions including direct [1,2] proton transfer, [1,2] hydride transfer, and the oxa-Michael reaction. Possible stereochemical configurations are examined for the three pathways.

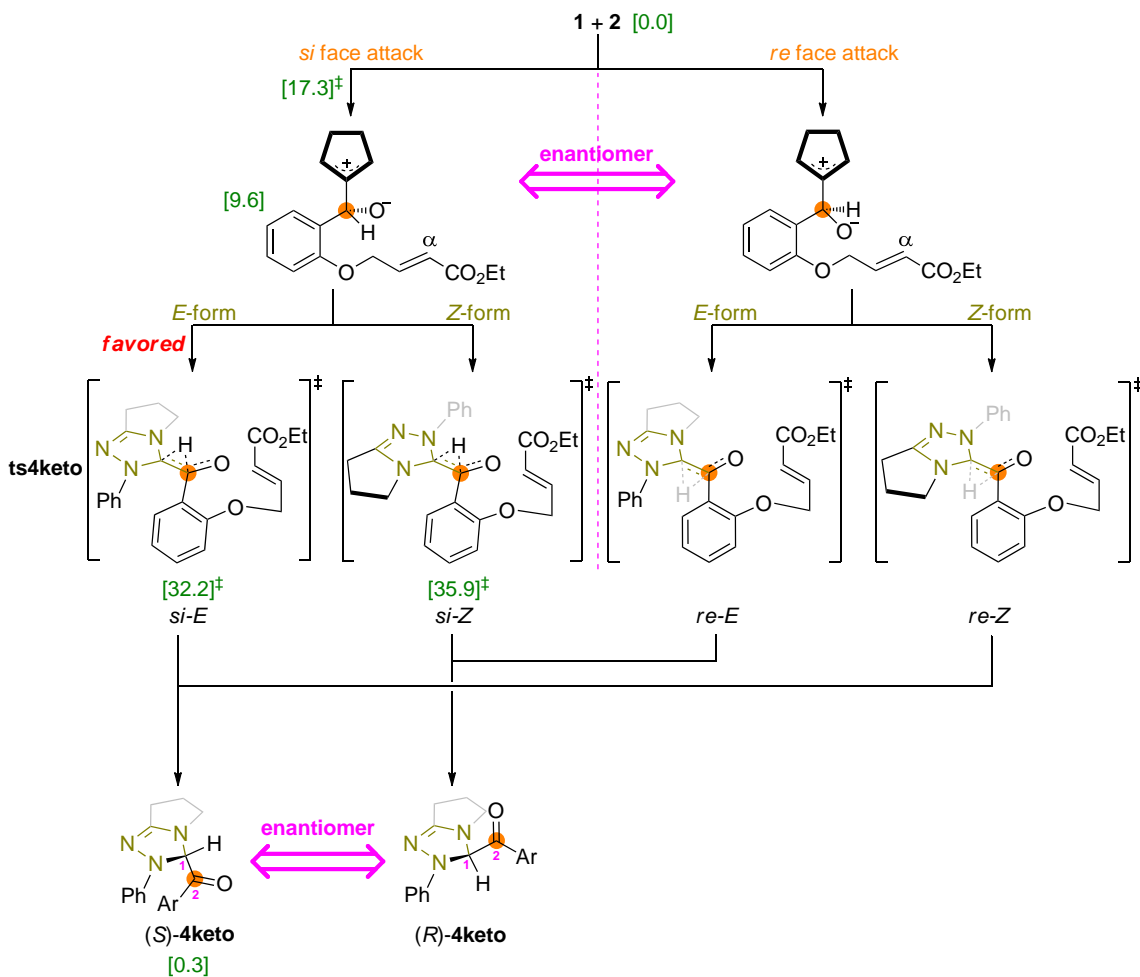
3.2.1 Direct [1,2] proton transfer

Scheme S2: Direct [1,2] proton transfer, leading to the (*E*)- or (*Z*)-configured BI with respect to the C1=C2 double bond. The reported activation energies (in kcal mol⁻¹) are relative to the reference energy of separated reactants, **1** + **2**.



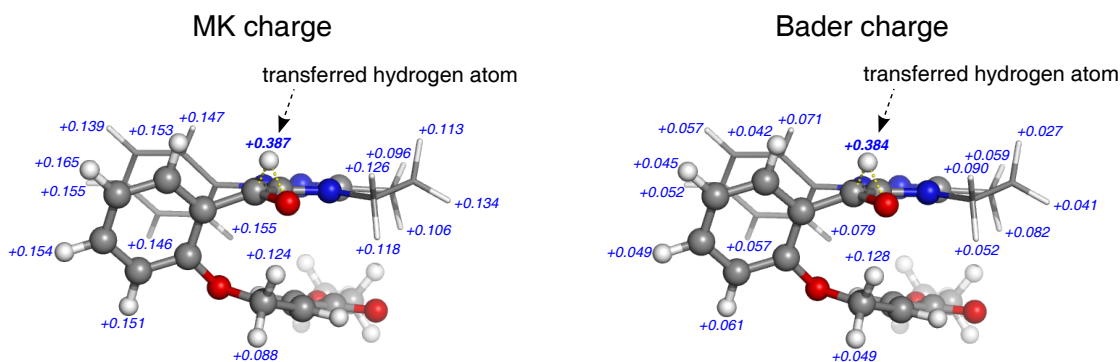
3.2.2 Direct [1,2] hydride transfer

Scheme S3: Direct [1,2] hydride transfer, leading to the ketone species with the (*R*)- or (*S*)-configuration at the C1 atom. The reported activation energies (in kcal mol⁻¹) are relative to the reference energy of separated reactants, **1** + **2**.



The Merz-Kollman (MK) and the Bader charges are computed to characterize the types of transferred hydrogen atoms. According to the MK and Bader charge analyses of **ts4**, the transferred hydrogen atom displays a positive charge of ca. +0.38e (Figure S3a), which suggests that the process **3** \rightarrow **4** proceeds through a proton transfer. In **ts4keto**, the transferred hydrogen atom displays a MK charge of $-0.005e$ while the charges of other hydrogen atoms range between and +0.070e and +0.206e (Figure S3b). The Bader charge analysis yields a charge of $-0.024e$ at the transferred hydrogen atom, compared to charges of +0.018 to +0.086e at other hydrogen atoms. Therefore, the process **3** \rightarrow **4keto** is described as a hydride transfer.

a) **ts4**



b) **ts4keto**

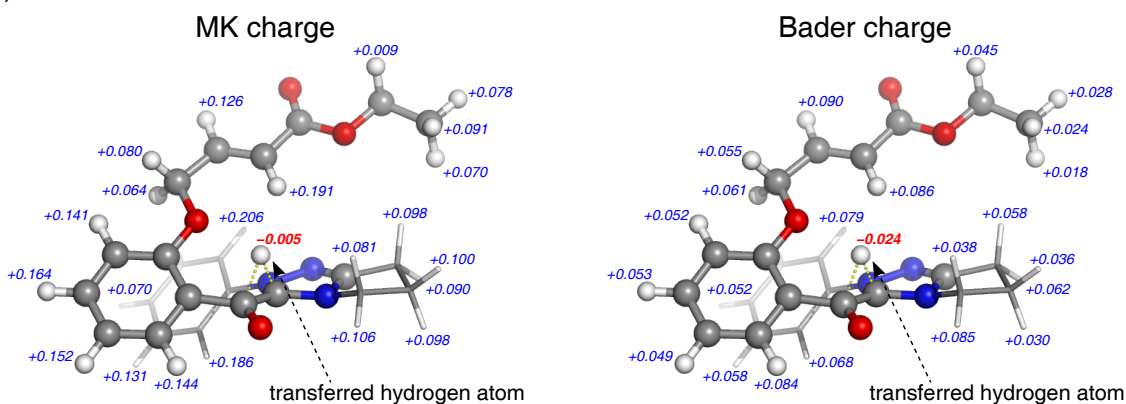


Figure S3: Charge analyses (in e) of **ts4** and **ts4keto**.

3.2.3 Oxa-Michael reaction

Unlike concerted [1,2] proton transfer and [1,2] hydride transfer, the oxa-Michael reaction proceeds in a stepwise mechanism via oxa-conjugate addition and subsequent proton transfer. The stereochemical configurations involved in the oxa-Michael reaction are designated according to the order of the reaction events, illustrated in Scheme S4. In principle, the proton transfer involves 32 possible stereoisomeric TSs (2^5), and half of isomers are excluded because of the structural restriction imposed by the seven-membered ring generated from the oxa-conjugate addition.

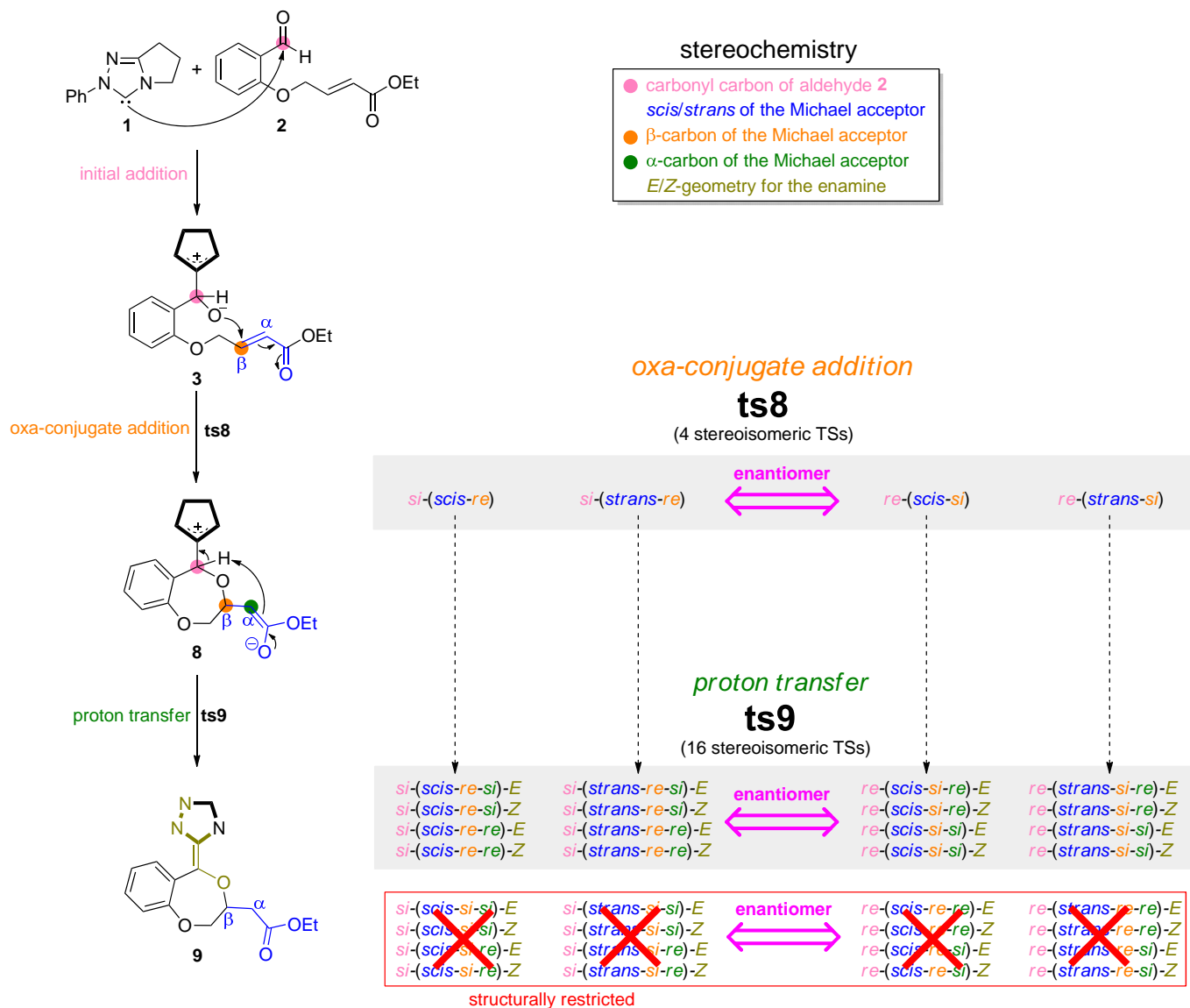
i) oxa-conjugate addition

Figure S4 depicts four stereoisomeric TSs for the oxa-conjugate addition, where two pairs of isomers are in an enantiomeric relationship. The enolate structures generated via the four TSs can undergo the proton transfer, leading to the enol ether intermediates.

ii) proton transfer

In Figure S6, 16 stereochemical configurations are divided into *syn* and *anti* addition: the *syn* mode is the addition of two substituents to the same side of the $C_\alpha=C_\beta$ alkene, and vice versa. The proton transfer features a broader range of barriers from 22.6 to 33.7 kcal mol⁻¹. The stereochemical mode of *si-(scis-re-si)-E* is the most energetically favored. The *syn* addition (ΔG^\ddagger : 22.6–28.7 kcal mol⁻¹) is preferred to the *anti* addition (ΔG^\ddagger : 30.1–33.7 kcal mol⁻¹).

Scheme S4: Stereochemistry of the oxa-Michael reaction (**3** → **8** → **9**). The stereoisomeric TSs with respect to the oxa-conjugate addition (**ts8**) are designated by the sequence composed by three symbols, such as *si*-(*scis*-*re*). The sequence composed by five symbols such as *si*-(*scis*-*re*-*si*)-*E* is used to characterize the stereoisomeric TSs with respect to the proton transfer (**ts9**).



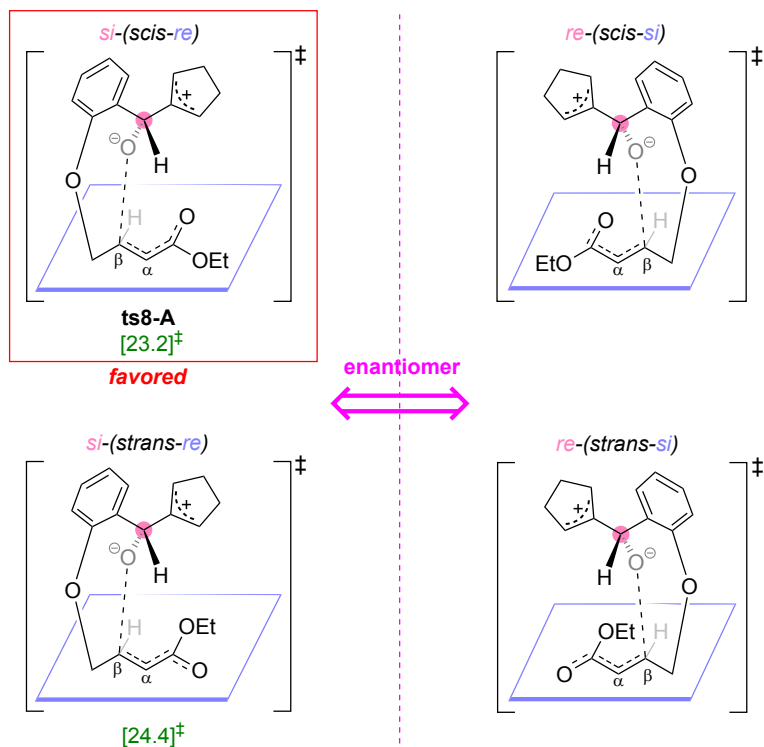


Figure S4: Four stereoisomeric TSs involved in the oxa-conjugate addition (**ts8**). The reported activation energies are relative to the reference energy of separated reactants, **1** + **2**.

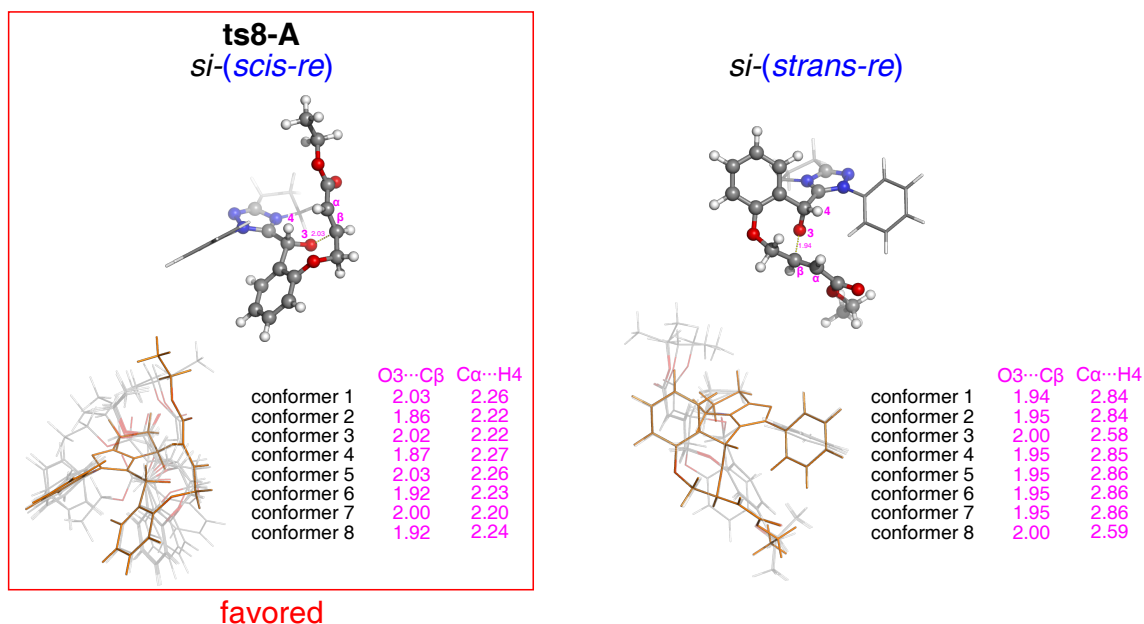


Figure S5: Optimized TS structures of **ts8** in terms of stereochemistry of *si*-(*scis-re*) and *si*-(*strans-re*). The most stable conformer is shown by the ball-and-stick representation, and eight low-energy conformers are aligned with respect to the five-membered NHC ring. Bond lengths are given in Å.

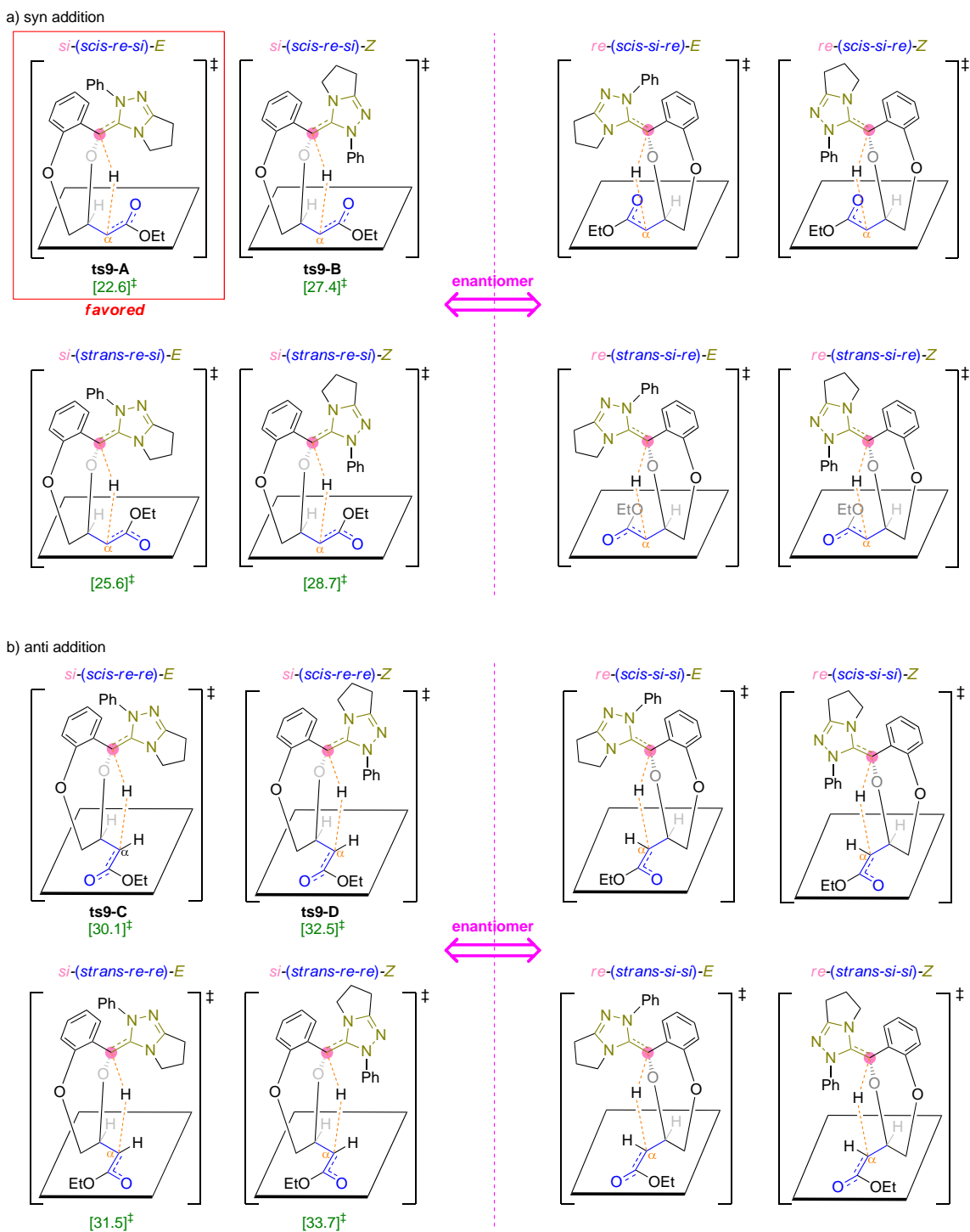


Figure S6: 16 stereoisomeric TSs involved in the proton transfer (**ts9**). The proton transfer of the oxa-Michael reaction can proceed in (a) syn, and (b) anti modes. The reported activation energies are relative to the reference energy of separated reactants, **1** + **2**.

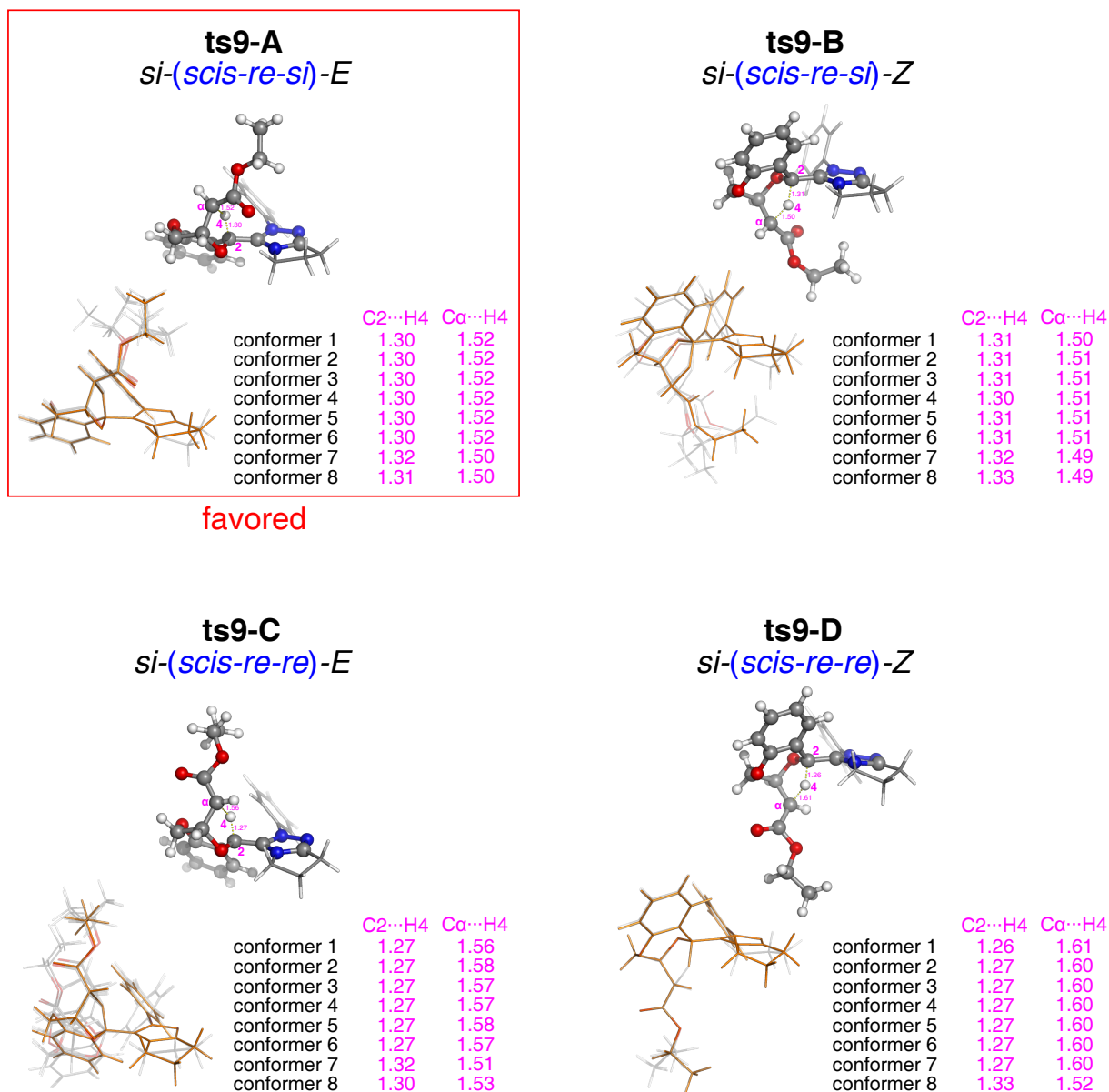


Figure S7: Optimized TS structures of **ts9** in terms of stereochemistry of *si-(scis-re-si)-E*, *si-(scis-re-si)-Z*, *si-(scis-re-re)-E*, and *si-(scis-re-re)-Z*. The most stable conformer is shown by the ball-and-stick representation, and eight low-energy conformers are aligned with respect to the five-membered NHC ring. Bond lengths are given in Å.

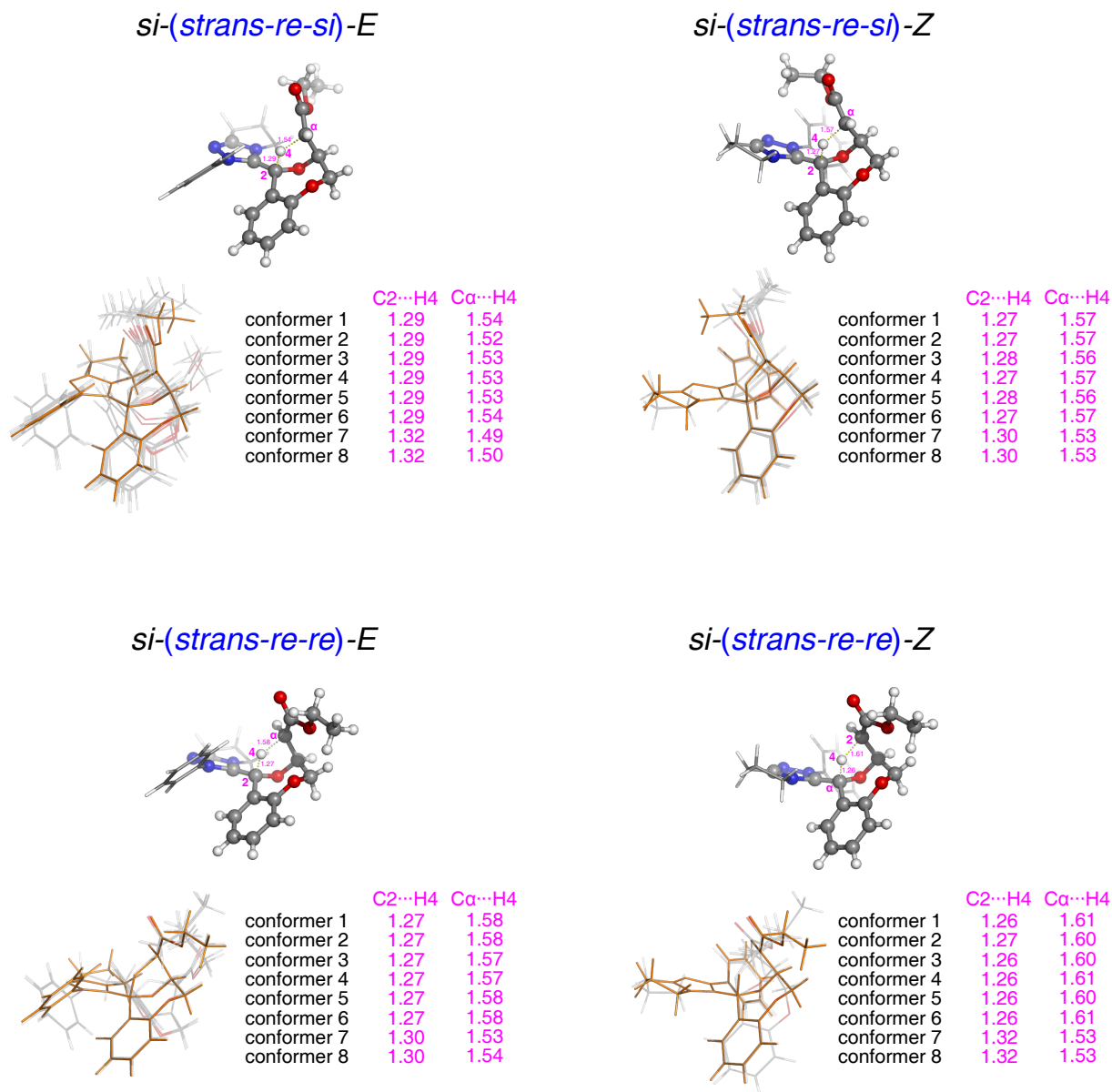


Figure S8: Optimized TS structures of **ts9** in terms of stereochemistry of *si-(strans-re-si)-E*, *si-(strans-re-si)-Z*, *si-(strans-re-re)-E*, and *si-(strans-re-re)-Z*. The most stable conformer is shown by the ball-and-stick representation, and eight low-energy conformers are aligned with respect to the five-membered NHC ring. Bond lengths are given in Å.

iii) enol ether

The oxa-Michael reaction can produce four stereoisomers of enol ether **9** (Figure S9), which differ in the stereogenic center of the β -carbon as well as the olefin geometry of the enamine.

The *E*-isomer is slightly more stable than the *Z*-isomer by 0.5 kcal mol⁻¹.

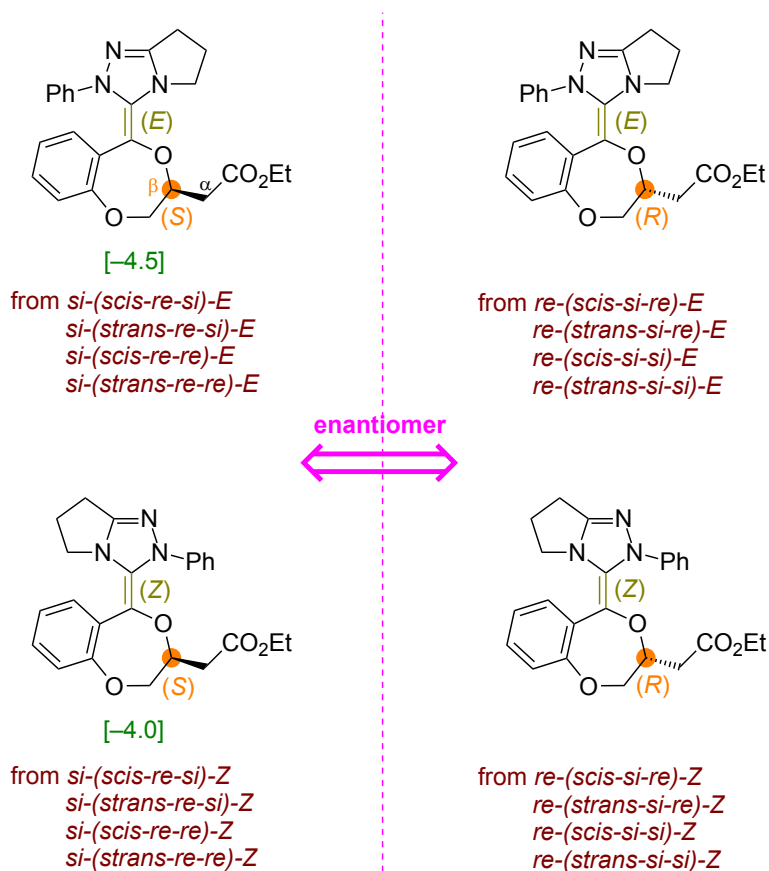


Figure S9: Four stereoisomers of enol ether **9**. The reported energies are relative to the reference energy of separated reactants, **1** + **2**.

Summary of energy profiles

The energy profiles for the oxa-Michael reaction are summarized in Figure S10, where the most energetically favored route is shown by the green dashed line. Along the lowest energy pathway, the activation barriers for initial addition, oxa-conjugate addition and proton transfer are 17.3, 23.2 and 22.6 kcal mol⁻¹, respectively.

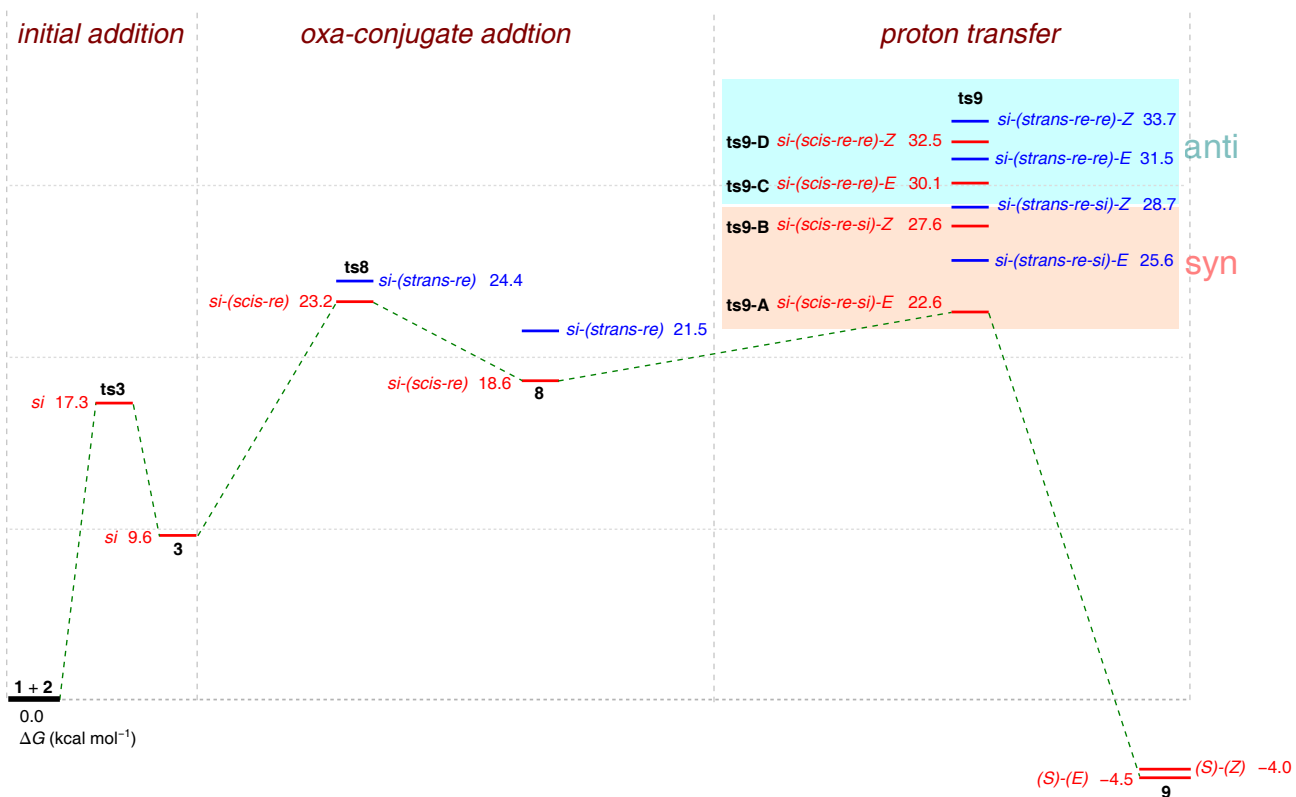
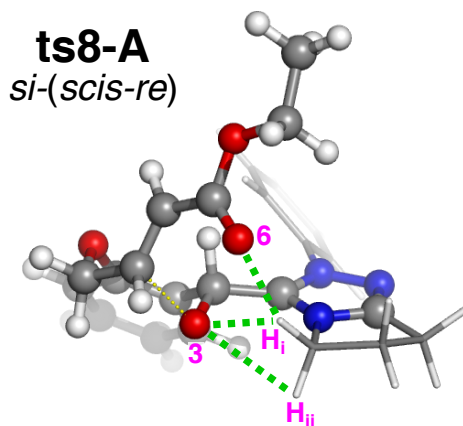


Figure S10: Free energy profiles (in kcal mol^{-1}) for the formation of enol ether **9**. The oxa-Michael reactions with respect to the *scis*- and *strans*-enones are shown in red and blue, respectively.

a)



$\Delta\Delta G$		O6...H _i	O3...H _i	O3...H _{ii}
0.0	conformer 1	2.29	2.49	2.82
0.3	conformer 2	5.16	2.46	3.54
0.3	conformer 3	2.26	2.51	2.80
0.5	conformer 4	4.86	2.71	2.88
0.7	conformer 5	2.30	2.49	2.81
0.7	conformer 6	4.63	2.42	3.27
0.9	conformer 7	2.24	2.83	2.46
0.9	conformer 8	4.75	2.43	3.30

b)

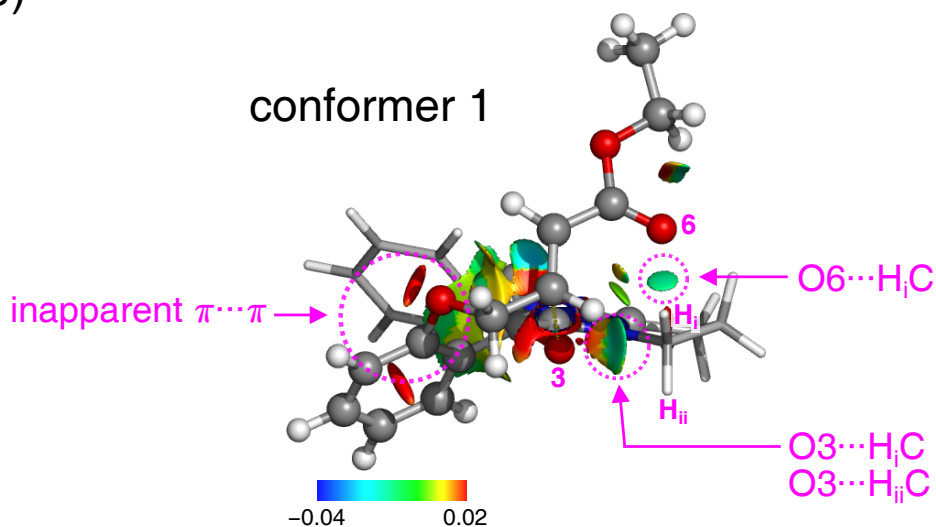
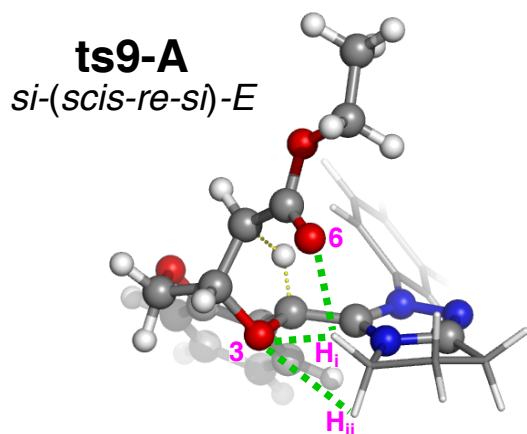


Figure S11: (a) Structural analysis of **ts8-A**. Relative free energies and distances are given in kcal mol⁻¹ and Å, respectively. For the low energy conformers, the O...HC distances smaller than 2.60 Å are marked in orange. (b) NCI analysis of the lowest energy conformer. The NCI surface corresponds to $s = 0.5$ au and the NCI color scale ranges from 0.04 to 0.02 au.

a)



$\Delta\Delta G$		O6...H _i	O3...H _i	O3...H _{ii}
0.0	conformer 1	2.17	2.51	2.98
0.0	conformer 2	2.19	2.51	2.96
0.1	conformer 3	2.15	2.85	2.55
0.3	conformer 4	2.15	2.85	2.55
0.7	conformer 5	2.14	2.84	2.55
0.7	conformer 6	2.17	2.51	2.97
3.2	conformer 7	2.12	2.51	2.99
3.5	conformer 8	2.10	2.86	2.55

b)

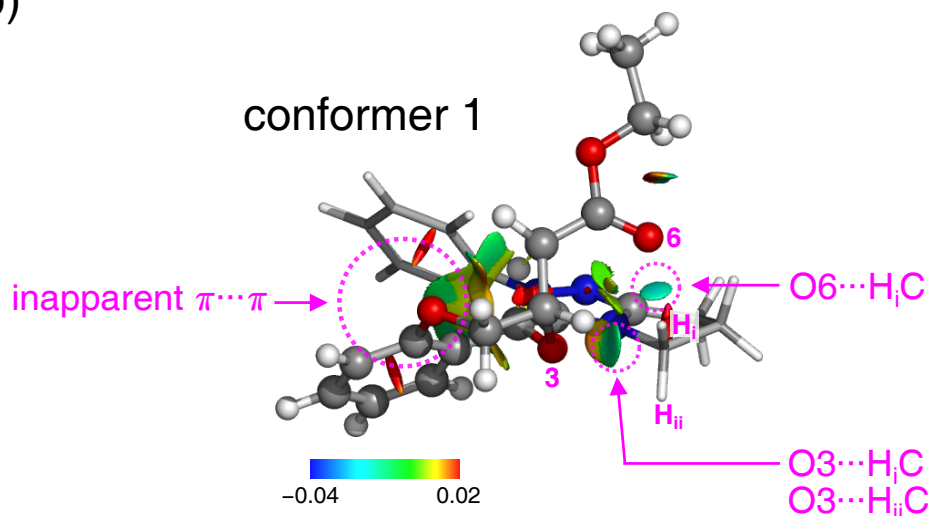


Figure S12: (a) Structural analysis of **ts9-A**. Relative free energies and distances are given in kcal mol⁻¹ and Å, respectively. For the low energy conformers, the O...HC distances smaller than 2.60 Å are marked in orange. (b) NCI analysis of the lowest energy conformer. The NCI surface corresponds to $s = 0.5$ au and the NCI color scale ranges from 0.04 to 0.02 au.

3.2.4 Proton transfer with a chiral carbene

Figure S13 shows possible stereoisomeric TSs of the proton transfer using a chiral carbene. The stereochemical configuration of *si*-(*scis-re-si*)-*E* is still the most energetically favored. Except for the moiety of the Bn group, the lowest energy TS with the chiral carbene is conformationally similar to that with the achiral carbene (Figures S12 and S14).

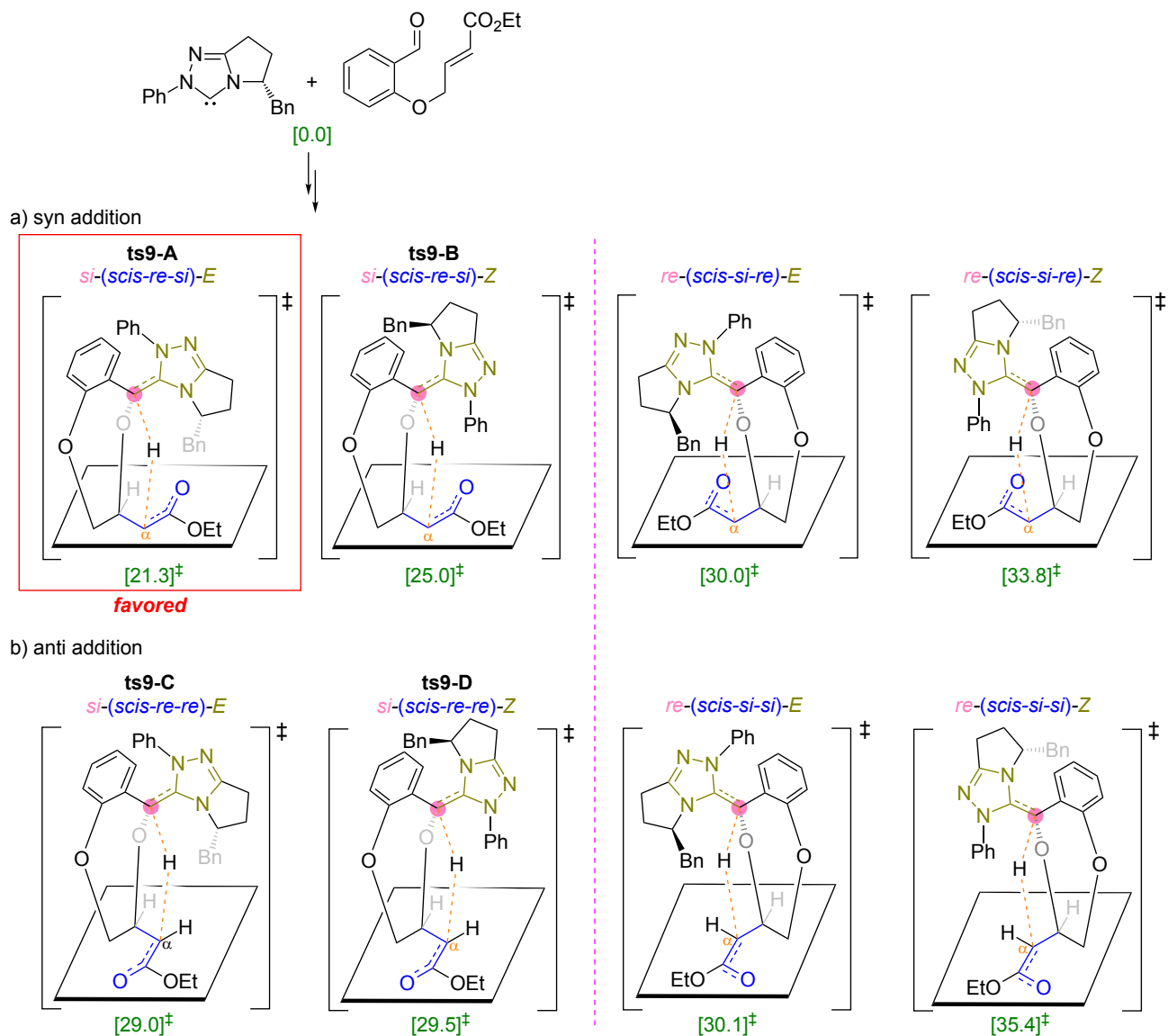
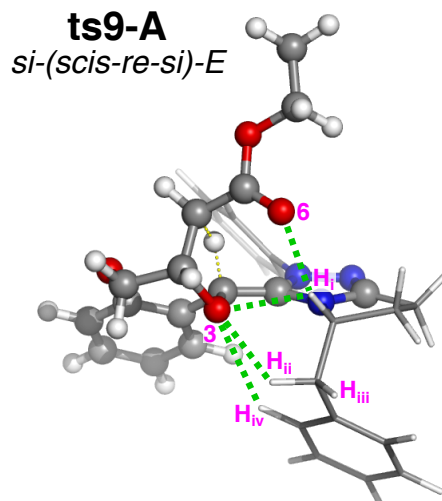


Figure S13: Stereoisomeric TSs with respect to the proton transfer using a chiral carbene. The reported activation energies (in kcal mol⁻¹) are relative to the reference energy of separated reactants.

a)



$\Delta\Delta G$		O6 \cdots H _i	O3 \cdots H _i	O3 \cdots H _{ii}	O3 \cdots H _{iii}	O3 \cdots H _{iv}
0.0	conformer 1	2.20	2.57	2.34	3.85	3.16
0.5	conformer 2	2.20	2.58	2.33	3.86	3.14
0.7	conformer 3	2.21	2.58	2.33	3.86	3.13
0.9	conformer 4	2.19	2.50	3.98	2.46	3.03
1.2	conformer 5	2.22	2.50	3.97	2.45	2.99
1.3	conformer 6	2.19	2.50	3.97	2.46	3.03
2.4	conformer 7	2.35	2.43	4.15	4.27	3.46
2.6	conformer 8	2.30	2.44	4.16	4.29	3.46

b)

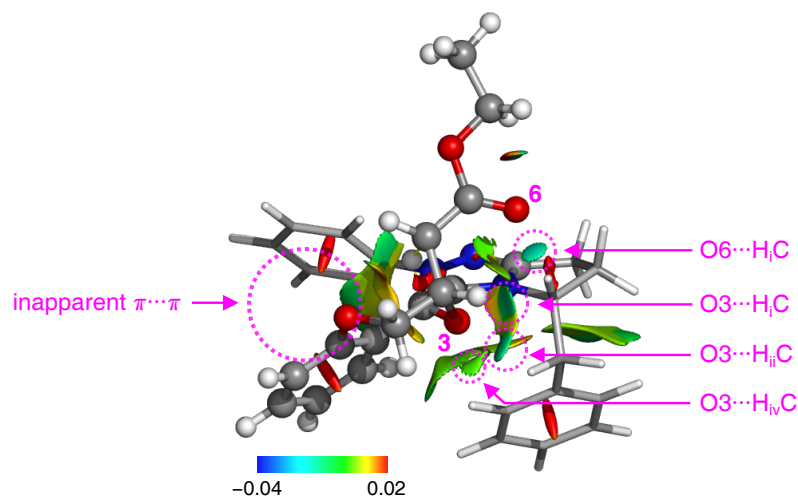
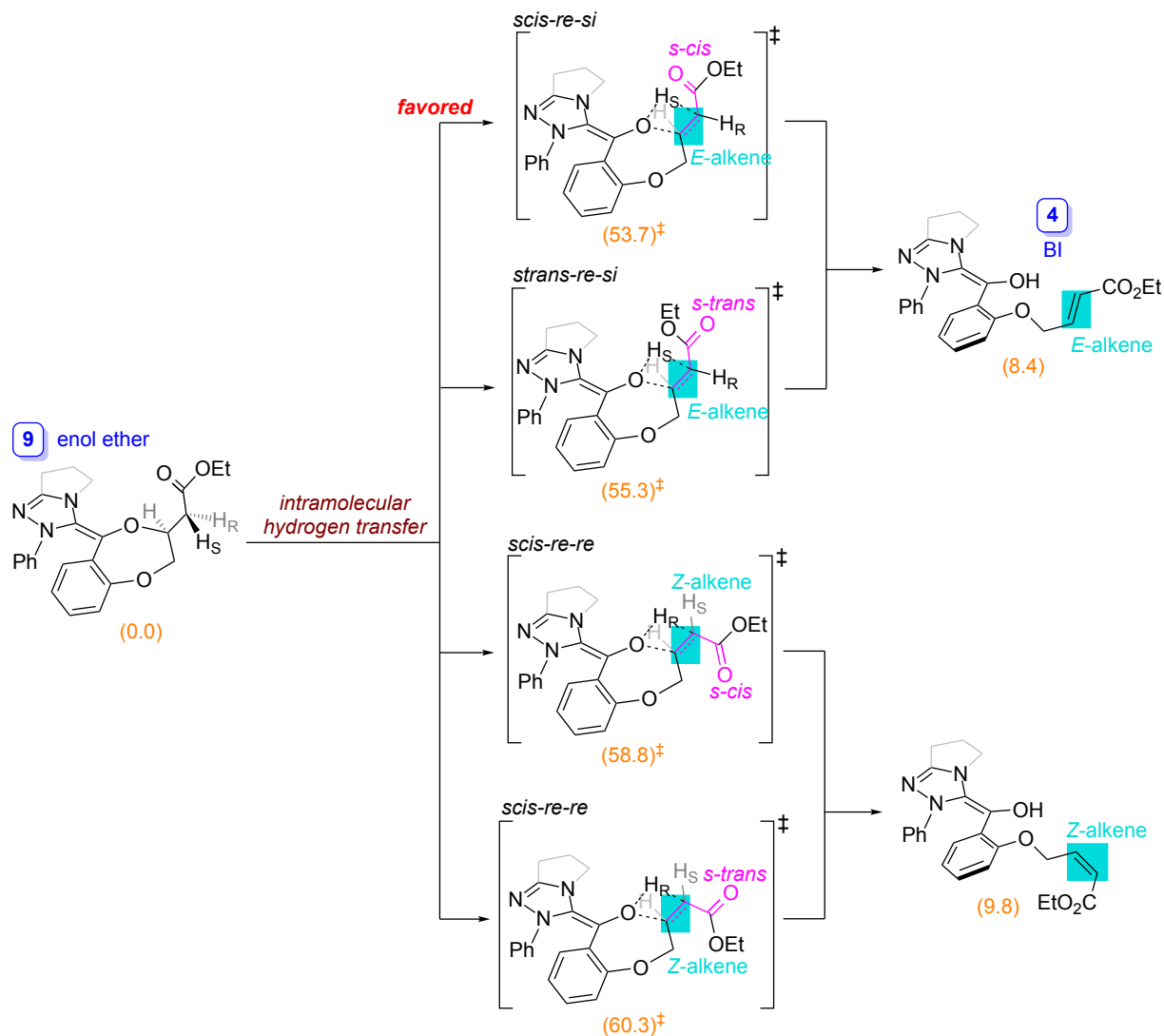


Figure S14: (a) Structural analysis of **ts9-A** with a chiral carbene. Relative free energies and distances are given in kcal mol⁻¹ and Å, respectively. For the low energy conformers, the O \cdots HC distances smaller than 2.60 Å are marked in orange. (b) NCI analysis of the lowest energy conformer. The NCI surface corresponds to $s = 0.5$ au and the NCI color scale ranges from 0.04 to 0.02 au.

3.3 Formation of the BI

3.3.1 Intramolecular mechanism

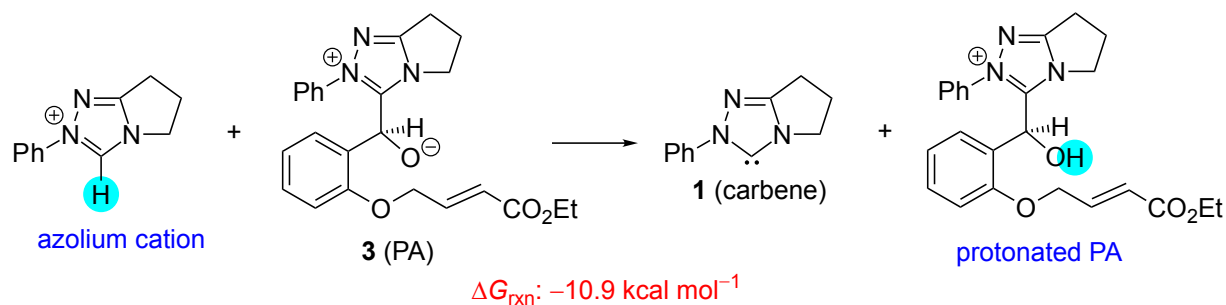
Scheme S5: Intramolecular hydrogen transfer. Four possible stereoisomeric TSs are involved in the intramolecular hydrogen transfer, while the (*E*)- or the (*Z*)-configured Michael acceptor are generated. The reported activation energies (in kcal mol⁻¹), shown in orange, are relative to the reference energy of enol ether **9**.



3.3.2 Intermolecular mechanism

Catalyst **1** and the PA **3** can accept a proton through the carbene and the oxyanion, respectively. In order to compare their basicity, the relative stability of their protonated states is examined by computing the reaction energy shown in Scheme S6, in which the proton is transferred from the triazolium precatalyst to the PA. The computed reaction energy of $-10.9 \text{ kcal mol}^{-1}$ indicates that the PA is more basic than the carbene.

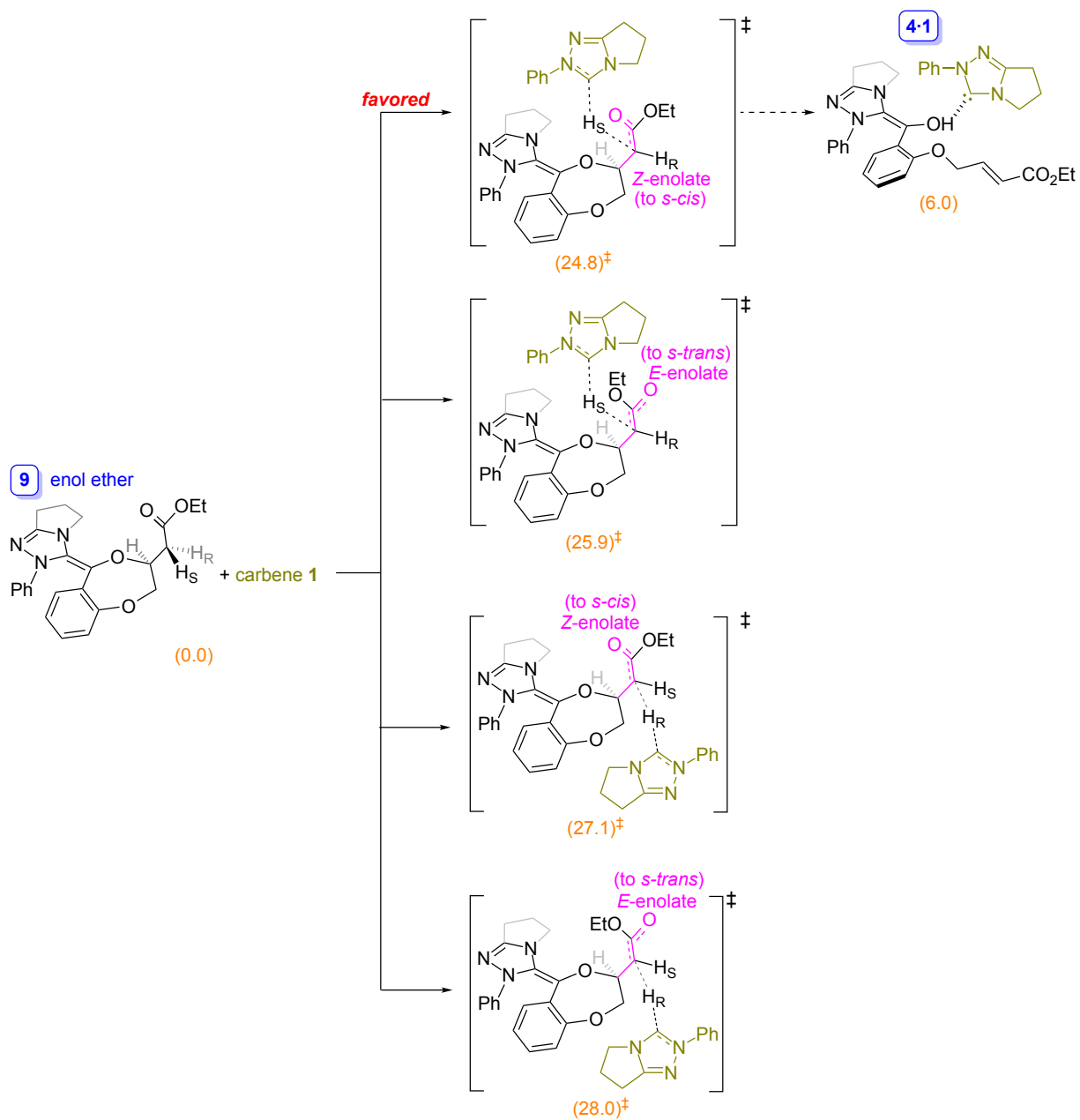
Scheme S6: Comparison of the basicity between carbene **1** and the PA **3**.



i) deprotonation by the carbene

The carbene is first used as the base to capture the α -proton of **9**. Scheme S7 shows four possible stereoisomeric TSs that differ in the prochiral α -proton and the conformation of the (*Z*)/(*E*)-enolate (related to the *s-cis*/*s-trans* conformations of the α,β -unsaturated ester). Calculations show that the proton abstraction requires an activation energy of at least $24.8 \text{ kcal mol}^{-1}$, which is higher than the barrier to the oxa-Michael reaction (23.2 and $22.6 \text{ kcal mol}^{-1}$).

Scheme S7: Deprotonation of enol ether **9** by carbene **1**. After the C–O bond cleavage, (*Z*)- and (*E*)-enolates lead to *s-cis* and *s-trans* enones, respectively. The free energies shown in orange (in kcal mol⁻¹) are relative to the reference energy of **9** + **1**.



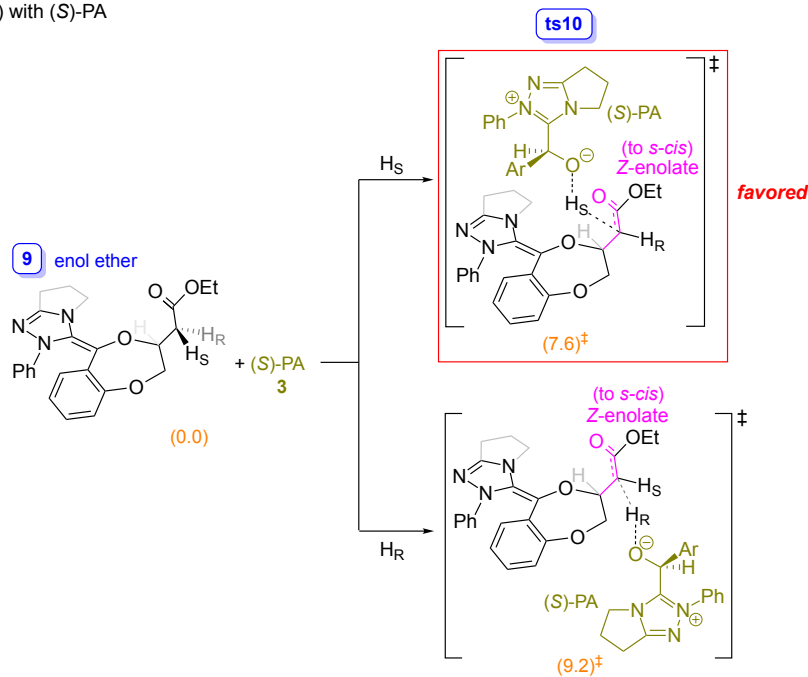
ii) PA-assisted process

In addition to the carbene, the two stereoisomers of (*S*)-PA and (*R*)-PA are also employed as the bases. Scheme S8 illustrates four possible stereoisomeric TSs for the α -deprotonation, which differ in the (*S*)-PA and (*R*)-PA isomers, as well as the prochiral α -proton of H_S and H_R. The lowest barrier to the proton abstraction is calculated to be 7.6 kcal mol⁻¹.

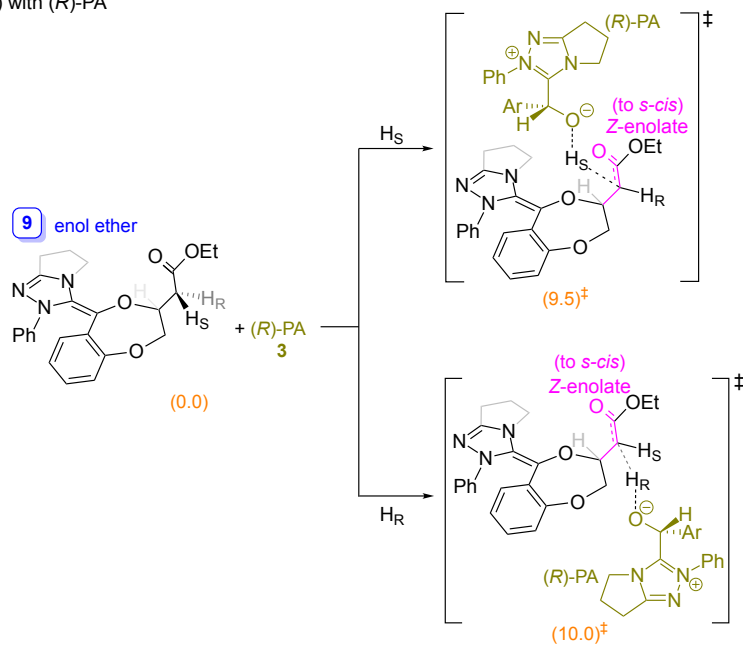
Figure S15 shows eight stereoisomeric TSs with respect to the C–O _{β} bond cleavage, which differ in the PA isomers, the olefin geometry of the Michael acceptor, and its *s-cis* and *s-trans* configurations. Regardless of the stereochemical configurations of the PA, the TS leading to the (*E*)-Michael acceptor is found to be always favored over the competing TS leading to the (*Z*)-Michael acceptor. The lowest energy TS involves the participation of the (*S*)-PA, which is slightly favored by 0.6 kcal mol⁻¹ over the involvement of the (*R*)-PA. Figure S17 summarizes the computed energy profiles for the retro oxa-Michael reaction, where the most energetically preferred pathway is shown by the green line. The barrier for the C–O _{β} bond breaking step ($\Delta G_{\text{ts11}}^\ddagger$: 10.3 kcal mol⁻¹) is higher than that for the deprotonation step ($\Delta G_{\text{ts10}}^\ddagger$: 7.6 kcal mol⁻¹), and the C–O _{β} bond cleavage is thus rate-determining in the base-assisted reaction.

Scheme S8: Deprotonation of enol ether **9** (a) by the (*S*)-PA and (b) by the (*R*)-PA. After the C–O bond cleavage, (*Z*)- and (*E*)-enolates lead to *s-cis* and *s-trans* enones, respectively. The free energies shown in orange (in kcal mol⁻¹) are relative to the reference energy of **9** + **3**.

a) with (*S*)-PA



b) with (*R*)-PA



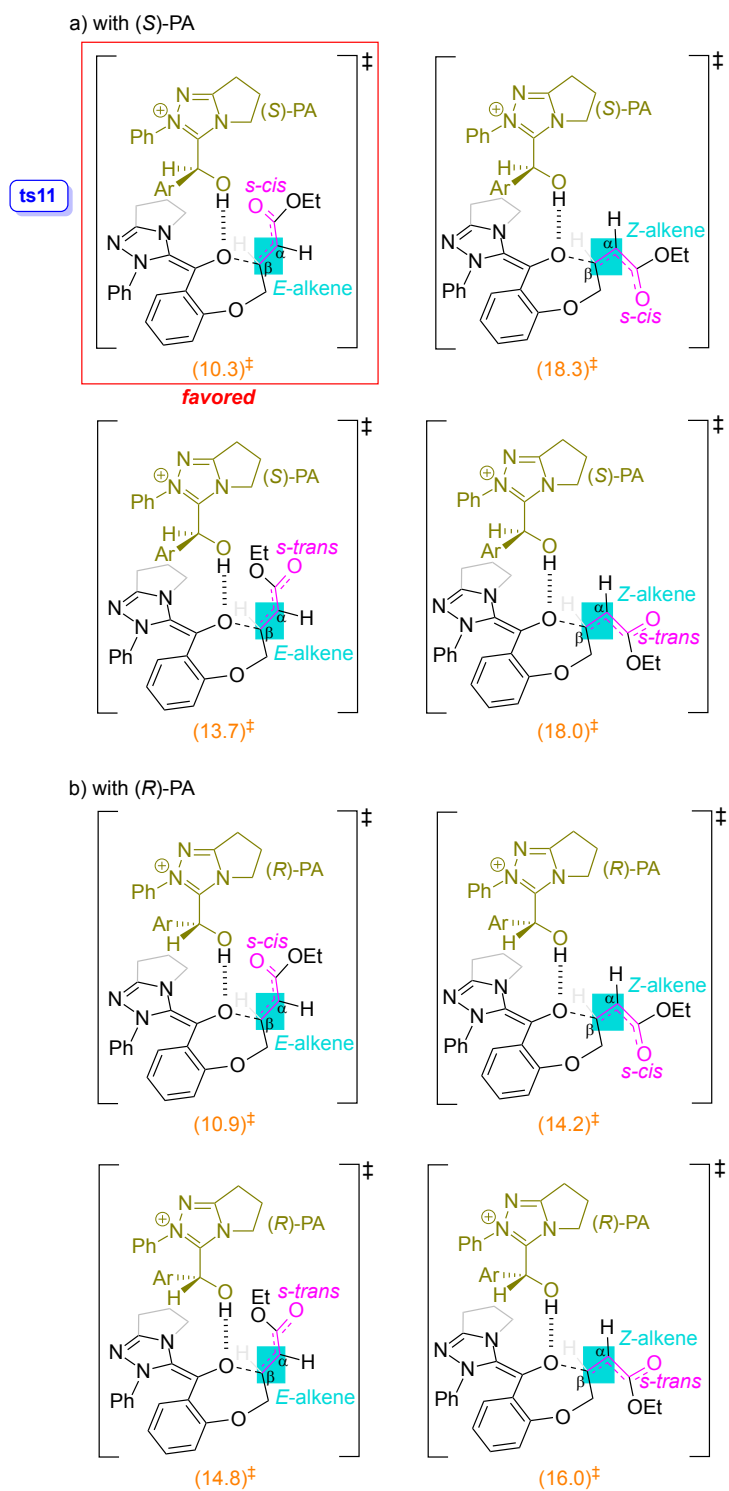
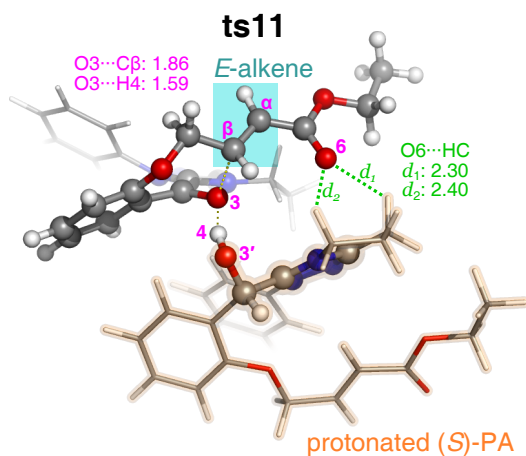


Figure S15: Eight stereoisomeric TSs with respect to the C–O_β bond cleavage. The (*R*)-PA and the (*S*)-PA are used as the bases. The free energies shown in orange (in kcal mol⁻¹) are relative to the reference energy of **9** + **3**.

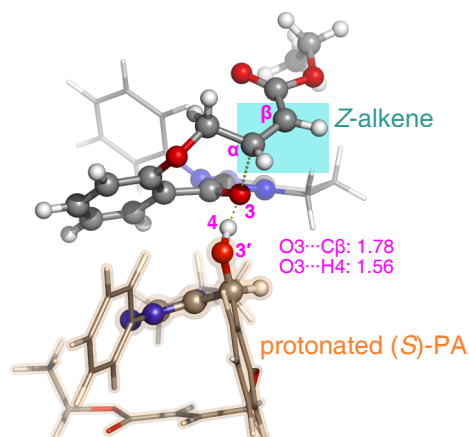
a) with (*S*)-PA



favored

(to the *E*-configured Michael acceptor)

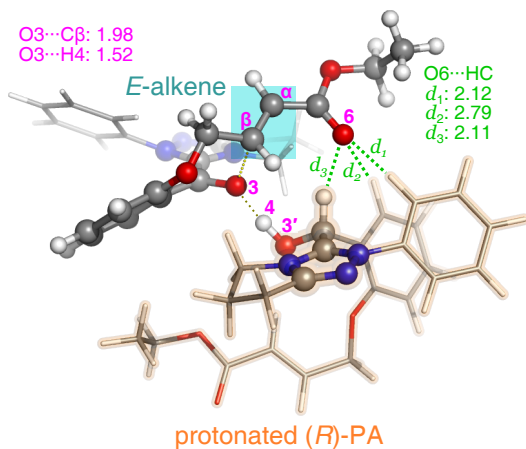
VS



disfavored

(to the *Z*-configured Michael acceptor)

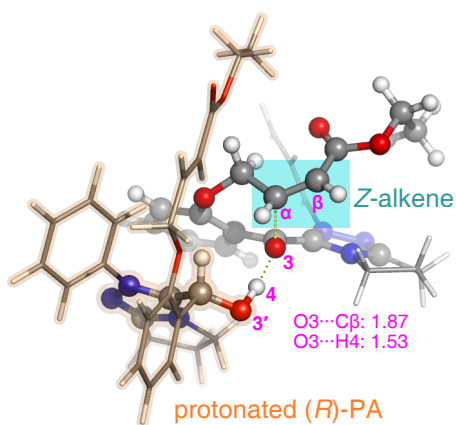
b) with (*R*)-PA



favored

(to the *E*-configured Michael acceptor)

VS



disfavored

(to the *Z*-configured Michael acceptor)

Figure S16: Lowest-energy conformers of the stereoisomeric TSs with respect to C–O bond cleavage. The (*R*)/(*S*)-PA moiety is highlighted in orange. The *E*/*Z*-geometry of the Michael acceptor is shown in cyan. Distances are given in Å.

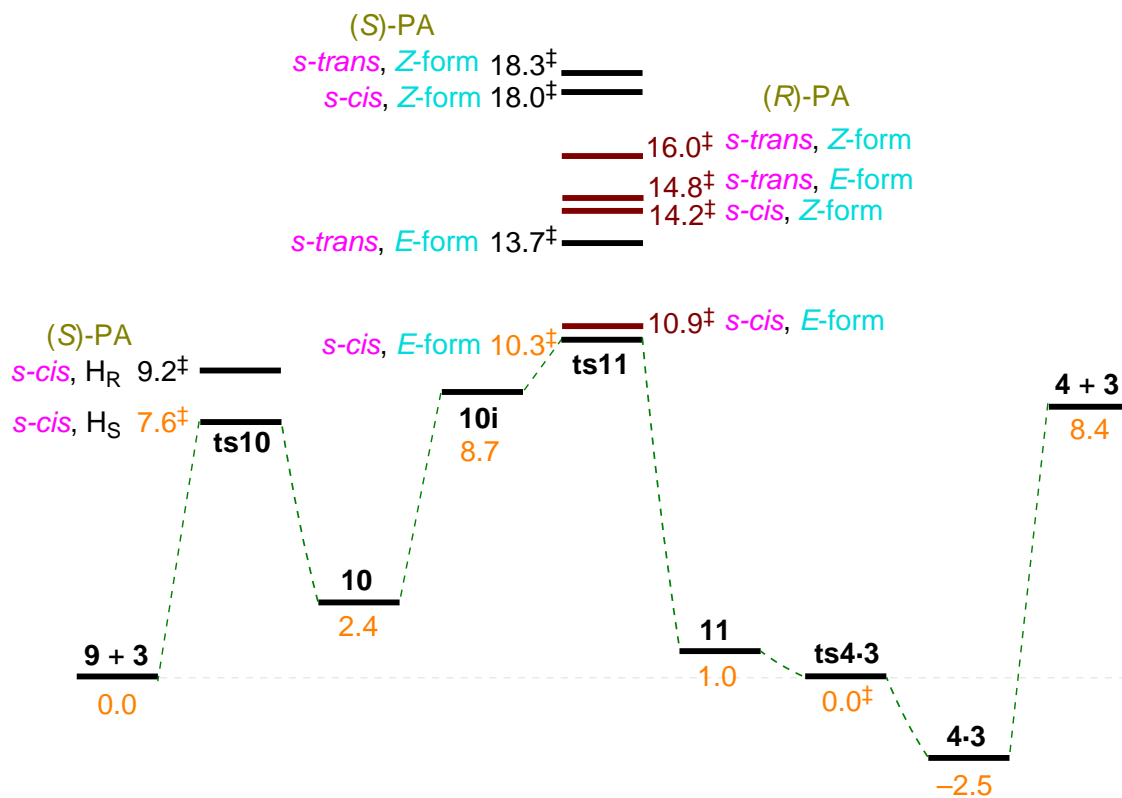
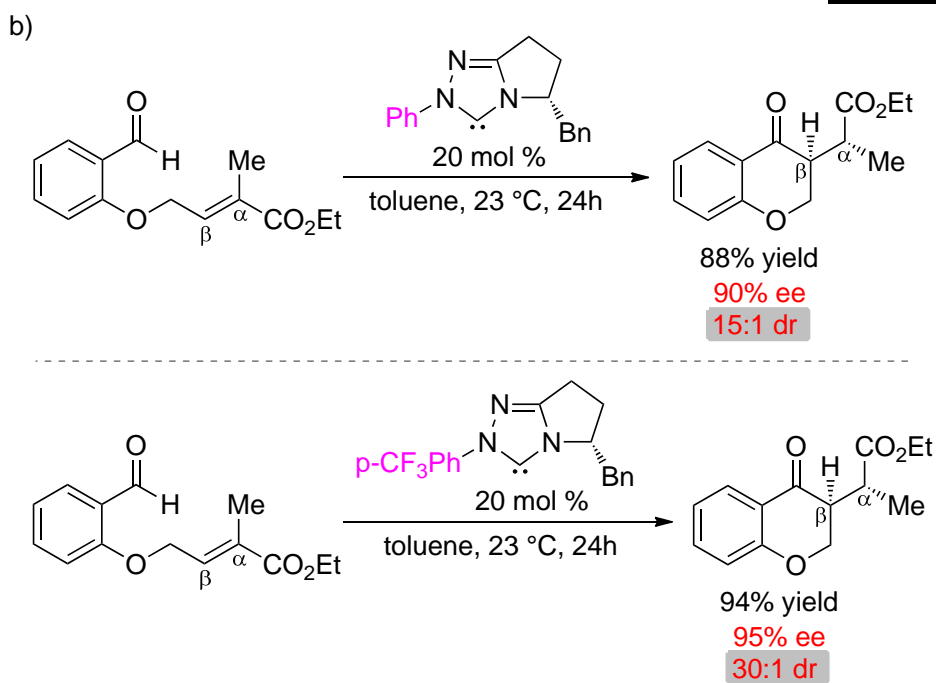
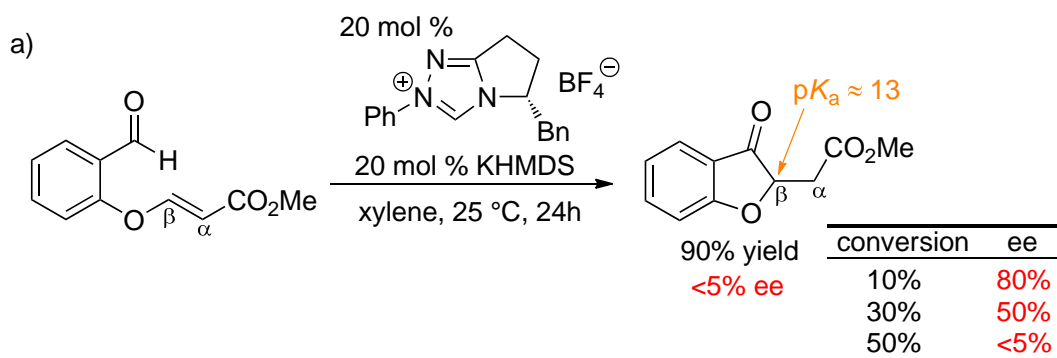


Figure S17: Computed energy profile (in kcal mol⁻¹) for the BI formation assisted by the PA. The symbols shown in cyan indicate the olefin geometry of the Michael acceptor to be re-generated. For consistency, the (*Z*)/(*E*)-configurations of the enolates in **ts10**, **10**, and **10i** (shown in magenta) are represented by the corresponding *s-cis*/*s-trans* of the enones. The reported free energies are relative to the reference energy of **9 + 3**.

iii) observed product epimerization

Scheme S9a shows formation of a benzofuran product catalyzed by a chiral triazolium pre-catalyst in the presence of KHMDS.⁵ Product epimerization involves deprotonation/protonation at the β -position ($pK_a \approx 13$). According to chiral HPLC analysis, the Stetter product was formed in 80% ee at 10% conversion. As the reaction progressed, the benzofuran underwent severe epimerization, with rapid erosion to 50% ee at 30% conversion. The epimerization may also be caused by a phenoxide elimination/oxa-conjugate addition sequence, triggered by the deprotonation at the α -position. In enantio- and diastereoselective intramolecular Stetter reactions, the use of the carbene, instead of its triazolium salt, was found to efficiently avoid product epimerization.⁶ When the α -methyl α, β -unsaturated ethyl ester was employed as the substrate, the Stetter product was generated in 90% ee and 15:1 dr (Scheme S9b). Diastereoselectivity can be improved by utilizing the more electron-deficient carbene with the *p*-trifluoromethylphenyl group (with 30:1 dr). Therefore, the degree of epimerization is also influenced by the electronic nature of the carbene catalyst.⁶

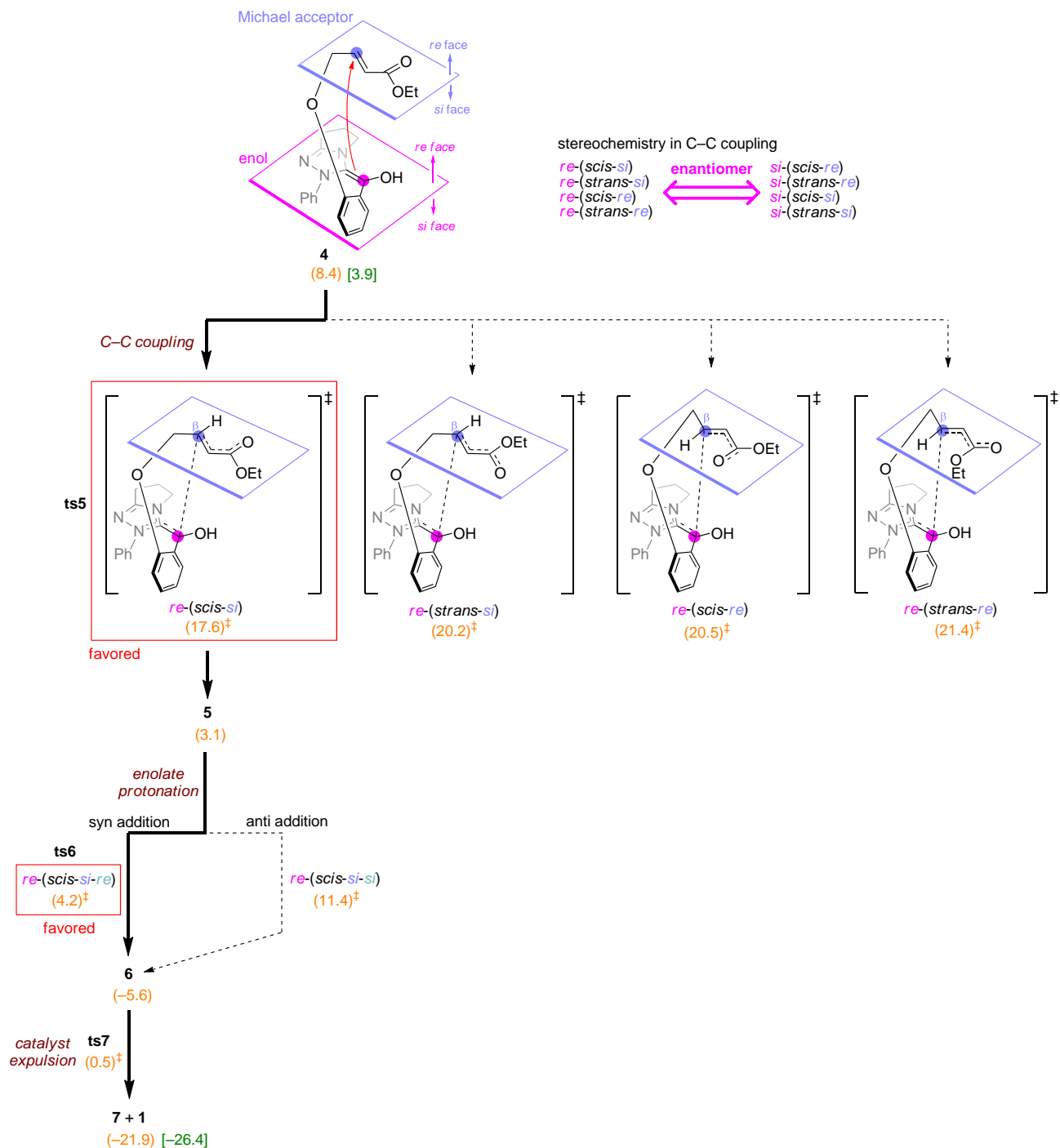
Scheme S9: (a) Epimerization of the benzofuran product.⁵ (b) Erosion of diastereoselectivity.⁶



3.4 C–C Michael reaction

The first step of the C–C Michael reaction is the C–C coupling between the nucleophilic enol and the electrophilic Michael acceptor (**4** \rightarrow **5**). In regard to stereochemical aspects, the C–C coupling can proceed via eight stereoisomeric TSs that differ in the prochiral faces of the enol and the Michael acceptor, as well as the *s-trans* and the *s-cis* configurations of the Michael acceptor. Because of an enantiomeric relationship, only four stereoisomeric TSs are examined, and are referred to as *re*-(*scis-si*), *re*-(*strans-si*), *re*-(*scis-re*) and *re*-(*strans-re*), shown in Scheme S10. Along the most favored route in terms of *re*-(*scis-si*), the resultant enolate (**5**) can undergo stereoselective protonation from either the *re* or the *si* face at the β -carbon atom: the TS with respect to the *re* face is energetically preferred to that with respect to the *si* face, with an 7.2 kcal mol⁻¹ difference in free energy of activation.

Scheme S10: Computed energetics of the C–C Michael reaction (**4** → **5** → **6**) and catalyst expulsion (**6** → **7** + **1**). The free energies shown in orange (in kcal mol⁻¹) are relative to the reference energy of enol ether **9**.



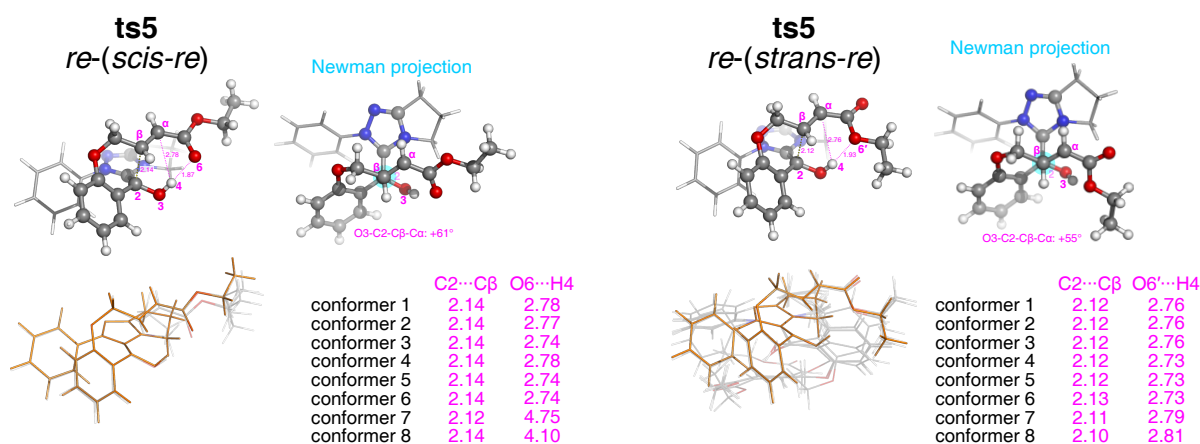
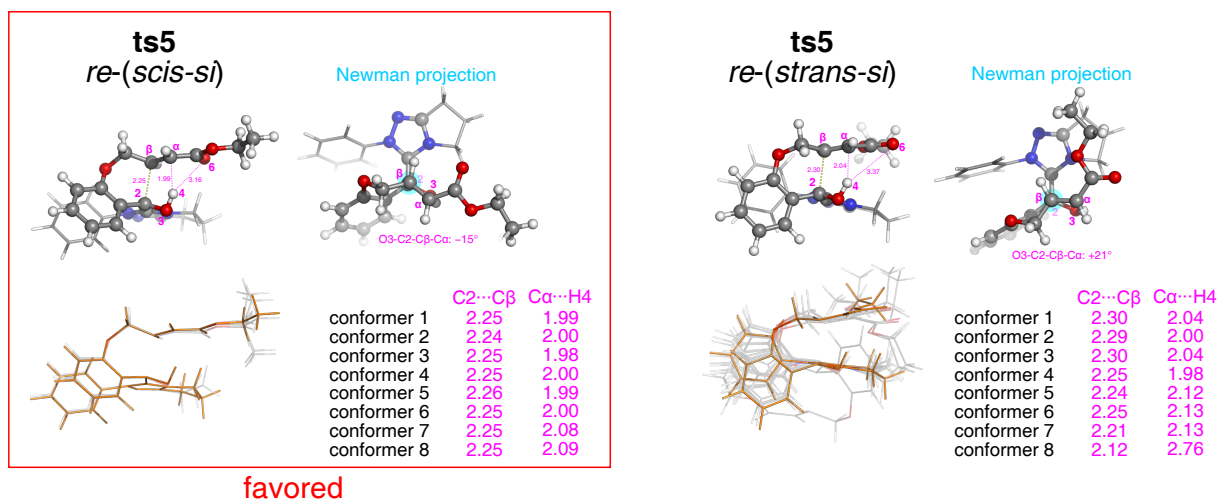


Figure S18: Optimized structures of **ts5** in terms of four stereochemical configurations of *re-(scis-si)*, *re-(strans-si)*, *re-(scis-re)* and *re-(strans-si)*. The Newman projections along the Cβ–C2 bond to form, highlighted in cyan, are also shown for the most stable conformer. Distances are in Å.

Table S2: Free energy profiles based on the most stable conformer for each species (in the second column). The Boltzmann-weighted energies are also listed for comparison (in the third column).

	ΔG (most stable conformer)	ΔG (Boltzmann-weighted)
1 + 2	0.0	0.0
ts3	17.3	17.3
3	9.6	9.6
ts8-A	23.3	23.2
8-A	18.8	18.6
ts9-A	22.9	22.6
9	-4.5	-4.5
ts4keto	32.3	32.2
4keto	0.3	0.3
ts4	52.6	52.5
4	3.9	3.9

	ΔG (most stable conformer)	ΔG (Boltzmann-weighted)
9 + 3	0.0	0.0
ts10	8.1	7.6
10	2.9	2.4
10i	9.1	8.7
ts11	10.8	10.3
11	1.5	1.0
ts4·3	0.6	0.0
4·3	-2.1	-2.5
ts5-A + 3	17.7	17.6
5-A + 3	3.3	3.1
ts6-A + 3	4.2	4.2
6 + 3	-5.6	-5.6
ts7 + 3	0.6	0.5
9 + 1 + 3	-21.9	-21.9

4 Kinetics simulations

4.1 Rate equation for each species

According to the reaction profile in Scheme 12, the rate equations are written as

$$\frac{d[\mathbf{1}]}{dt} = -k_3[\mathbf{1}][\mathbf{2}] + k_{-3}[\mathbf{3}] + k_5[\mathbf{4}] \quad (\text{s1})$$

$$\frac{d[\mathbf{2}]}{dt} = -k_3[\mathbf{1}][\mathbf{2}] + k_{-3}[\mathbf{3}] \quad (\text{s2})$$

$$\frac{d[\mathbf{3}]}{dt} = +k_3[\mathbf{1}][\mathbf{2}] - k_{-3}[\mathbf{3}] - k_8[\mathbf{3}] + k_{-8}[\mathbf{8-A}] - k_{11}[\mathbf{3}][\mathbf{9}] + k_{-11}[\mathbf{4}\cdot\mathbf{3}] + k_{43d}[\mathbf{4}\cdot\mathbf{3}] - k_{43a}[\mathbf{4}][\mathbf{3}] \quad (\text{s3})$$

$$\frac{d[\mathbf{8-A}]}{dt} = +k_8[\mathbf{3}] - k_{-8}[\mathbf{8-A}] - k_9[\mathbf{8-A}] \quad (\text{s4})$$

$$\frac{d[\mathbf{9}]}{dt} = +k_9[\mathbf{8-A}] - k_{11}[\mathbf{3}][\mathbf{9}] + k_{-11}[\mathbf{4}\cdot\mathbf{3}] \quad (\text{s5})$$

$$\frac{d[\mathbf{4}\cdot\mathbf{3}]}{dt} = +k_{11}[\mathbf{3}][\mathbf{9}] - k_{-11}[\mathbf{4}\cdot\mathbf{3}] - k_{43d}[\mathbf{4}\cdot\mathbf{3}] + k_{43a}[\mathbf{4}][\mathbf{3}] \quad (\text{s6})$$

$$\frac{d[\mathbf{4}]}{dt} = +k_{43d}[\mathbf{4}\cdot\mathbf{3}] - k_{43a}[\mathbf{4}][\mathbf{3}] - k_5[\mathbf{4}] \quad (\text{s7})$$

$$\frac{d[\mathbf{7}]}{dt} = +k_5[\mathbf{4}]. \quad (\text{s8})$$

The initial concentrations of the substrate and the catalyst are set as $[\mathbf{1}]_0 = 0.005$ M and $[\mathbf{2}]_0 = 0.025$ M. The rate constants are estimated by the Eyring-Polanyi equation using the DFT-computed barriers (Table S3). The reaction temperature is set at 0 °C according to previous kinetic experiments.⁷ The coupled differential equations of eqs. s1–s8 are numerically solved by the Mathematica software.

Table S3: Rate constants calculated at 0°C by the Eyring-Polanyi equation using DFT-computed activation energies ($\Delta G_{\text{act}}^\ddagger$ in kcal mol⁻¹).

	rate constant	$\Delta G_{\text{act}}^\ddagger$
k_3	$8.20 \times 10^{-2} \text{ M}^{-1} \text{ s}^{-1}$	17.3
k_{-3}	$3.93 \times 10^6 \text{ s}^{-1}$	7.7
k_8	$7.48 \times 10^1 \text{ s}^{-1}$	13.6
k_{-8}	$1.19 \times 10^9 \text{ s}^{-1}$	4.6
k_9	$3.59 \times 10^9 \text{ s}^{-1}$	4.0
k_{11}	$3.27 \times 10^4 \text{ M}^{-1} \text{ s}^{-1}$	10.3
k_{-11}	$3.27 \times 10^2 \text{ s}^{-1}$	12.8
k_{43d}	$1.06 \times 10^4 \text{ s}^{-1}$	10.9 + 0.01
k_{43a}	$5.59 \times 10^{12} \text{ M}^{-1} \text{ s}^{-1}$	0.0 + 0.01
k_5	$2.06 \times 10^5 \text{ s}^{-1}$	9.2
$k_{1+2 \rightarrow 9} \equiv \frac{k_3 k_8 k_9}{k_8 k_9 + k_{-3} k_9 + k_{-3} k_{-8}}$	$1.17 \times 10^{-6} \text{ M}^{-1} \text{ s}^{-1}$	
$k_{3 \rightarrow 9} \equiv \frac{k_8 k_9}{k_9 + k_{-8}}$	$5.62 \times 10^1 \text{ s}^{-1}$	
$k_{9 \rightarrow 4} \equiv \frac{k_{11} k_{43d}}{k_{43d} + k_{-11}}$	$3.17 \times 10^4 \text{ M}^{-1} \text{ s}^{-1}$	

4.2 Kinetic simulations at five reaction stages

The catalytic cycle is composed of five sequential processes (Figure 4a): initial addition, oxa-Michael reaction, BI formation, C–C Michael reaction, and catalyst expulsion. Each process of the catalytic cycle is gradually combined to perform kinetic simulations, shown in Figure S19. Each elementary step is considered reversible in the simulations. The enol ether is the dominant intermediate prior to the C–C Michael reaction (Figure S19c). Before the product forms, enol ether **9** and intermediate **6** coexist (Figure S19d). However, **6** could not be accumulated if the step of catalyst expulsion is included in the kinetic model (Figure S20a). For the ease of the simulation, the formation of the complex **4·3** from **4** and **3** is assumed to require a small activation energy of 0.01 kcal mol⁻¹, shown in Figure S20a. Increasing the barrier to 0.5 kcal mol⁻¹ does not significantly alter the kinetic pattern (Figure S20b). The same treatment is used to deal with the equilibrium between **10** and **10i**. When **4·3** is eliminated in the reaction profile, the result of the simulation remains almost unchanged (Figure S20a vs. Figure S20c). Therefore, the kinetics is not affected by the state of the hydrogen-bonded complex **4·3**.

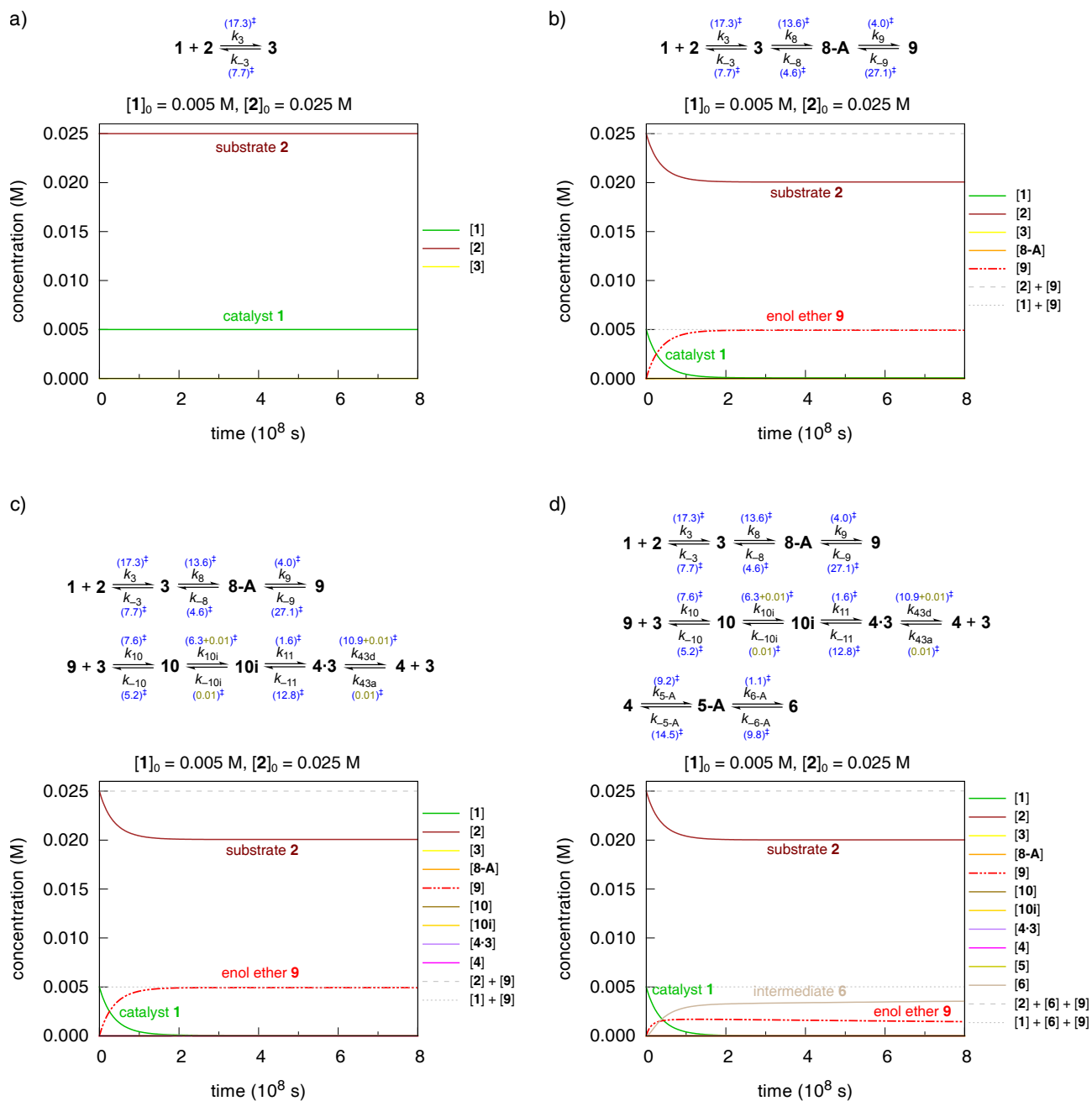


Figure S19: Kinetic simulations at different reaction stages.

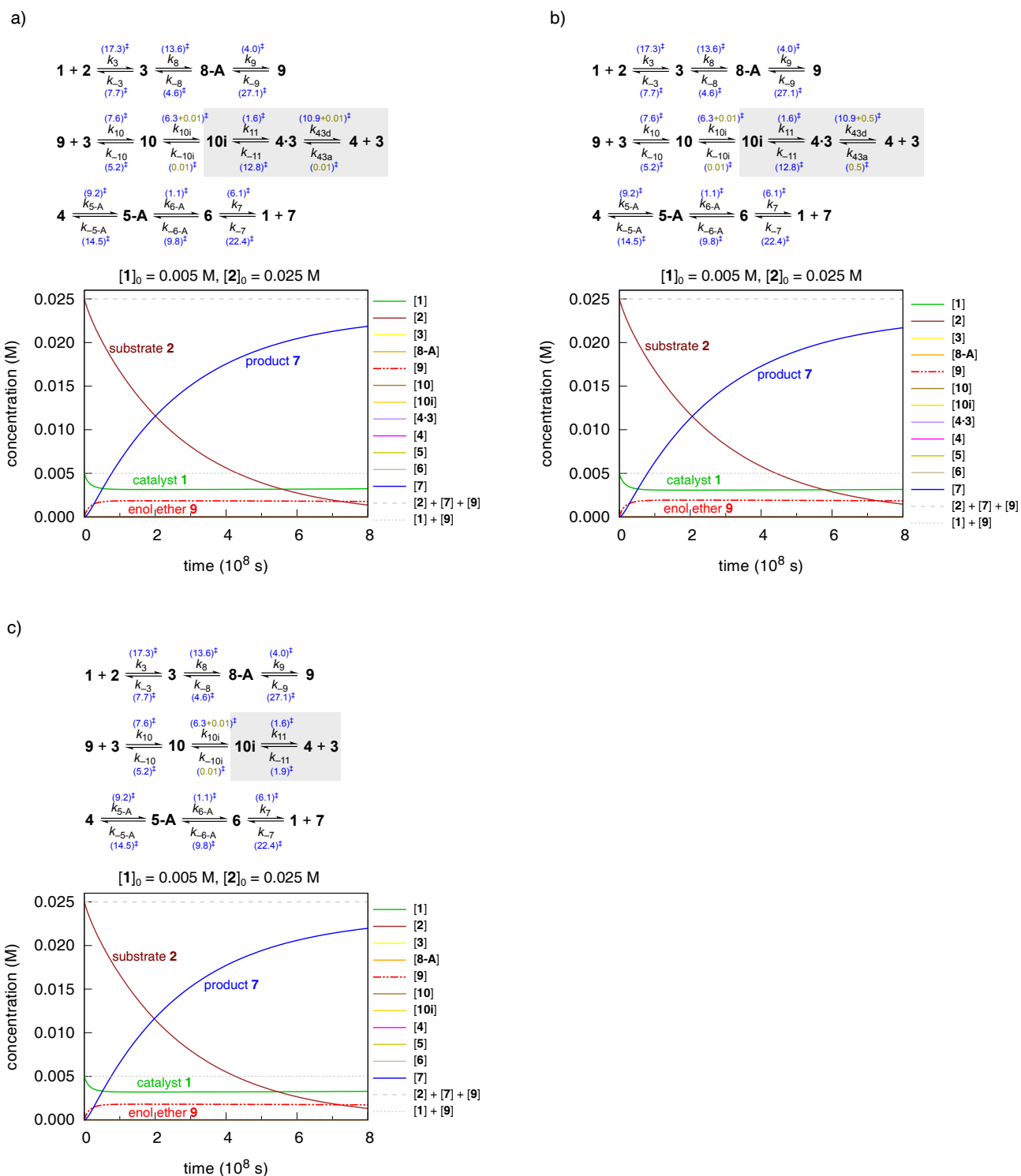


Figure S20: Kinetic simulations including all five reaction stages. The gray regions indicate the BI formation with or without the hydrogen-bonded complex ($4\cdot 3$) considered.

4.3 Determination of the reaction order by the VTNA

Because the kinetic simulations show the build-up of enol ether **9** (that exists in a concentration of 0.0018 M under the steady-state condition), the concentration of the catalyst present during catalysis is not equal to its initial concentration ($[\mathbf{1}]_0 = 0.005$ M). In order to identify the reaction order over the course of the reaction, we employ the variable time normalization analysis (VTNA), which can be applied to the condition where catalyst deactivation or product inhibition occurs.^{8–10}

The reference reaction is set using the initial condition of $[\mathbf{1}]_0 = 0.005$ M and $[\mathbf{2}]_0 = 0.025$ M. The VTNA is first carried out by changing the initial concentration of the catalyst from 0.004 M to 0.006 M (meanwhile the initial concentration of the other species is fixed). Figure S21a shows the product concentration profiles against the variable time scale normalized in the catalyst concentration, $\sum[\mathbf{1}]^\alpha \Delta t$, where $\alpha = 0, 1$, and 2 . The best overlay is obtained with $\alpha = 1$ in the overall regime. A similar procedure is performed by varying the initial concentration of the substrate, and the effect of different reaction orders is illustrated in Figure S21b. The first order in substrate leads to the best overlay. According to the VTNA, the catalytic reaction is determined to be first order in catalyst and first order in substrate, that is $d[\mathbf{7}]/dt \propto [\mathbf{1}]^1[\mathbf{2}]^1$.

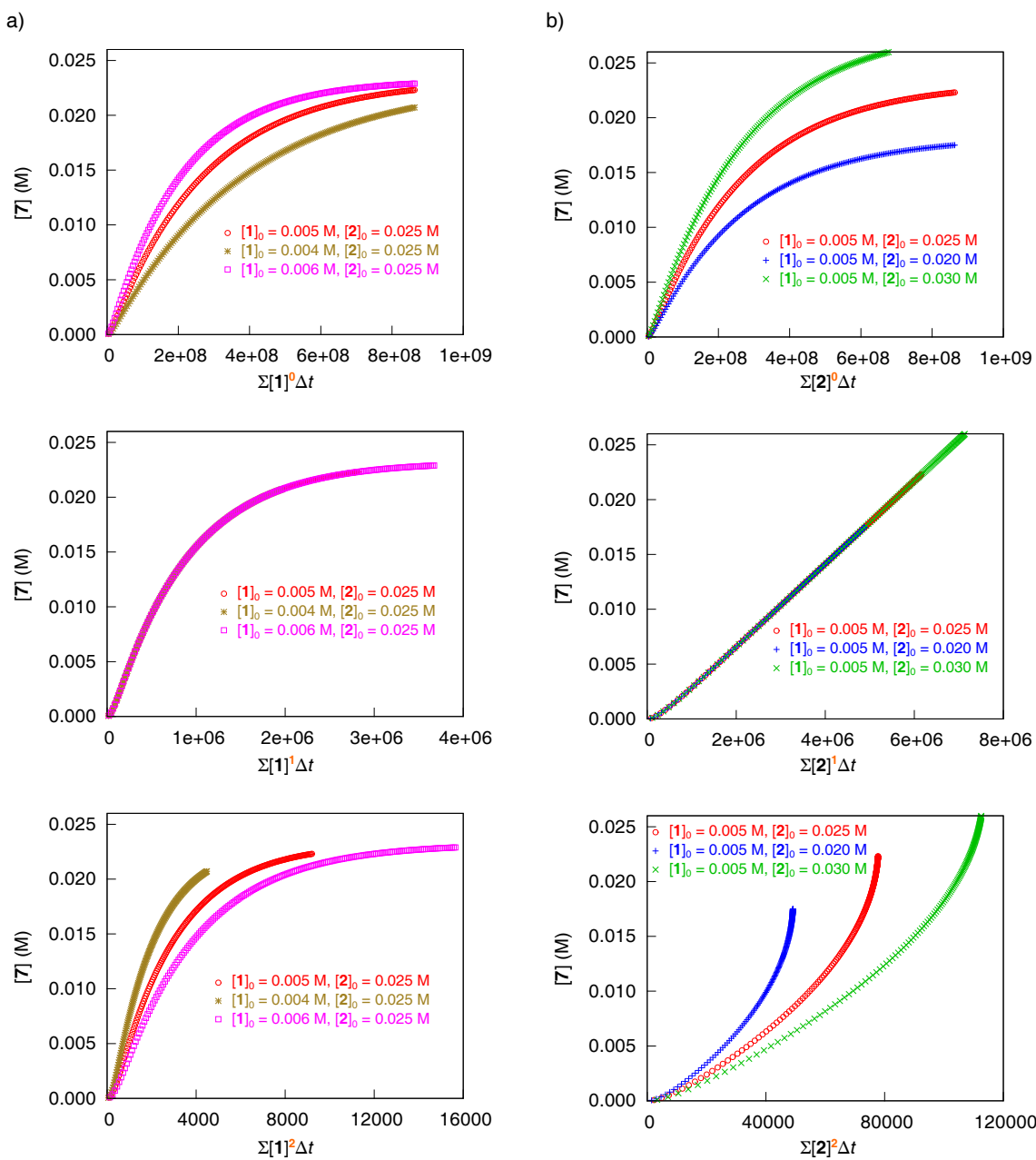
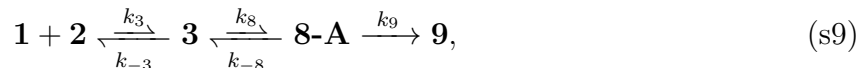


Figure S21: Variable time normalization analysis: (a) variation of the initial concentration of catalyst **1**, where the initial concentration of substrate **2** is fixed; (b) variation of the initial concentration of substrate **2**, where the initial concentration of catalyst **1** is fixed.

4.4 Rate constant for enol ether formation

If we only consider the formation of the enol ether, the reaction profile is written as



where the initial addition ($\mathbf{1} + \mathbf{2} \rightarrow \mathbf{3}$) is followed by the oxa-Michael reaction ($\mathbf{3} \rightarrow \mathbf{8-A} \rightarrow \mathbf{9}$). The steady-state approximation (eqs. s10 and s11) is used to solve the concentration of the two intermediates, $\mathbf{3}$ and $\mathbf{8-A}$.

$$\frac{d[\mathbf{3}]}{dt} = +k_3[\mathbf{1}][\mathbf{2}] - k_{-3}[\mathbf{3}] - k_8[\mathbf{3}] + k_{-8}[\mathbf{8-A}] \approx 0 \quad (\text{s10})$$

$$\frac{d[\mathbf{8-A}]}{dt} = +k_8[\mathbf{3}] - k_{-8}[\mathbf{8-A}] - k_9[\mathbf{8-A}] \approx 0 \quad (\text{s11})$$

The concentration of $\mathbf{8-A}$ is expressed in terms of $[\mathbf{1}]$ and $[\mathbf{2}]$ as

$$[\mathbf{8-A}] = \frac{k_3 k_8}{k_8 k_9 + k_{-3} k_9 + k_{-3} k_{-8}} [\mathbf{1}][\mathbf{2}]. \quad (\text{s12})$$

Substitution of eq. s12 to eq. s13 yields the rate law for enol ether formation, written as

$$\frac{d[\mathbf{9}]}{dt} = k_9[\mathbf{8-A}] \quad (\text{s13})$$

$$= \frac{k_3 k_8 k_9}{k_8 k_9 + k_{-3} k_9 + k_{-3} k_{-8}} [\mathbf{1}][\mathbf{2}] \quad (\text{s14})$$

$$= k_{1+2 \rightarrow 9} [\mathbf{1}][\mathbf{2}] \quad (\text{s15})$$

where the rate constant $k_{1+2 \rightarrow 9}$ is given by

$$k_{1+2 \rightarrow 9} \equiv \frac{k_3 k_8 k_9}{k_8 k_9 + k_{-3} k_9 + k_{-3} k_{-8}} \quad (\text{s16})$$

$$= \frac{1}{\frac{1}{k_3} + \frac{k_{-3}}{k_3} \frac{1}{k_8} + \frac{k_{-3}}{k_3} \frac{k_{-8}}{k_8} \frac{1}{k_9}}. \quad (\text{s17})$$

Rate constant related to activation energies and rate-determining TSs

The rate constant $k_{1+2\rightarrow 9}$ in eq. s17 is expressed in terms of energy as

$$k_{1+2\rightarrow 9} = \left(\frac{1}{k_3} + \frac{k_{-3}}{k_3} \frac{1}{k_8} + \frac{k_{-3}}{k_3} \frac{k_{-8}}{k_8} \frac{1}{k_9} \right)^{-1} \quad (\text{s18})$$

$$= \left[\frac{1}{A} \exp\left(\frac{\Delta G_3^\ddagger}{RT}\right) + \frac{1}{A} \exp\left(\frac{\Delta G_3 + \Delta G_8^\ddagger}{RT}\right) + \frac{1}{A} \exp\left(\frac{\Delta G_3 + \Delta G_8 + \Delta G_9^\ddagger}{RT}\right) \right]^{-1}. \quad (\text{s19})$$

The term A denotes the pre-exponential factor of the Eyring-Polanyi equation,

$$k = A \cdot \exp\left(\frac{-\Delta G^\ddagger}{RT}\right), \quad A \equiv \frac{k_{\text{Boltz}} T}{h}$$

where k_{Boltz} , T , and h indicate the Boltzmann constant, the temperature, and the Planck constant, respectively. The relationship between the rate-constant representation (eq. s18) and the energy representation (eq. s19) is illustrated in Figure S22.

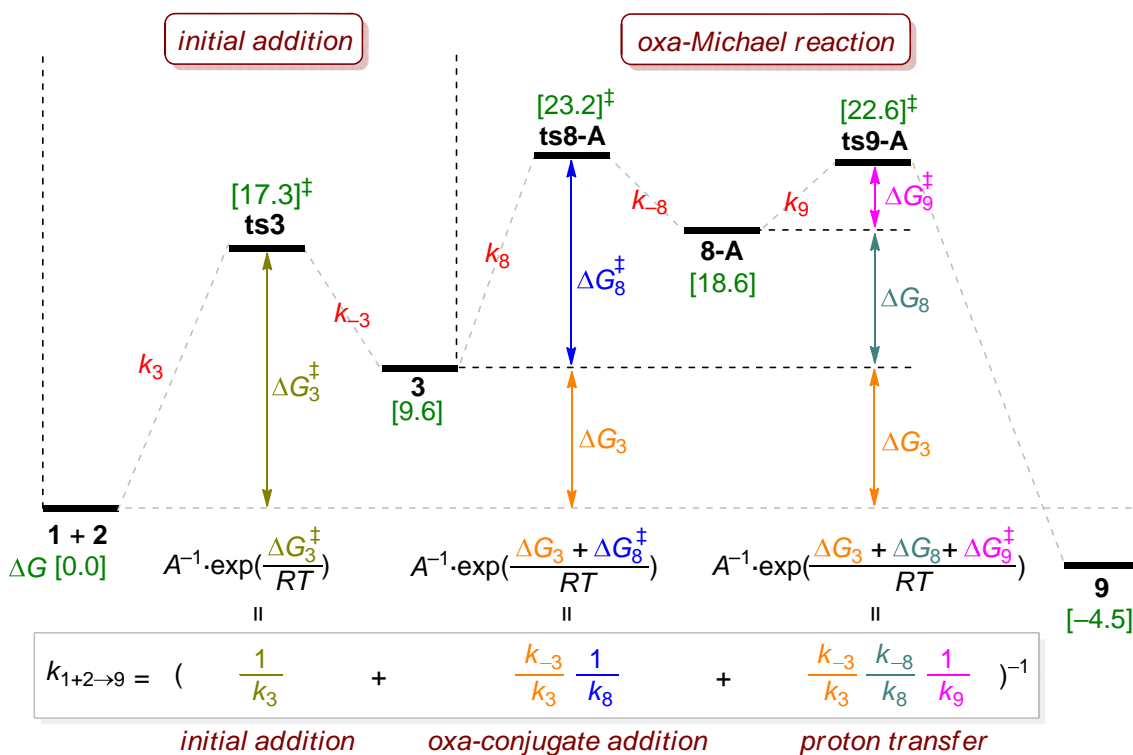


Figure S22: Relationship between the rate-constant representation (eq. s18) and the energy representation (eq. s19).

According to the DFT-computed energy profile shown in Figure S22, the magnitudes of the activation barriers follow the order of

$$\Delta G_3^\ddagger < \Delta G_3 + \Delta G_8^\ddagger \approx \Delta G_3 + \Delta G_8 + \Delta G_9^\ddagger. \quad (\text{s20})$$

Therefore, the first term can be neglected in eq. s18, providing

$$k_{1+2 \rightarrow 9} \approx \left(\frac{k_{-3}}{k_3} \frac{1}{k_8} + \frac{k_{-3}}{k_3} \frac{k_{-8}}{k_8} \frac{1}{k_9} \right)^{-1}. \quad (\text{s21})$$

Finally, the rate constant $k_{1+2 \rightarrow 9}$ is primarily determined by the two events of oxa-conjugate addition and proton transfer.

4.5 Steady-state approximation

Under the steady-state condition, the concentrations of all intermediates remain essentially constant, namely

$$\frac{d[\mathbf{3}]}{dt} \approx 0, \frac{d[\mathbf{8-A}]}{dt} \approx 0, \frac{d[\mathbf{9}]}{dt} \approx 0, \frac{d[\mathbf{4}\cdot\mathbf{3}]}{dt} \approx 0, \frac{d[\mathbf{4}]}{dt} \approx 0, \quad (\text{s22})$$

where the rate equations are presented in eqs. s3–s7. Because the amount of catalyst is conserved, the relationship of mass balance is given by

$$\begin{aligned} [\mathbf{1}]_0 &= [\mathbf{1}] + [\mathbf{3}] + [\mathbf{8-A}] + [\mathbf{9}] + 2 \cdot [\mathbf{4}\cdot\mathbf{3}] + [\mathbf{4}] \\ &\approx [\mathbf{1}] + [\mathbf{9}]. \end{aligned} \quad (\text{s23})$$

The kinetic simulation shows that the catalyst resting state consists of $\mathbf{1}$ (unbound form) and $\mathbf{9}$ (bound form) so that the approximation of eq. s23 is valid. The simultaneous equations of eqs. s22 and s23 are algebraically solved using the Mathematica software, and the concentration of the BI is expressed in terms of $[\mathbf{1}]_0$ and $[\mathbf{2}]$ as

$$[\mathbf{4}] = \frac{1}{\frac{k_8 k_9 + k_{-3} k_9 + k_{-3} k_{-8}}{k_3 k_8 k_9} \cdot k_5 + \frac{k_{-11} k_{43a}}{k_{11} k_{43d}} [\mathbf{2}]} [\mathbf{1}]_0 [\mathbf{2}] - \frac{k_8 k_9}{k_9 + k_{-8}} \frac{1}{\frac{k_8 k_9 + k_{-3} k_9 + k_{-3} k_{-8}}{k_3 k_8 k_9} \frac{k_{11} k_{43d}}{k_{-11} + k_{43d}} \cdot k_5 + \frac{k_{-11} k_{43a}}{k_{-11} + k_{43d}} [\mathbf{2}]} [\mathbf{2}]$$

Thus, the rate law of product formation is written as

$$\begin{aligned} \frac{d[\mathbf{7}]}{dt} &= k_5 [\mathbf{4}] \\ &= \frac{1}{\frac{k_8 k_9 + k_{-3} k_9 + k_{-3} k_{-8}}{k_3 k_8 k_9} + \frac{k_{-11} k_{43a}}{k_{11} k_{43d}} \frac{1}{k_5} [\mathbf{2}]} [\mathbf{1}]_0 [\mathbf{2}] - \frac{k_8 k_9}{k_9 + k_{-8}} \frac{1}{\frac{k_8 k_9 + k_{-3} k_9 + k_{-3} k_{-8}}{k_3 k_8 k_9} \frac{k_{11} k_{43d}}{k_{-11} + k_{43d}} + \frac{k_{-11} k_{43a}}{k_{-11} + k_{43d}} \frac{1}{k_5} [\mathbf{2}]} [\mathbf{2}] \end{aligned} \quad (\text{s24})$$

Since $\frac{k_8k_9+k_{-3}k_9+k_{-3}k_{-8}}{k_3k_8k_9}$ corresponds to the highest activation barrier (ca. 23 kcal mol⁻¹), the second term of the denominator can be neglected in eq. s24 , which is re-expressed as

$$\begin{aligned} \frac{d[\mathbf{7}]}{dt} &= \frac{k_3k_8k_9}{k_8k_9 + k_{-3}k_9 + k_{-3}k_{-8}} [\mathbf{1}]_0 [\mathbf{2}] \\ &\quad - \frac{k_3k_8k_9}{k_8k_9 + k_{-3}k_9 + k_{-3}k_{-8}} \cdot \frac{k_8k_9}{k_9 + k_{-8}} \cdot \frac{k_{-11} + k_{43d}}{k_{11}k_{43d}} [\mathbf{2}] \end{aligned} \quad (\text{s25})$$

$$= \frac{k_3k_8k_9}{k_8k_9 + k_{-3}k_9 + k_{-3}k_{-8}} \left[[\mathbf{1}]_0 - \frac{k_8k_9}{k_9 + k_{-8}} \cdot \left(\frac{k_{11}k_{43d}}{k_{-11} + k_{43d}} \right)^{-1} \right] \cdot [\mathbf{2}] \quad (\text{s26})$$

$$= k_{\text{cat}} ([\mathbf{1}]_0 - [\mathbf{9}]_{\text{steady-state}}) \cdot [\mathbf{2}] \quad (\text{s27})$$

where

$$k_{\text{cat}} \equiv \frac{k_3k_8k_9}{k_8k_9 + k_{-3}k_9 + k_{-3}k_{-8}} \quad (\text{s28})$$

$$[\mathbf{9}]_{\text{steady-state}} \equiv \frac{k_8k_9}{k_9 + k_{-8}} \cdot \left(\frac{k_{11}k_{43d}}{k_{-11} + k_{43d}} \right)^{-1}. \quad (\text{s29})$$

When the steady-state condition is reached, the concentration of the catalyst ($[\mathbf{1}]_{\text{steady-state}}$) is not equal to its initial concentration ($[\mathbf{1}]_0$). In other words, the catalyst is partially consumed on the enol ether formation. The rate law is finally expressed in terms of $[\mathbf{1}]_{\text{steady-state}}$ and $[\mathbf{2}]$ as

$$\frac{d[\mathbf{7}]}{dt} = k_{\text{cat}} [\mathbf{1}]_{\text{steady-state}} \cdot [\mathbf{2}] \quad (\text{s30})$$

where

$$[\mathbf{1}]_{\text{steady-state}} \equiv [\mathbf{1}]_0 - [\mathbf{9}]_{\text{steady-state}}. \quad (\text{s31})$$

Direct substitution of the computed rate constants presented in Table S3 to eq. s24 also gives the same numerical outcome,

$$\begin{aligned}
\frac{d[\mathbf{7}]}{dt} &= \frac{1}{8.53 \times 10^5 + \underline{2.12} \times 10^{14}[\mathbf{2}]}[\mathbf{1}]_0[\mathbf{2}] - \frac{2.78 \times 10^{21}}{1.35 \times 10^{30} + \underline{3.34} \times 10^{25}[\mathbf{2}]}[\mathbf{2}] \\
&\approx 1.17 \times 10^{-6}[\mathbf{1}]_0[\mathbf{2}] - 2.05 \times 10^{-9}[\mathbf{2}] \\
&\approx 1.17 \times 10^{-6}([\mathbf{1}]_0 - 0.0018)[\mathbf{2}].
\end{aligned} \tag{s32}$$

Concentration of the enol ether

By using the relationship between the rate-constant and the energy representations depicted in Figure S23, eq. s29 can be simplified as

$$[\mathbf{9}]_{\text{steady-state}} = \frac{k_{3 \rightarrow 9}}{k_{9 \rightarrow 4}} \tag{s33}$$

where $k_{3 \rightarrow 9}$ and $k_{9 \rightarrow 4}$ correspond to the rate constants for the oxa-Michael reaction step $\mathbf{3} \rightarrow \mathbf{9}$ and the BI formation $\mathbf{9} \rightleftharpoons \mathbf{4}$, respectively.

$$k_{3 \rightarrow 9} \equiv \frac{k_8 k_9}{k_9 + k_{-8}} = \left(\frac{1}{k_8} + \frac{k_{-8}}{k_8} \frac{1}{k_9} \right)^{-1} \tag{s34}$$

$$k_{9 \rightarrow 4} \equiv \frac{k_{11} k_{43d}}{k_{43d} + k_{-11}} = \left(\frac{1}{k_{11}} + \frac{k_{-11}}{k_{11}} \frac{1}{k_{43d}} \right)^{-1}. \tag{s35}$$

The two rate constants of $k_{3 \rightarrow 9}$ and $k_{9 \rightarrow 4}$ are indeed relevant to formation and consumption of the enol ether, respectively. The concentration of the enol ether that forms in the steady-state regime is the ratio of $k_{3 \rightarrow 9}$ to $k_{9 \rightarrow 4}$. If $k_{9 \rightarrow 4}$ is much greater than $k_{3 \rightarrow 9}$, $[\mathbf{9}]_{\text{steady-state}}$ would become smaller. Namely, when the enol ether is consumed faster than it is generated, it could not be significantly accumulated.

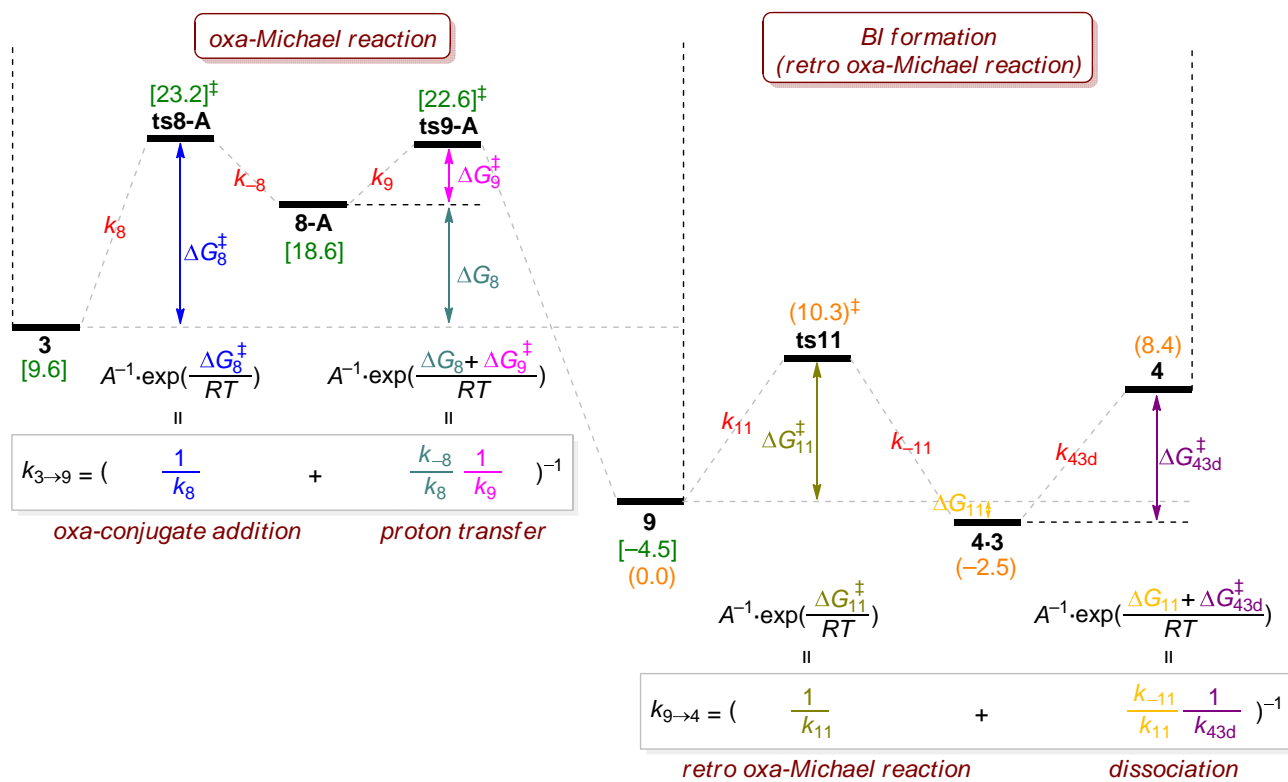


Figure S23: Relationship between the rate-constant representation and the energy representation in eqs. s34 and s35.

4.6 Kinetic simulation with increasing k_{11} and k_{-11}

According to eq. s35, if $k_{9 \rightarrow 4}$ with respect to the retro oxa-Michael reaction is raised, the amount of the enol ether that builds up during catalysis would decrease. In order to confirm this, a kinetic simulation is performed by artificially lowering the activation energy of **ts11** by 0.5 kcal mol⁻¹ (the barrier heights with respect to k_{11} and k_{-11} are decreased to 9.8 and 12.3 kcal mol⁻¹, respectively) while other parameters remain unchanged. Kinetic simulations reveal that the concentration of the enol ether decreases to 0.00073 M (Figure S24a), compared to 0.0018 M in the reaction profile with k_{11} and k_{-11} unchanged (Figure 5a). The VTNA shows that the catalytic rate constant is not affected by the magnitudes of k_{11} and k_{-11} (Figure S24b). The catalytic pattern observed in the kinetic simulation can also be reproduced by eqs. s28 and s29 derived by the steady-state approximation.

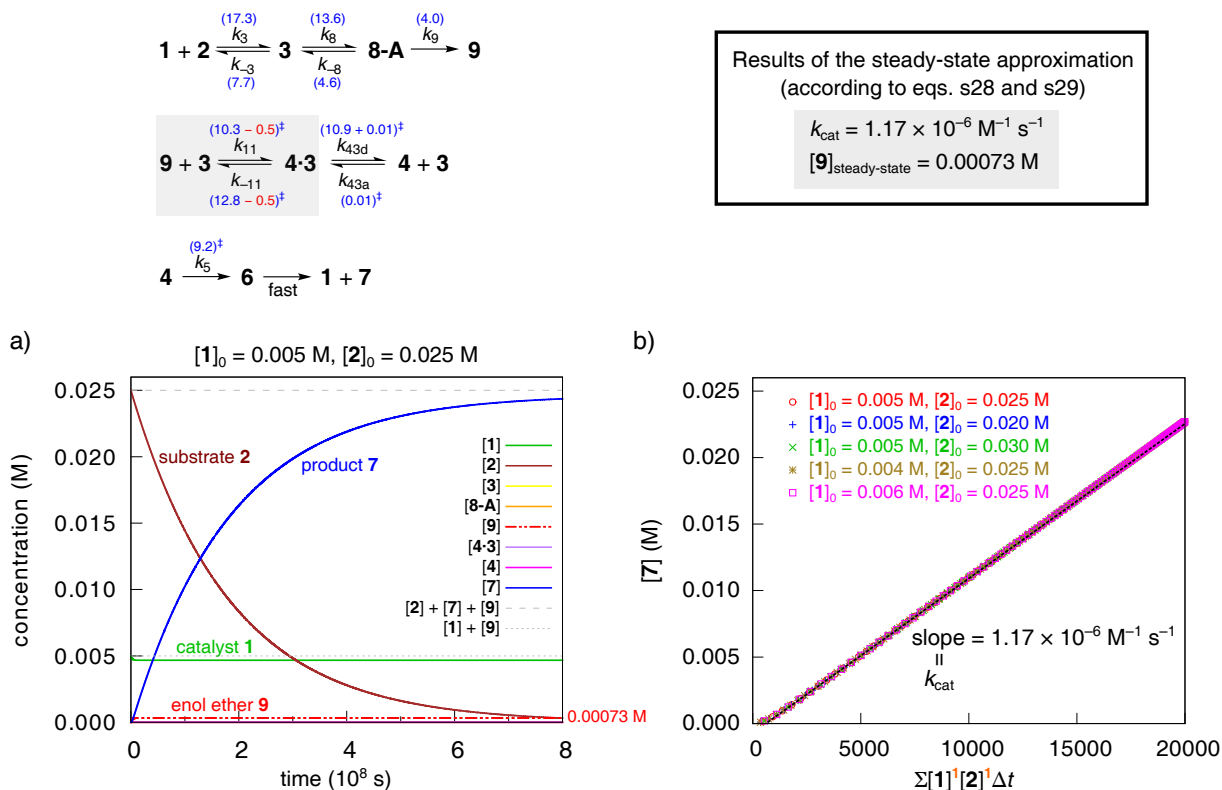


Figure S24: (a) Kinetic simulation using the initial concentrations of $[1]_0 = 0.005 \text{ M}$ and $[2]_0 = 0.025 \text{ M}$. The barrier heights with respect to k_{11} and k_{-11} are lowered by 0.5 kcal mol⁻¹ while other parameters remain unchanged. (b) VTNA using the data obtained from kinetic simulations.

4.7 NHC-assisted mechanism

When carbene **1** acts as a base that assists in the retro oxa-Michael reaction (Scheme S7), the computed barrier for the deprotonation step is 24.8 kcal mol⁻¹, and the BI·NHC complex (**4·1**) is 6.0 kcal mol⁻¹ higher in energy than the state of **9** + **1**. The NHC-assisted mechanism thus requires an activation energy of at least 24.8 kcal mol⁻¹. The reaction profile based on the NHC-assisted mechanism is depicted at the top of Figure S25, where the step of **9** + **1** ⇌ **4·1** is assumed to proceed through an energy barrier of 24.8 kcal mol⁻¹ for the forward reaction. Kinetic simulations demonstrate that the enol ether could not be consumed so that the catalytic cycle is impeded by the slow retro oxa-Michael reaction. Therefore, the NHC-assisted mechanism is less efficient than the PA-assisted mechanism.

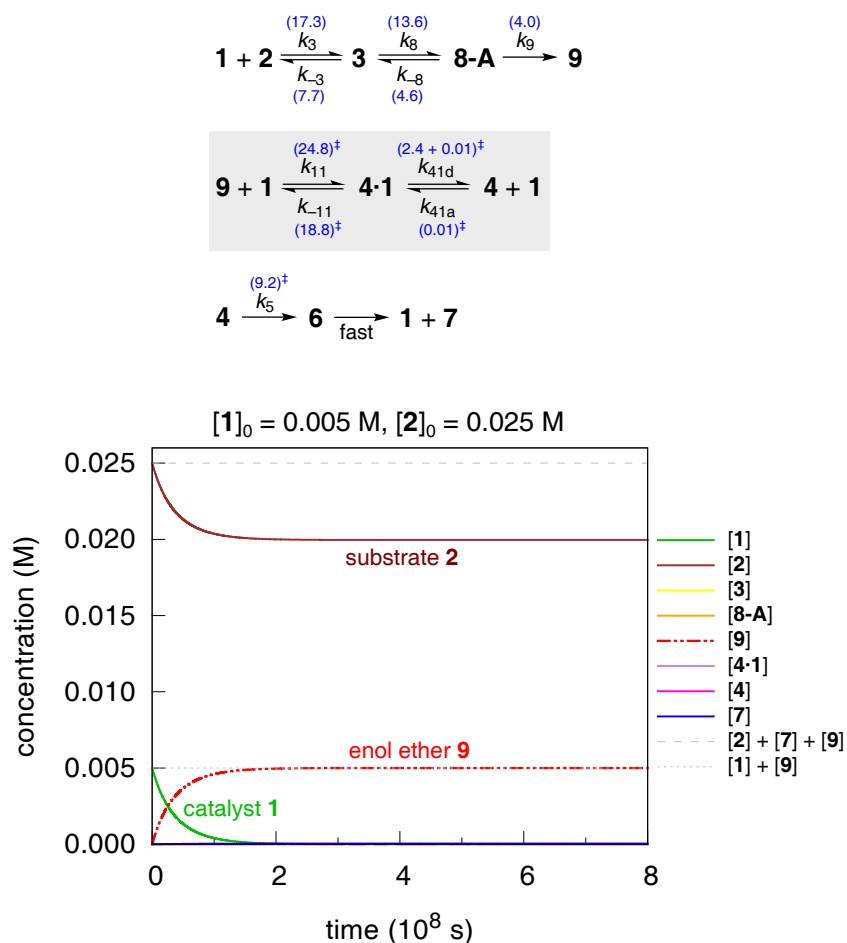


Figure S25: Kinetic simulation based on the reaction profile of the NHC-assisted mechanism.

5 Cartesian coordinates of optimized structures

For each species, the coordinates and the energies of the lowest energy conformer are provided. Other energy terms, *i.e.* thermal correction to free energy based on the rigid-rotor-harmonic-oscillator (RRHO) treatment, include zero-point energy, thermal correction, and entropic effects. In addition to the standard RRHO value computed by the Gaussian package, the quasi-RRHO approximation is employed to correct the contribution from low frequencies. The imaginary frequency with respect to the bond forming/breaking process is given for the TS located. Note that the listed thermal correction to free energy are calculated under standard conditions of 0°C and 1 atm. In solution phase, a change in concentration (0°C and 1 M in solution) leads to a difference in free energy of 1.8 kcal mol⁻¹. Single-point electronic energies with a larger basis set of def2-TZVP are also presented.

```

1
charge, 2S+1 = 0, 1
--- OPT at ωB97X-D/6-311G** in SMD ---
E(ele) = -589.95978138 a.u.
Correction to G = 0.168392 a.u.(RRHO)
Correction to G = 0.173680 a.u.(quasi-RRHO)
--- SP at ωB97X-D/def2-TZVP in SMD ---
E(ele) = -590.03136335 a.u.
C 0.728892 1.238118 -0.017913
N -0.022553 0.109499 -0.030952
N 1.964584 0.686878 -0.035791
N 0.683541 -1.085724 -0.059599
C 1.906059 -0.677252 -0.064753
C 3.328286 1.198727 -0.070933
C 4.147412 -0.057212 0.297529
C 3.273976 -1.269668 -0.114826
H 3.556159 1.562071 -1.075862
H 3.451830 2.015920 0.637817
H 5.122744 -0.063404 -0.187918
H 4.306971 -0.079141 1.377752
H 3.496924 -1.599081 -1.133743
H 3.390406 -2.125614 0.548844
C -1.444797 0.052287 -0.004721
C -2.187186 1.230370 -0.032968
C -2.087115 -1.180902 0.047611
C -3.572640 1.165641 -0.007137
H -1.674705 2.181835 -0.073454
C -3.475241 -1.229681 0.071640
H -1.498454 -2.087617 0.068228
C -4.225096 -0.061199 0.044898
H -4.145102 2.086172 -0.029108
H -3.969764 -2.193733 0.112525
H -5.307986 -0.104797 0.064164

C 2.863617 0.527746 0.019437
C 2.182477 -0.530952 -0.608463
C 4.250203 0.611811 -0.095158
C 2.900685 -1.480118 -1.336005
C 4.966741 -0.328191 -0.815978
C 4.282424 -1.369657 -1.432331
H 4.747095 1.438611 0.399730
H 2.399246 -2.302970 -1.827460
H 6.044060 -0.253768 -0.898955
H 4.828081 -2.114737 -2.000759
O 0.839891 -0.554967 -0.458272
C 0.097274 -1.591177 -1.066931
H 0.423584 -2.570561 -0.691488
H 0.249049 -1.586351 -2.154912
C -1.350988 -1.415562 -0.777127
H -2.003831 -2.172401 -1.204843
C -1.887195 -0.435717 -0.059286
H -1.289417 0.345803 0.391678
C -3.352753 -0.385873 0.148086
O -4.156007 -1.177996 -0.291050
O -3.688445 0.668222 0.898177
C -5.089920 0.836220 1.176912
H -5.457336 -0.056238 1.689784
H -5.629658 0.926066 0.230829
C -5.239872 2.073797 2.027851
H -4.865445 2.955837 1.503270
H -6.296018 2.233345 2.259290
H -4.693466 1.969526 2.968009

ts3
charge, 2S+1 = 0, 1
--- OPT at ωB97X-D/6-311G** in SMD ---
E(ele) = -1394.60341952 a.u.
Correction to G = 0.397588 a.u.(RRHO)
Correction to G = 0.410130 a.u.(quasi-RRHO)
imaginary frequency = 189i
--- SP at ωB97X-D/def2-TZVP in SMD ---
E(ele) = -1394.77505069 a.u.
C 0.373675 -0.233845 1.655096
N -0.928202 -0.467060 1.399433
N 0.355146 1.061664 2.006702
N -1.748009 0.635931 1.563858
C -0.914941 1.550912 1.939125
C 1.345738 2.061928 2.397812
C 0.442531 3.172577 2.973095
C -0.938547 2.999951 2.289148
H 2.045306 1.626321 3.106946
H 1.893781 2.382356 1.509024
H 0.332650 3.025572 4.049598
H 0.864232 4.163211 2.807799

7
charge, 2S+1 = 0, 1
--- OPT at ωB97X-D/6-311G** in SMD ---
E(ele) = -804.69268153 a.u.
Correction to G = 0.207780 a.u.(RRHO)
Correction to G = 0.215278 a.u.(quasi-RRHO)
--- SP at ωB97X-D/def2-TZVP in SMD ---
E(ele) = -804.79482594 a.u.
C -1.194374 -0.585913 -0.538538
H 1.122328 -1.635488 -1.210791
O -1.318246 -1.476229 -1.351199
C -2.340032 0.198474 -0.026717
C -2.132461 1.248484 0.878953
C -3.648720 -0.146553 -0.384397
C -3.223983 1.918423 1.434347
C -4.729040 0.521538 0.154504

2
charge, 2S+1 = 0, 1
--- OPT at ωB97X-D/6-311G** in SMD ---
E(ele) = -804.64386182 a.u.
Correction to G = 0.201858 a.u.(RRHO)
Correction to G = 0.210153 a.u.(quasi-RRHO)
--- SP at ωB97X-D/def2-TZVP in SMD ---
E(ele) = -804.74769740 a.u.
C 2.136042 1.553712 0.798228
H 1.040852 1.430775 0.850968
O 2.678172 2.480659 1.353411

```



```

charge, 2S+1 = 0, 1
--- OPT at  $\omega$ B97X-D/6-311G** in SMD ---
E(ele) = -1394.59667357 a.u.
Correction to G = 0.399761 a.u. (RRHO)
Correction to G = 0.411259 a.u. (quasi-RRHO)
imaginary frequency = 11551
--- SP at  $\omega$ B97X-D/def2-TZVP in SMD ---
E(ele) = -1394.76720601 a.u.
C 0.200609 0.726828 -0.914895
N -0.317500 1.846482 -0.353134
N 1.307330 1.163296 -1.545027
N 0.422055 2.972377 -0.653238
C 1.393274 2.512767 -1.369276
C 2.403566 0.602152 -2.341139
C 3.408864 1.771937 -2.323856
C 2.586378 3.059204 -2.075363
H 2.785903 -0.288003 -1.848159
H 2.033052 0.363222 -3.338949
H 4.102532 1.618282 -1.495251
H 3.985205 1.821205 -3.246705
H 3.115689 3.803083 -1.481746
H 2.272704 3.530598 -3.011117
C -1.402099 1.956338 0.566719
C -2.358170 2.940416 0.354468
C -1.488202 1.083324 1.642388
C -3.429959 3.038625 1.229801
H -2.255998 3.618602 -0.487096
C -2.573467 1.181940 2.501697
H -0.723857 0.333116 1.805331
C -3.544946 2.153781 2.296276
H -4.182197 3.802526 1.071548
H -2.654313 0.495630 3.336007
H -4.390722 2.224781 2.970289
C -0.201507 -0.648337 -0.756980
H 0.338216 -0.973725 0.378940
O 0.619753 -1.502108 -1.495043
C -1.648539 -1.026555 -0.808270
C -2.041896 -2.294346 -0.342125
C -2.641183 -0.189206 -1.321940
C -3.384978 -2.658682 -0.345309
C -3.980823 -0.548651 -1.317782
C -4.356487 -1.787046 -0.814497
H -2.361277 0.774995 -1.730650
H -3.645001 -0.638862 0.037196
H -4.724330 0.135620 -1.709885
H -5.399373 -2.083132 -0.801628
O -1.174754 -3.206208 0.193310
C -0.043253 -3.625669 -0.574208
H -0.359444 -3.856212 -1.597647
H 0.300011 -4.541757 -0.089504
C 1.074679 -2.597967 -0.597551
H 1.944310 -3.001730 -1.119633
C 1.355525 -2.046448 0.752971
H 0.900098 -2.521627 1.613391
C 2.610546 -1.397934 0.961822
O 3.399762 -1.024743 0.097095
O 2.860910 -1.151194 2.278887
C 4.056429 -0.432754 2.572236
H 4.024829 0.549584 2.089243
H 4.919830 -0.968371 2.166741
C 4.149631 -0.298318 4.075368
H 3.286343 0.242161 4.471795
H 4.187783 -1.281660 4.550559
H 5.055155 0.251182 4.347110

```

```

ts9-B in terms of  $si$ -( $scis$ - $re$ - $si$ )-Z
charge, 2S+1 = 0, 1
--- OPT at  $\omega$ B97X-D/6-311G** in SMD ---
E(ele) = -1394.58865016 a.u.
Correction to G = 0.399862 a.u. (RRHO)
Correction to G = 0.411009 a.u. (quasi-RRHO)
imaginary frequency = 11761
--- SP at  $\omega$ B97X-D/def2-TZVP in SMD ---
E(ele) = -1394.75931319 a.u.
C -0.068350 -0.394017 -0.862641
N -1.249909 -0.051311 -1.412030
N 0.111032 -1.674692 -1.252166
N -1.827111 -1.097460 -2.106699
C -0.972003 -2.057625 -1.982203
C 1.018235 -2.769515 -0.923517
C 0.585495 -3.830940 -1.957333

```

```

C -0.884646 -3.506825 -2.324662
H 2.056546 -2.460820 -1.031139
H 0.841343 -3.076409 0.109853
H 1.211799 -3.739928 -2.846847
H 0.700217 -4.840162 -1.565311
H -1.119874 -3.709203 -3.368616
H -1.590914 -4.064035 -1.703684
C -1.909861 1.223430 -1.448315
C -1.964312 1.889818 -2.663821
C -2.509046 1.727957 -0.305027
C -2.632669 3.104691 -2.735972
H -1.491483 1.457740 -3.537994
C -3.171534 2.945386 -0.391702
H -2.436623 1.183462 0.631405
C -3.233991 3.632454 -1.599198
H -2.680732 3.637622 -3.678413
H -3.641834 3.357378 0.493699
H -3.754167 4.582178 -1.655312
C 0.805285 0.305183 0.047485
H 0.663637 -0.351987 1.176061
O 0.269761 1.482050 0.546016
C 2.257287 0.397365 -0.303179
C 3.182363 0.832369 0.668206
C 2.752058 0.090489 -1.574621
C 4.536673 0.913740 0.355313
C 4.104656 0.159731 -1.878968
C 5.004308 0.569375 -0.904259
H 2.056896 -0.205673 -2.353963
H 5.213931 1.244154 1.134291
H 4.448207 -0.090376 -2.876297
H 6.063846 0.635524 -1.123919
O 2.862969 1.115508 1.965774
C 1.820950 2.046004 2.275883
H 1.961219 2.962114 1.691827
H 1.957846 2.268903 3.335757
C 0.433335 1.485480 2.025561
H -0.328174 2.192563 2.359843
C 0.283822 0.104296 2.554920
H 1.076309 -0.302703 3.170989
C -1.025885 -0.419065 2.763119
O -2.081527 0.042249 2.339328
O -1.010451 -1.600035 3.452428
C -2.244479 -2.310931 3.522036
H -3.062951 -1.613972 3.712809
H -2.138087 -2.976561 4.380758
C -2.504873 -3.103767 2.253362
H -1.673600 -3.785025 2.048625
H -3.417392 -3.697961 2.358956
H -2.633428 -2.428853 1.404170

```

```

ts9-C in terms of  $si$ -( $scis$ - $re$ - $re$ )-E
charge, 2S+1 = 0, 1
--- OPT at  $\omega$ B97X-D/6-311G** in SMD ---
E(ele) = -1394.58340304 a.u.
Correction to G = 0.398749 a.u. (RRHO)
Correction to G = 0.410507 a.u. (quasi-RRHO)
imaginary frequency = 10501
--- SP at  $\omega$ B97X-D/def2-TZVP in SMD ---
E(ele) = -1394.75444412 a.u.
C 1.267584 -0.962343 -0.275126
N 2.024275 -0.383691 0.684026
N 1.762551 -2.209520 -0.370806
N 2.998729 -1.231650 1.165464
C 2.797961 -2.326278 0.510093
C 1.499760 -3.431024 -1.133625
C 2.794405 -4.230610 -0.875251
C 3.376777 -3.698870 0.457696
H 0.610105 -3.915332 -0.729168
H 1.327146 -3.195656 -2.179399
H 2.601745 -5.301878 -0.843149
H 3.503350 -4.037646 -1.682826
H 3.020506 -4.275538 1.315561
H 4.465403 -3.694728 0.480838
C 1.862352 0.910091 1.266501
C 0.607460 1.317598 1.698899
C 2.972272 1.736072 1.374774
C 0.462484 2.594503 2.225207
H -0.246577 0.654797 1.624706
C 2.816411 3.004004 1.916137
H 3.939129 1.384544 1.035762
C 1.561831 3.437724 2.329704

```

```

ts9-D in terms of  $si$ -( $scis$ - $re$ - $re$ )-Z
charge, 2S+1 = 0, 1
--- OPT at  $\omega$ B97X-D/6-311G** in SMD ---
E(ele) = -1394.57762497 a.u.
Correction to G = 0.397351 a.u. (RRHO)
Correction to G = 0.409653 a.u. (quasi-RRHO)
imaginary frequency = 9661
--- SP at  $\omega$ B97X-D/def2-TZVP in SMD ---
E(ele) = -1394.75018575 a.u.
C 1.022748 0.876146 0.286142
N 2.177129 0.336593 0.721681
N 0.829459 1.932951 1.101628
N 2.692417 1.012604 1.811626
C 1.847851 1.970613 2.003763
C -0.227581 2.908060 1.354306
C 0.132107 3.380439 2.780491
C 1.643676 3.090600 2.965854
H -0.173504 3.705593 0.611320
H -1.203527 2.428773 1.285590
H -0.107797 4.432664 2.924773
H -0.439034 2.798223 3.505653
H 2.260391 3.944979 2.674001
H 1.905589 2.814384 3.985706
C 2.910703 -0.779500 0.210412
C 3.247938 -0.832667 -1.133710
C 3.302246 -1.770769 1.097999
C 3.981222 -1.914455 -1.598086
H 2.924206 -0.050080 -1.807523
C 4.043158 -2.844424 0.623295
H 3.026716 -1.696752 2.142664
C 4.379754 -2.918954 -0.722991
H 4.242128 -1.970899 -2.648230
H 4.350266 -3.626843 1.307136
H 4.953619 -3.761333 -1.091703
C 0.034305 0.374704 -0.646467
H -0.839475 -0.111103 0.128223
O 0.381170 -0.2839145 -1.233566
C -0.551624 1.355103 -1.614102
C -1.745000 1.002829 -2.269075
C 0.038272 2.580122 -1.930093
C -2.331952 1.886849 -3.169976
C -0.551020 3.462936 -2.826550
C -1.747064 3.116198 -3.441269
H 0.984572 2.850844 -1.471430
H -3.259952 1.587949 -3.643269
H -0.071628 4.409224 -3.049874

```



```

E(ele) = -1394.61534332 a.u.
Correction to G = 0.401566 a.u.(RRHO)
Correction to G = 0.412772 a.u.(quasi-RRHO)
imaginary frequency = 263i
--- SP at  $\omega_{B97X-D}/def2-TZVP$  in SMD ---
E(ele) = -1394.78415232 a.u.
C -0.159592 0.967550 -0.468469
N -1.248425 1.632444 0.025150
N 0.772400 1.951130 -0.598251
N -0.984959 2.977524 0.252135
C 0.235814 3.115398 -0.133587
C 2.152208 2.088355 -1.062330
C 2.282243 3.622004 -1.176070
C 1.242451 4.213495 -0.194925
H 2.828186 1.655672 -0.321460
H 2.281846 1.571408 -2.009311
H 3.295427 3.953276 -0.951856
H 2.038991 3.935637 -2.193809
H 1.671928 4.366707 0.799068
H 0.814858 5.157072 -0.530793
C -2.604390 1.202043 0.107827
C -3.250782 1.243156 1.334766
C -3.263936 0.771913 -1.036261
C -4.572078 0.828316 1.418479
H -2.710164 1.580925 2.209525
C -4.579476 0.341298 -0.940881
H -2.742761 0.756675 -1.985401
C -5.233446 0.368035 0.285152
H -5.081654 0.851163 2.374766
H -5.091504 -0.015700 -1.826600
H -6.261112 0.030534 0.357729
C 0.800212 -0.408013 -0.667988
H 1.794056 -1.147275 -0.984508
D 1.129477 -0.660547 -1.524303
C -1.031027 -1.385641 -0.690945
C -1.725377 -1.693222 0.482094
C -1.420625 -2.015553 -1.874639
C -2.834303 -2.528920 0.462089
C -2.517906 -2.863726 -1.901017
C -3.240519 -3.101278 -0.734890
H -0.859848 -1.809690 -2.779403
H -3.357945 -2.722935 1.390772
H -2.818171 -3.331247 -2.832135
H -4.108659 -3.750740 -0.753365
D -1.309634 -1.175305 1.677892
C 0.024229 -1.577378 1.993752
H 0.125416 -2.654747 1.817766
H 0.127715 -1.397306 3.066958
C 1.118473 -0.833372 1.282496
H 1.228159 0.214171 1.548347
C 2.263536 -1.507809 0.911186
H 2.263632 -2.588237 0.814335
C 3.534101 -0.831213 0.788563
D 3.750358 0.354517 0.987240
D 4.521829 -1.679296 0.424363
C 5.830550 -1.116132 0.295058
H 6.118131 -0.643229 1.238151
H 5.816329 -0.338594 -0.474434
C 6.773659 -2.237809 -0.072702
H 6.783487 -3.007045 0.703196
H 6.477236 -2.702189 -1.016357
H 7.788804 -1.847711 -0.184237

ts5-B
charge, 2S+1 = 0, 1
--- OPT at  $\omega_{B97X-D}/6-311G^{**}$  in SMD ---
E(ele) = -1394.61144048 a.u.
Correction to G = 0.402074 a.u.(RRHO)
Correction to G = 0.413149 a.u.(quasi-RRHO)
imaginary frequency = 374i
--- SP at  $\omega_{B97X-D}/def2-TZVP$  in SMD ---
E(ele) = -1394.7799913 a.u.
C -0.046324 0.640902 -0.616976
N -0.923779 1.520363 -0.037848
N 1.097953 1.373017 -0.748191
N -0.335423 2.754182 0.208288
C 0.863062 2.619358 -0.241086
C 2.354370 1.311047 -1.498873
C 3.136124 2.458014 -0.838231
C 2.065770 3.488865 -0.406054
H 2.831951 0.341934 -1.412768
H 2.145042 1.506306 -2.554373
H 3.651546 2.068701 0.042539
H 3.877445 2.883939 -1.513507
H 2.324086 4.020161 0.509288
H 1.877976 4.230913 -1.186913
C -2.340520 1.433560 0.047284
C -2.973767 1.871439 1.203808
C -3.074772 0.940139 -1.023370
C -4.354696 1.796520 1.291716
H -2.378956 2.254118 2.023381
C -4.456816 0.849567 -0.917659
H -2.570712 0.619119 -1.926113
C -5.098809 1.275417 0.237119
H -4.851794 2.132368 2.194519
H -5.028460 0.447430 -1.745776
H -6.177580 1.205007 0.316671
C -0.080219 -0.759896 -0.766036
H 1.588968 -1.643479 -1.253111
O 0.834763 -1.225375 -1.705777
C -1.306323 -1.571314 -0.636698
C -1.986246 -1.631124 0.585109
C -1.775424 -2.350953 -1.696036
C -3.149176 -2.381647 0.716626
C -2.931614 -3.105470 -1.568163
C -3.628803 -3.107823 -0.362805
H -1.220810 -2.341256 -2.626818
H -3.661629 -2.379373 1.671385
H -3.291764 -3.689138 -2.407820
H -4.537988 -3.689381 -0.258617
D -1.581433 -0.887685 1.649747
C -0.232506 -0.995850 2.108916
H -0.195298 -1.799082 2.855525
H -0.039837 -0.049799 2.617932
C 0.846893 -1.262622 1.094288
H 0.859343 -2.266324 0.674924
C 2.073305 -0.652960 1.299428
H 2.184082 0.170346 1.994060
C 3.225372 -1.083149 0.575215
O 3.230277 -1.860789 -0.381714
D 4.369855 -0.510239 1.005927
H 5.562590 -0.836797 0.283900
H 5.432136 -0.577955 -0.771036
H 5.736904 -1.914350 0.339892
C 6.698656 -0.060694 0.907769
H 6.815477 -0.322766 1.961915
H 7.632910 -0.292837 0.389847
H 6.525089 1.016068 0.836345

5
charge, 2S+1 = 0, 1
--- OPT at  $\omega_{B97X-D}/6-311G^{**}$  in SMD ---
E(ele) = -1394.63945762 a.u.
Correction to G = 0.403654 a.u.(RRHO)
Correction to G = 0.415323 a.u.(quasi-RRHO)
--- SP at  $\omega_{B97X-D}/def2-TZVP$  in SMD ---
E(ele) = -1394.80970831 a.u.
C 0.081311 0.726767 0.669766
N 0.283518 -0.042580 1.746410
N 0.817721 1.818256 0.891670
N 1.142768 0.532930 2.644863
C 1.442744 1.665159 2.093614
C 1.164409 3.079005 0.213427
C 2.383796 3.541470 1.038140
C 2.275860 2.854668 2.420294
H 1.409101 2.876625 -0.825480
H 0.312836 3.755926 0.276638
H 3.294990 3.207029 0.538988
H 2.420145 4.626754 1.118646
H 3.241318 2.579676 2.841907
H 1.751495 3.478946 3.148951
C -0.159555 -1.388090 1.985886
C -1.467023 -1.635593 2.370978
C 0.765136 -2.410162 1.820344
C -1.864354 -2.952016 2.568685
H -2.165062 -0.818731 2.498066
C 0.357772 -3.719221 2.028874
H 1.774835 -1.272727 1.508212
C -0.956801 -3.989517 2.395838
H -2.887414 -3.162071 2.856238
H 1.065133 -4.528760 1.894650
H -1.274169 -5.014759 2.547576

ts6-A
charge, 2S+1 = 0, 1
--- OPT at  $\omega_{B97X-D}/6-311G^{**}$  in SMD ---
E(ele) = -1394.63406307 a.u.
Correction to G = 0.400475 a.u.(RRHO)
Correction to G = 0.411621 a.u.(quasi-RRHO)
imaginary frequency = 1238i
--- SP at  $\omega_{B97X-D}/def2-TZVP$  in SMD ---
E(ele) = -1394.80446629 a.u.
C 0.221796 -0.916520 -0.186814
N -0.222067 -0.731759 -1.434392
N 1.236439 -1.773073 -0.317666
N 0.521982 -1.413444 -2.363669
C 1.404438 -2.029043 -1.643555
C 2.298127 -2.341825 0.516849
C 2.901582 -3.387399 -0.441680
C 2.605881 -2.879187 -1.873209
H 2.993521 -1.539356 0.763562
H 1.886020 -2.750082 1.432765
H 3.967472 -3.522032 -0.236334
H 2.407596 -4.349143 -0.287036
H 3.414174 -2.248713 -2.253270
H 2.429639 -3.679659 -0.502013
C -1.273126 0.129438 -1.891852
C -2.596744 -0.255224 -1.753163
C -0.916077 1.331155 -2.488215
C -3.591011 0.601551 -2.207718
H -2.844027 -1.199608 -1.283910
C -1.917838 2.175322 -2.943764
H 0.132054 1.591183 -2.575548
C -3.253012 1.812429 -2.798779
H -4.630769 0.319966 -2.092728
H -1.655540 3.119547 -3.405903
H -4.033580 2.478381 -3.148404
C -0.228613 -0.297656 1.138787
H 1.297289 0.196280 2.157716
D 0.572197 -0.778577 2.130559
C -1.702836 -0.620788 1.340344
C -2.662567 0.384763 1.463875
C -2.125452 -1.950230 1.359691
C -4.018688 0.060758 1.538840
C -3.467466 -2.282524 1.443818
C -4.417270 -1.263863 1.517797
H -1.376764 -2.733617 1.293621
H -4.737828 0.867801 1.615909
H -3.775043 -3.321668 1.452886
H -5.472717 -1.506178 1.577123
D -2.338821 1.696330 1.493762
C -1.003215 1.961929 1.919864

```

H -0.892381 1.634867 2.961701 H -8.014109 0.726300 0.726869 C 0.760507 2.835351 -0.731215
H -0.890856 3.044921 1.875003 C 2.126980 1.672202 -2.256054
C 0.028402 1.276917 1.046904 C 2.281106 3.188400 -2.485894
H -0.092611 1.627881 0.020633 C 1.716346 3.869042 -1.215954
C 1.417552 1.482327 1.600165 H 2.981750 1.228764 -1.747725
H 1.530533 2.235509 2.376062 H 1.915675 1.103269 -3.155677
C 2.483328 1.440440 0.639022 H 3.319202 3.460133 -2.672867
O 2.440710 0.901676 -0.464709 H 1.689112 3.489970 -3.353357
O 3.631469 2.011522 1.083942 H 2.493111 4.012719 -0.459959
C 4.765632 1.916228 0.223544 H 1.243092 4.830446 -1.411528
H 4.526505 2.349966 -0.751582 C -1.583607 0.942865 0.923147
H 5.017667 0.863064 0.060579 C -2.413785 -0.077706 0.479611
C 5.905412 2.652869 0.889584 C -1.761001 1.512297 2.178796
H 6.799926 2.603790 0.262581 C -3.403194 -0.564123 1.323544
H 5.649743 3.704148 1.042961 H -2.289285 -0.484940 -0.514386
H 6.139813 2.210634 1.861030 C -2.766092 1.030625 3.005606

ts6-B
charge, 2S+1 = 0, 1
--- OPT at ω B97X-D/6-311G** in SMD ---
E(ele) = -1394.62184589 a.u.
Correction to G = 0.400551 a.u. (RRHO)
Correction to G = 0.411455 a.u. (quasi-RRHO)
imaginary frequency = 1110i
--- SP at ω B97X-D/def2-TZVP in SMD ---
E(ele) = -1394.79231759 a.u.

C 0.368999 -1.220700 -0.211509
N 1.463332 -1.475548 0.516284
N -0.221896 -2.412177 -0.352030
N 1.592357 -2.807463 0.824689
C 0.548399 -3.343989 0.277078
C -1.395320 -2.987315 -1.025152
C -1.463124 -4.380096 -0.365623
C -0.028512 -4.708209 0.115434
H -2.273273 -2.374828 -0.847730
H -1.196802 -3.021865 -2.095675
H -2.133154 -4.337187 0.495258
H -1.848198 -5.128177 -1.056735
H -0.004223 -5.283503 1.039572
H 0.540204 -5.255656 -0.641115
C 2.464220 -0.553351 0.975911
C 3.666162 -0.480468 0.287034
C 2.217008 0.219127 2.098686
C 4.633759 0.410205 0.724282
H 3.824917 -1.098849 -0.587299
C 3.111755 1.111107 2.525478
H 1.276399 0.127923 2.626270
C 4.394046 1.209125 1.837687
H 5.570852 0.490027 0.186698
H 3.004831 1.732725 3.392539
H 5.149300 1.912067 2.169618
C -0.195271 0.088443 -0.757662
H -2.056235 -0.083029 -1.033232
O -1.101713 -0.219620 -1.726148
C 0.955800 0.950896 -1.249579
C 1.312177 2.127160 -0.589259
C 1.708582 0.544813 -2.350492
C 2.453381 2.832786 -0.972953
C 2.829376 1.252245 -2.753395
C 3.210221 2.390189 -2.043583
H 1.400019 -0.345255 -2.889147
H 2.713211 3.732211 -0.427317
H 3.403992 0.924040 -3.611856
H 4.091833 2.947487 -2.341110
O 0.575504 2.618214 0.430918
C -0.815913 2.276460 0.345005
H -1.219500 2.654110 -0.597129
H -1.300229 2.804516 1.162530
C -1.003157 0.774205 0.462608
H -0.550728 0.470292 1.411105
C -2.413368 0.255669 0.309881
H -2.603682 -0.667989 0.855263
C -3.560895 1.124323 0.297455
O -3.615243 2.313575 0.030582
O -4.705536 0.425679 0.572942
C -5.924992 1.155536 0.465654
H -6.028831 1.556147 -0.547539
H -5.909331 2.007282 1.152404
C -7.054705 0.206258 0.796882
H -7.069481 -0.637687 0.102300
H -6.948731 -0.184797 1.812176

6
charge, 2S+1 = 0, 1
--- OPT at ω B97X-D/6-311G** in SMD ---
E(ele) = -1394.65202000 a.u.
Correction to G = 0.403045 a.u. (RRHO)
Correction to G = 0.414694 a.u. (quasi-RRHO)
--- SP at ω B97X-D/def2-TZVP in SMD ---
E(ele) = -1394.82314229 a.u.

C 0.049139 -0.546663 0.799464
N -0.692552 -1.410224 0.093276
N 0.841968 -1.328714 1.534761
N -0.366789 -2.720985 0.342027
C 0.569777 -2.627067 1.230807
C 1.922539 -1.174332 2.512461
C 2.562928 -2.577087 2.469220
C 1.446969 -3.547358 2.008631
H 2.567019 -0.354838 2.215020
H 1.487265 -0.93245 3.482342
H 3.367948 -2.581141 1.731081
H 2.984343 -2.857394 3.433800
H 1.815615 -4.376972 1.407294
H 0.892420 -3.959726 2.856311
C -1.646293 -1.123020 -0.936059
C -2.912684 -0.669496 -0.603874
C -1.261961 -1.322130 -2.255605
H -3.810478 -0.388380 -1.626219
H -3.185985 -0.526596 0.434239
C -2.170504 -1.046958 -3.266935
H -0.257481 -1.667720 -2.466712
C -3.441156 -0.575237 -2.952200
H -4.798737 -0.019023 -1.379943
H -1.883613 -1.192685 -4.301767
H -4.145569 -0.351830 -3.745343
C 0.129222 1.019914 0.856370
H 2.408847 1.802331 0.130840
O 1.029128 1.374541 1.747206
C -1.307278 1.479483 1.206509
C -2.035477 2.361855 0.410147
C -1.901876 1.008923 2.376381
C -3.352533 2.694602 0.733550
C -3.205440 1.334591 2.714874
C -3.938161 2.171926 1.873496
H -1.316343 0.363189 3.023986
H -3.891644 3.369159 0.078192
H -3.649437 0.946372 3.624552
H -4.961554 2.433976 2.119404
O -1.517898 2.920264 -0.711158
C -0.095862 2.912027 -0.760534
H 0.299967 3.546709 0.043595
H 0.162383 3.352940 -1.724472
C 0.459262 1.506118 -0.622000
H -0.032461 0.883117 -1.373590
C 1.963815 1.526304 -0.834865
H 2.269826 2.276780 -1.569601
C 2.562420 0.213491 -1.244937
O 1.995356 -0.854788 -1.277487
O 3.851192 0.353523 -1.569821
C 4.556503 -0.839132 -1.951961
H 4.046534 -1.298206 -2.802511
H 4.528723 -1.549563 -1.121316
C 5.971170 -0.439841 -2.296056
H 6.465385 0.022179 -1.438376
H 6.542518 -1.324479 -2.588612
H 5.984088 0.268700 -3.127388

ts7
charge, 2S+1 = 0, 1
--- OPT at ω B97X-D/6-311G** in SMD ---
E(ele) = -1394.64522414 a.u.
Correction to G = 0.404874 a.u. (RRHO)
Correction to G = 0.415606 a.u. (quasi-RRHO)
imaginary frequency = 183i
--- SP at ω B97X-D/def2-TZVP in SMD ---
E(ele) = -1394.81423708 a.u.

base-assisted mechanism
TS with respect to Hs deprotonation of 9 by 1
charge, 2S+1 = 0, 1
--- OPT at ω B97X-D/6-311G** in SMD ---
E(ele) = -1984.58615987 a.u.
Correction to G = 0.591835 a.u. (RRHO)
Correction to G = 0.608700 a.u. (quasi-RRHO)
imaginary frequency = 965i
--- SP at ω B97X-D/def2-TZVP in SMD ---
E(ele) = -1984.82351671 a.u.

C 1.356467 -1.536995 -0.127132
N 2.587093 -2.168657 0.070394
N 0.473300 -2.601556 -0.144472
N 2.428579 -3.546362 0.314610
C 1.165086 -3.730679 0.180468
C -0.973156 -2.769460 -0.048613
C -1.095831 -4.298517 -0.179774
C 0.223940 -4.873008 0.384963
H -1.316177 -2.414838 0.925588
H -1.509326 -2.227824 -0.826157
H -1.974375 -4.676776 0.342384
H -1.189532 -4.562082 -1.235718
H 0.144972 -5.082584 1.455745
H 0.552197 -5.784842 -0.113339
C 3.879228 -1.707592 -0.244099
C 4.097611 -0.814195 -1.290236
C 4.957580 -2.164936 0.513686
C 5.382117 -0.360021 -1.555101


```

O   -1.329716   3.251636   0.025852   C   -1.015573   -4.099779   1.517013   C   1.637568   3.664817   3.516651
O   0.258189   4.819754   0.369468   C   -2.548407   -4.030375   1.695435   C   3.673383   2.562452   4.210578
C   -0.631959   5.404991   1.306100   H   0.269148   -2.674314   0.425475   C   2.702961   3.534241   4.402010
H   -0.837894   4.702289   2.122937   H   -0.430835   -2.029593   1.939757   H   4.308451   0.920955   2.983831
H   -1.588672   5.638572   0.829249   H   -0.768055   -4.805349   0.720447   H   0.898499   4.437753   3.682600
C   0.029620   6.657752   1.837873   H   -0.503383   -4.411609   2.427120   H   4.502568   2.469638   4.901341
H   0.977521   6.421888   2.329026   H   -3.060753   -4.965978   1.473349   H   2.769766   4.208686   5.248306
H   0.231942   7.361109   1.026405   H   -2.815341   -3.715197   2.707763   O   0.598252   2.883899   1.458061
H   -0.622978   7.148613   2.565708   C   -4.464059   -0.792969   -1.379309   C   -0.673900   3.460150   1.679936
C   -2.057614   -0.409372   0.120707   C   -4.017415   -0.353854   -2.623343   H   -1.004070   3.811257   0.697402
N   -1.461652   -0.267589   1.301162   C   -5.826856   -0.744403   -1.077875   H   -0.622361   4.340554   2.329187
N   -1.427804   -0.907325   -0.714692   C   -4.924125   0.154867   -3.543517   C   -1.689855   2.487016   2.178421
N   -0.471886   -1.211644   1.235159   H   -2.965528   -0.410155   -2.868172   H   -2.701800   2.878415   2.220056
C   -0.465288   -1.564307   -0.012949   C   -6.723641   -0.243781   -2.008863   C   -1.462274   1.210704   2.472489
C   -1.414314   -1.223314   -2.146074   H   -6.169208   -1.112853   -0.119406   H   -0.469489   0.778010   2.436110
C   -0.566001   -2.512429   -2.161088   C   -6.278224   0.218781   -3.243312   C   -2.538584   0.254355   2.977733
C   0.310474   -2.478662   -0.885913   H   -4.561756   0.500699   -4.505083   O   -2.338056   -0.879360   3.172772
H   -2.429669   -1.362497   -2.511810   H   -7.779668   -0.210210   -1.763957   O   -3.763585   0.757049   2.609419
H   -0.928962   -0.404382   -2.675761   H   -6.981222   -0.915017   -3.964512   C   -4.875453   -0.131491   2.797733
H   -1.221101   -3.383994   -2.117690   C   -1.381456   -0.087099   -0.693955   H   -4.892831   -0.438654   3.865770
H   0.038670   -2.568493   -3.064797   H   0.798056   -0.406480   0.862463   H   -4.735567   -1.021971   2.199775
H   0.431170   -3.462325   -0.436630   O   -0.018076   -0.282436   -0.554930   C   -6.126024   0.622557   2.432996
H   1.292141   -2.041496   -1.077190   C   -1.786948   1.253934   -1.114801   H   -6.261394   1.506817   3.060891
C   -1.756034   0.327741   2.568092   C   -0.958184   2.037741   -1.944894   H   -6.084086   0.938917   1.387898
C   -1.840361   -0.506573   3.675311   C   -2.959906   1.856668   -0.636841   H   -6.997377   -0.025369   2.559594

base-assisted mechanism
ts11
charge, 2S+1 = 0, 1
--- OPT at  $\omega$ B97X-D/6-311G** in SMD ---
E(ele) = -2789.27693150 a.u.
Correction to G = 0.829211 a.u.(RRHO)
Correction to G = 0.852623 a.u.(quasi-RRHO)
imaginary frequency = 25i
--- SP at  $\omega$ B97X-D/def2-TZVP in SMD ---
E(ele) = -2789.60948451 a.u.
C   2.663111   0.752162   0.736865
N   3.796938   0.455647   1.531521
N   1.760291   1.240184   1.681359
N   3.518174   0.657393   2.905579
C   2.326394   1.133664   2.910049
C   0.502717   1.965393   1.691455
C   0.071582   1.791151   3.158780
C   1.389134   1.644898   3.956992
H   0.677272   3.013702   1.429703
H   -0.195707   1.555989   0.969481
H   -0.536891   2.627201   3.504044
H   -0.519989   0.877935   3.255697
H   1.749163   2.608753   4.327827
H   1.306481   0.966554   4.805821
C   5.150441   0.497512   1.162856
C   6.097940   -0.070385   2.021592
C   5.574245   1.073864   -0.034243
C   7.439489   -0.065422   1.675325
H   5.767671   -0.498717   2.958903
C   6.920602   1.063252   -0.373437
H   4.852228   1.530414   -0.696714
C   7.862163   0.492729   0.472289
H   8.162043   -0.509264   2.351836
H   7.230507   1.511100   -1.311249
H   8.911600   0.484715   0.201210
C   2.349264   0.418640   -0.547122
H   0.342934   -0.167335   -2.046078
O   1.134175   0.772728   -1.030443
C   3.185861   -0.391980   -1.450197
C   3.148507   -0.184901   -2.841971
C   3.915548   -1.493894   -0.984052
C   3.782205   -1.075056   -3.707062
C   4.565451   -2.365582   -1.841545
C   4.484827   -2.163507   -3.215556
H   3.945749   -1.679529   0.083206
H   3.716518   -0.880439   -4.771330
H   5.119986   -3.205874   -1.439389
H   4.978816   -2.841215   -3.902934
O   2.484399   0.837543   -3.448795
C   2.410435   2.100732   -2.804599
H   2.466927   2.841462   -3.606811
H   3.275706   2.252689   -2.150867
C   1.132753   2.325046   -2.049480
H   0.239986   1.995044   -2.571667
C   1.018100   3.476155   -1.280048

```


charge, 2S+1 = 0, 1
--- OPT at ω B97X-D/6-311G** in SMD ---
E(ele) = -320.82331345 a.u.
Correction to G = 0.084463 a.u. (RRHO)
Correction to G = 0.088367 a.u. (quasi-RRHO)
--- SP at ω B97X-D/def2-TZVP in SMD ---
E(ele) = -320.86408245 a.u.
C -0.027187 -0.285778 -0.157390
N -0.319325 0.763711 -0.941255
N -1.146127 -1.050964 -0.338650
N -1.524487 0.707489 -1.589357
C -2.007194 -0.424923 -1.194310
C 0.511196 1.928745 -1.159750
H -0.018787 2.828179 -0.841507
H 1.420216 1.809975 -0.574465
H 0.761713 2.013661 -2.218626
C -1.382405 -2.337921 0.289492
H -2.270046 -2.297449 0.923914
H -1.511065 -3.114814 -0.466699
H -0.515686 -2.575666 0.902035
H -2.960995 -0.827516 -1.496286

model thiazol-2-ylidene

charge, 2S+1 = 0, 1
--- OPT at ω B97X-D/6-311G** in SMD ---
E(ele) = -608.30257078 a.u.
Correction to G = 0.054448 a.u. (RRHO)
Correction to G = 0.057450 a.u. (quasi-RRHO)
--- SP at ω B97X-D/def2-TZVP in SMD ---
E(ele) = -608.33831197 a.u.
C 0.228572 -0.262589 -0.302818
S -1.013703 -1.451132 -0.246841
N -0.317408 0.797258 -0.915158
C -2.202344 -0.465307 -1.048713
C -1.643898 0.720528 -1.335957
C 0.452307 2.017414 -1.144014
H 0.519823 2.222867 -2.214325
H -0.024102 2.860703 -0.639854
H 1.448724 1.863955 -0.737570
H -3.209276 -0.790680 -1.259841
H -2.098745 1.566345 -1.831072

substrate used by the Suresh group

charge, 2S+1 = 0, 1
--- OPT at ω B97X-D/6-311G** in SMD ---
E(ele) = -1073.53908284 a.u.
Correction to G = 0.269927 a.u. (RRHO)
Correction to G = 0.279613 a.u. (quasi-RRHO)
--- SP at ω B97X-D/def2-TZVP in SMD ---
E(ele) = -1073.67181957 a.u.
C 0.841588 -2.461027 1.784703
H 0.169204 -1.961076 2.502130
O 1.861703 -2.990063 2.159321
C 0.415907 -2.426906 0.367499
C -0.763143 -1.781438 -0.028587
C 1.222769 -3.017907 -0.606027
C -1.115607 -1.722504 -1.374336
C 0.885073 -2.958997 -1.945960
C -0.286655 -2.307159 -2.321154
H 2.127172 -3.516621 -0.276123
H -2.025885 -1.222999 -1.679949
H 1.522547 -3.414009 -2.693999
H -0.565519 -2.252829 -3.367428
O -1.525868 -1.234801 0.963139
C -2.567904 -0.391532 0.628719
C -2.296150 0.915841 0.209983
C -0.903223 1.367903 0.097714
H -0.200555 0.906730 0.784999
C -0.464295 2.280560 -0.773343
H -1.143318 2.766901 -1.468198
C 0.916793 2.823285 -0.801442
O 1.101096 3.943021 -1.237252
C 2.061408 2.015168 -0.269713
C 3.116066 2.697900 0.339462
C 2.134597 0.627945 -0.413497
C 4.209950 2.002598 0.831236
H 3.061259 3.776788 0.425588
C 3.240495 -0.064171 0.064443
H 1.340407 0.085969 -0.914792
C 4.272503 0.619256 0.695217

H 5.016516 2.538365 1.318729
H 3.293225 -1.139746 -0.053929
H 5.127548 0.073664 1.078322
C -3.385384 1.742606 -0.077990
C -4.687278 1.279424 0.043308
C -4.927441 -0.024120 0.462669
C -3.862342 -0.866143 0.754832
H -3.203249 2.769657 -0.373456
H -5.516421 1.941513 -0.176405
H -5.943322 -0.387297 0.564947
H -4.019263 -1.887796 1.079334

8-membered product

charge, 2S+1 = 0, 1
--- OPT at ω B97X-D/6-311G** in SMD ---
E(ele) = -1073.57382127 a.u.
Correction to G = 0.275265 a.u. (RRHO)
Correction to G = 0.284137 a.u. (quasi-RRHO)
--- SP at ω B97X-D/def2-TZVP in SMD ---
E(ele) = -1073.70499200 a.u.
C 0.046678 -1.152626 -0.174429
H 0.489872 1.085311 -1.606828
O 0.791103 -1.360993 -1.104532
C -0.441018 -2.268323 0.691577
C -1.478945 -2.163821 1.628160
C 0.248210 -3.484009 0.604308
C -1.775914 -3.230124 2.472385
C -0.048325 -4.547054 1.435023
C -1.060231 -4.411179 2.382434
H 1.043124 -3.555076 -0.128219
H -2.582422 -3.110689 3.185494
H 0.508273 -5.472974 1.355225
H -1.301876 -5.233835 3.045953
O -2.255106 -1.048320 1.808284
C -2.757604 -0.379575 0.709448
C -1.898539 0.314321 -0.137875
C -0.418421 0.261180 0.171131
H -0.298391 0.376480 1.252717
C 0.421878 1.305871 -0.538710
H -0.039966 2.294388 -0.439319
C 1.827547 1.389946 0.028502
O 2.147303 0.752979 1.007914
C 2.807646 2.302759 -0.643359
C 2.469706 3.087805 -1.747212
C 4.105634 2.366740 -0.132259
C 3.414762 3.923729 -2.327846
H 1.469740 3.054618 -2.163066
C 5.048922 3.199041 -0.713375
H 4.355972 1.752679 0.724415
C 4.704022 3.979687 -1.812595
H 3.144518 4.530474 -3.184501
H 6.054779 3.240634 -0.311346
H 5.441402 4.631432 -2.267983
C -2.454083 0.988950 -1.222371
C -3.828361 0.994500 -1.427568
C -4.667928 0.318568 -0.550814
C -4.130783 -0.376104 0.524724
H -1.810126 1.522956 -1.911142
H -4.243153 1.530948 -2.273001
H -5.740338 0.323271 -0.707270
H -4.758226 -0.918247 1.221892

enol ether derived from model 1,2,4-triazol-5-ylidene

charge, 2S+1 = 0, 1
--- OPT at ω B97X-D/6-311G** in SMD ---
E(ele) = -1394.39054469 a.u.
Correction to G = 0.386599 a.u. (RRHO)
Correction to G = 0.398283 a.u. (quasi-RRHO)
--- SP at ω B97X-D/def2-TZVP in SMD ---
E(ele) = -1394.55903983 a.u.
C -2.049301 -0.855231 -0.650864
N -3.392677 -0.813011 -0.373202
N -1.889931 -2.042259 -1.350251
N -4.050137 -1.914724 -0.876249
C -3.133080 -2.608741 -1.450690
C -4.030677 -0.005441 0.636207
H -3.357278 0.106376 1.491006
H -4.288096 0.989951 0.264575
H -4.936000 -0.524103 0.946329

C -0.733770 -2.414707 -2.147359
H 0.097798 -2.747007 -1.527631
H -1.027786 -3.229132 -2.809428
H -0.405712 -1.564259 -2.747321
H -3.303911 -3.539517 -1.967627
C -1.064916 0.031055 -0.289512
H 2.555296 -0.201618 1.039426
O 0.252163 -0.419589 -0.325550
C -1.244250 1.453537 -0.035060
C -0.406941 2.156300 0.853563
C -2.193447 2.220891 -0.731266
C -0.490901 3.529990 1.010224
C -2.305885 3.591827 -0.553777
C -1.442706 4.258519 0.307401
H -2.827933 1.725622 -1.458527
H 0.191196 4.011468 1.701829
H -3.050302 4.144509 -1.116204
H -1.508979 5.332599 0.435918
O 0.554915 1.495482 1.606658
C 0.064294 0.531543 2.460720
C 0.128535 -0.811796 2.097922
C 0.685736 -1.235424 0.761326
H 0.367344 -2.271709 0.580346
C 2.215348 -1.188201 0.725530
H 2.605025 -1.932965 1.422581
C 2.713363 -1.562908 -0.660192
O 2.719427 -2.729846 -0.997561
C 3.188566 -0.493636 -1.590479
C 2.871127 0.853245 -1.402920
C 3.947257 -0.872749 -2.700196
C 3.310322 1.804340 -2.314419
H 2.249060 1.156053 -0.579133
H 4.398342 0.080381 -3.501727
H 4.176038 -1.922739 -2.840254
C 4.078822 1.421439 -3.407402
H 3.046916 2.846041 -2.171142
H 4.996079 -0.219504 -4.453144
H 4.426674 2.167780 -4.113283
C -0.337940 -1.761752 3.002577
C -0.855781 -1.385850 4.235284
C -0.924168 -0.039587 4.573070
C -0.466417 0.921935 3.681630
H -0.304968 -2.811059 2.726184
H -1.213412 -2.140910 4.925752
H -1.332688 0.264401 5.530093
H -0.510294 1.978114 3.921547

enol ether derived from model thiazol-2-ylidene

charge, 2S+1 = 0, 1
--- OPT at ω B97X-D/6-311G** in SMD ---
E(ele) = -1681.88660578 a.u.
Correction to G = 0.354319 a.u. (RRHO)
Correction to G = 0.366046 a.u. (quasi-RRHO)
--- SP at ω B97X-D/def2-TZVP in SMD ---
E(ele) = -1682.04944621 a.u.
C 1.663015 0.353524 1.528520
S 3.028943 1.492549 1.645721
N 1.960741 -0.827858 2.215744
C 3.956550 0.286617 2.535460
C 3.253109 -0.824549 2.740068
C 0.921453 -1.519095 2.976960
H 0.031361 -1.659068 2.369013
H 1.301552 -2.496213 3.728093
H 0.647806 -0.947300 3.870999
H 4.969700 0.491097 2.842519
H 3.587174 -1.702978 3.274346
C 0.571346 0.552469 0.759832
H -1.341955 -1.512856 -1.799110
O -0.287219 -0.491779 0.476102
C 0.215578 1.820746 0.108261
C -0.133287 1.847915 -1.251519
C 0.147578 3.024631 0.814777
C -0.566554 3.013967 -1.863201
C -0.258993 4.202655 0.203824
C -0.631581 4.194800 -1.134552
H 0.387851 3.020599 1.872281
H -0.834683 2.981222 -2.912752
H -0.306918 5.119661 0.779503
H -0.966011 5.106428 -1.616408
O -0.096836 0.706475 -2.026478

C	1.111897	0.030148	-2.072035
C	1.296800	-1.105521	-1.285526
C	0.231405	-1.566363	-0.324832
H	0.672187	-2.318577	0.339938
C	-0.976466	-2.188875	-1.027608
H	-0.654398	-3.119424	-1.499905
C	-2.048520	-2.550272	-0.012108
D	-1.912626	-3.543305	0.672199
C	-3.254593	-1.677311	0.130825
C	-4.350830	-2.176043	0.838121
C	-3.304301	-0.381121	-0.385614
C	-5.484886	-1.398910	1.013315
H	-4.294702	-3.179040	1.244523
C	-4.435168	0.401914	-0.195753
H	-2.450158	0.032773	-0.905975
C	-5.527319	-0.106955	0.496840
H	-6.335503	-1.796088	1.555716
H	-4.459227	1.412846	-0.586301
H	-6.411853	0.504422	0.638620
C	2.509255	-1.780912	-1.378102
C	3.507726	-1.344685	-2.239793
C	3.306348	-0.206627	-3.009974
C	2.105969	0.487010	-2.922657
H	2.674201	-2.650696	-0.750565
H	4.445419	-1.884789	-2.298981
H	4.083809	0.146777	-3.677504
H	1.927607	1.380365	-3.509993

References

- (1) Riplinger, C.; Sandhoefer, B.; Hansen, A.; Neese, F. Natural triple excitations in local coupled cluster calculations with pair natural orbitals. *J. Chem. Phys.* **2013**, *139*, 134101.
- (2) Guo, Y.; Riplinger, C.; Becker, U.; Liakos, D. G.; Minenkov, Y.; Cavallo, L.; Neese, F. Communication: An improved linear scaling perturbative triples correction for the domain based local pair-natural orbital based singles and doubles coupled cluster method [DLPNO-CCSD(T)]. *J. Chem. Phys.* **2018**, *148*, 011101.
- (3) Neese, F.; Wennmohs, F.; Becker, U.; Riplinger, C. The ORCA quantum chemistry program package. *J. Chem. Phys.* **2020**, *152*, 224108.
- (4) Shida, N.; Kabuto, C.; Niwa, T.; Ebata, T.; Yamamoto, Y. Studies on s-Cis/s-Trans Preference of Acyclic α,β -Unsaturated Esters. Reactions, Supersonic Jet Spectroscopy, NOEs, and X-ray Analysis. *J. Org. Chem.* **1994**, *59*, 4068–4075.
- (5) Kerr, M. S.; De Alaniz, J. R.; Rovis, T. A highly enantioselective catalytic intramolecular stetter reaction. *J. Am. Chem. Soc.* **2002**, *124*, 10298–10299.
- (6) De Alaniz, J. R.; Rovis, T. A highly enantio- and diastereoselective catalytic intramolecular Stetter reaction. *J. Am. Chem. Soc.* **2005**, *127*, 6284–6289.
- (7) Moore, J. L.; Silvestri, A. P.; De Alaniz, J. R.; Dirocco, D. a.; Rovis, T. Mechanistic investigation of the enantioselective intramolecular stetter reaction: Proton transfer is the first irreversible step. *Org. Lett.* **2011**, *13*, 1742–1745.
- (8) Burés, J. Variable Time Normalization Analysis: General Graphical Elucidation of Reaction Orders from Concentration Profiles. *Angew. Chem. Int. Ed.* **2016**, *52*, 16084–16087.

- (9) Martínez-Carrión, A.; Howlett, M. G.; Alamillo-Ferrer, C.; Clayton, A. D.; Bourne, R. A.; Codina, A.; Vidal-Ferran, A.; Adams, R. W.; Burés, J. Kinetic treatments for catalyst activation and deactivation processes based on variable time normalization analysis. *Angew. Chem. Int. Ed.* **2019**, *58*, 10189–10193.
- (10) Nielsen, C. D.-T.; Burés, J. Visual kinetic analysis. *Chem. Sci.* **2019**, *10*, 348–353.